THE UNIVERSITY OF MICHIGAN
INDUSTRY PROGRAM OF THE COLLEGE OF ENGINEERING

THE USE OF STRONG SHOCK WAVES IN THE THERMAL DECOMPOSITION OF ETHANE AND ETHYLENE

Irving Franklin Miller

A dissertation submitted in partial fulfillment
of the requirements for the degree of
Doctor of Philosophy in the
University of Michigan
1959

October, 1959

IP-392

Doctoral Committee:

Professor Stuart W. Churchill, Chairman
Associate Professor Thomas C. Adamson, Jr.
Associate Professor Richard B. Bernstein
Assistant Professor Keith H. Coats
Associate Professor Edwin H. Young

ABSTRACT

A chemical shock tube was utilized to measure the rate of thermal decomposition of ethane to form ethylene and hydrogen and the rate of thermal decomposition of ethylene to form acetylene and hydrogen at high temperatures. The chemical shock tube is an instrument for producing, confining, and controlling shock waves. The reactant gas mixture is rapidly compressed and heated by the shock wave and then rapidly expanded and cooled by a rarefaction wave. In its simplest form, the shock tube consists of two chambers separated by a thin diaphragm. One section contains a driver gas at high pressure while the other contains the reactant gas at a low pressure. When the diaphragm is suddenly ruptured, the movement of the high pressure gas into the low pressure section causes a shock wave to propagate through the low pressure section. The mixture is quenched by a rarefaction wave reflected from the end of the high pressure section.

The temperature and pressure history in the shock tube is computed from the measured wave velocity, along with the initial conditions of the driver and reactant gases. If a reaction mechanism is postulated, a reaction rate constant can then be computed from the composition of the final mixture in the tube. When a first order mechanism is postulated, the computed rates obtained in this investigation at temperatures between about 2200°R and about 5000°R indicate a lower apparent energy of activation than previous data obtained at lower temperatures (less than 2000°R) in conventional reactors. How-

ever, the data obtained in this investigation along with the data obtained by previous investigations with both shock tubes and conventional reactors can be represented grossly by a single apparent energy of activation over the extreme range of temperatures from 1300°R to 5000°R. These data represent degrees of conversion of up to about 60% ethane converted to ethylene and up to 17% ethylene converted to acetylene. The reaction rate constants which fit all the data are, for ethane to ethylene and hydrogen,

$$\ln k_1 = 19.365 - \frac{41640}{T}$$

and for ethylene to acetylene and hydrogen,

$$\ln k_1 = 10.756 - \frac{18940}{T}$$

where k_1 is the first order rate constant ($sec.^{-1}$) and T is temperature (°R). These equations give apparent endothermic energies of activation, for ethane to ethylene and hydrogen, of 83,000 BTU/lb.-mole (46 kcal/gm.-mole), and for ethylene to acetylene and hydrogen, of 37,700 BTU/lb.-mole (21 kcal/gm.-mole). In previous investigations of the cracking of ethane and ethylene, a whole spectrum of products of decomposition was obtained, while in this research, only the principal products of decomposition (H_2, C_2H_4, C_2H_2) were obtained. This difference is undoubtedly attributable to the shorter residence times and hence lower conversions obtained in this research.

Additions of O_2, Air, CO, and Cl_2 in amounts of less than about 10% did not affect the reaction rates significantly. Carbon was not included in the analysis. However, hydrogen and carbon balances for the gaseous products and reactants indicate that a slight amount of carbon is formed in the ethylene

to acetylene reaction, but little or no carbon is formed during the ethane to ethylene reaction.

A significant percentage of acetylene can be made directly from ethane at the high temperatures achieved in a shock tube (4700°R and higher) and this reaction may have commercial possibilities. With the possibility of commercial applications in mind, a method for duplication of the conditions in the shock tube on a continuous basis was investigated theoretically. The system which was postulated was a convergent-divergent nozzle with a standing shock wave at the exit. The rate at which energy would have to be transferred through the wall of the nozzle to the high velocity gas stream is extremely and perhaps prohibitively high.

ACKNOWLEDGMENTS

The author wishes to express his appreciation to the members of the Doctoral Committee for their many helpful suggestions and constant encouragement during the conduct of this work. He would also like to thank the members of the staff of the Aircraft Propulsion Laboratory, whose help at critical stages in the work was indispensable. In addition, Mr. Edward J. Schaefer helped considerably in the design of some of the electronics equipment.

He would also like to thank the Standard Oil Foundation and the Union Carbide and Carbon Corporation for their financial support during the course of this work.

To the shop and laboratory personnel of the Department of Chemical and Metallurgical Engineering the author expresses his thanks for their assistance in some of the mechanical and analytical problems presented by this work.

Finally, he would like to thank Mrs. Thelma Dyer, who typed the first draft of this manuscript, and also the Engineering College Industry Program, which prepared this manuscript in its final form.

Special thanks are due Professor Joseph J. Martin and Assistant Professor Don E. Rogers for serving on the author's Doctoral Committee during most of the course of this work.

TABLE OF CONTENTS

		Page
ABSTRACT		ii
ACKNOWLEDGMENTS		v
LIST OF TABLES		viii
LIST OF FIGURES		ix
LIST OF APPENDICES		xi
I.	INTRODUCTION	1
	A. Scope of Research	1
	B. Review of the Literature	2
II.	THEORY	6
	A. Definition and Rankine-Hugoniot Equation	6
	B. The Shock Tube	8
	C. Pressure Rise Across a Shock Wave	11
	D. Temperature Rise Across a Shock Wave	14
	E. Gas Residence Time in the Reaction Zone	16
	F. Average Temperature in the Reaction Zone	28
	G. Chemical Kinetic Equations	33
III.	DESCRIPTION OF APPARATUS	38
	A. General Remarks	38
	B. Construction of the Shock Tube	41
	C. The Velocity Probes and Timing Circuit	49
	D. Operation of the Shock Tube	50
	E. Preparation of Reactant Mixtures	55
	F. Analytical Procedures	55
IV.	EXPERIMENTAL RESULTS	57
	A. Experimental Data Taken	57
	B. Cracking of Ethane	57
	C. Statistical Analysis of Ethane Data	65
	D. Uncertainty in the Value of k_1 for Ethane	67
	E. Analytical Methods for Eliminating Uncertainty	70
	F. The Effect of Certain Additives on Ethane Cracking	72

G. Cracking of Ethylene 74
H. Decomposition of a Mixture of Ethane and Ethylene 79
I. General Notes on the Decomposition of Hydrocarbons in the Shock Tube 80
J. Considerations for the Attainment of Continuous Decomposition by a Shock Wave 82

V. CONCLUSIONS 87

APPENDICES 89

BIBLIOGRAPHY 103

NOMENCLATURE 114

LIST OF TABLES

Table No.		Page
I	STANDARD DEVIATIONS	66
II	ANALYSIS OF HELIUM DRIVEN RUNS FOR ETHANE	72
III	ANALYSIS OF HELIUM DRIVEN RUNS FOR ETHYLENE	78
IV	PREDICTION OF CONVERSION FOR MIXTURE OF C_2H_6 AND C_2H_4	79
V	HEAT REQUIREMENT FOR STANDING SHOCK WAVE TO DUPLICATE SHOCK TUBE RUNS	85

LIST OF FIGURES

Figure No.		Page
1	Wave Diagram with Temperature and Pressure Profiles	10
2	Classical Taub Equation Curves for Some Representative Gases	15
3	Temperature Rise Across Shock	17
4	Wave Diagram for Interaction with Reflected Rarefaction	19
5	Distance Between Diaphragm Site and Interaction Point vs. Mach Number	27
6	Maximum Residence Time as a Function of Mach Number	29
7	Particle Paths for Flow in Shock Tube	30
8	Loading Side of Shock Tube	39
9	Test Side of Shock Tube	40
10	Diagram of the Shock Tube and Associated Lines	44
11	Method of Assembly of Test Section	45
12	"O" Ring Groove Detail	46
13	Detail of Flange	48
14	Block Diagram of Velocity Measurement Circuit	51
15	Circuit of Transducer Signal Amplifier	52
16	Circuit of Thyratron Pulse Maker	53
17	Data for the Reaction $C_2H_6 \rightleftharpoons C_2H_4 + H_2$	59
18	One Possible Way ln k_1 May Be Related to T	62

19 Least Squares Curves for Reaction $C_2H_6 \rightleftharpoons C_2H_4 + H_2$ 64

20 Uncertainty in the Value of $\ln k_1$ 69

21 $\ln k_1$ vs. $1/T$ for $C_2H_4 \rightleftharpoons C_2H_2 + H_2$ 75

22 Schematic Diagram of Converging-Diverging Nozzle 83

LIST OF APPENDICES

Appendix		Page
I -	FLOW EQUATIONS	89
	A. Derivation of Rankine-Hugoniot Equation	89
	B. Notes on the Derivation of the Taub Equation	90
	C. Notes on Particle Velocity	91
II -	SAMPLE CALCULATION	93
III -	EXPERIMENTAL INFORMATION	97
	A. Data Obtained During the Course of the Runs	97
	B. Reaction Parameters Calculated from Raw Data	100

I - INTRODUCTION

A. Scope of Research

The purpose of this dissertation is to examine the feasibility of promoting certain chemical reactions by means of shock waves, to examine the compositions of the products obtained from these reactions, and to interpret these results in terms of reaction rates and mechanisms. More specifically, attention was directed to the cracking of ethane to ethylene and the further cracking of ethylene to acetylene, with a view to obtaining rate equations as well as studying possible side reactions by various techniques including addition of contaminants.

Due to the current, wide interest in the use of shock waves as promoters of chemical reactions and in the use of the shock tube in chemical and chemical engineering research, a fairly extensive review of the pertinent literature is presented.

Equations are developed for the determination of the reaction rates in terms of the various directly measurable quantities and, in the course of this development, many of the very useful aerodynamic relationships for a shock wave are also developed.

The special features of the experimental equipment are presented, along with an analysis of many of the problems in the design. An unusual method of quenching the shock wave was utilized. This method is discussed, along with several problems involved in the analysis of the flow conditions

established by the use of this method.

One possible method of obtaining continuous reaction by shock waves is presented and an attempt at evaluation of the system is made to determine its feasibility for possible commercial application.

B. Review of the Literature

Although more work on shock waves has probably been done in the last ten years than in all time previous, the history of shock waves does go back about 150 years. According to Courant and Friedrichs (21), the existence of shock waves was first suggested on mathematical grounds. In 1808, Poisson determined a simple wave solution of the differential equation of flow of an isothermal gas. Challis (18) observed that this solution cannot always be solved uniquely for the velocity and Stokes (102) showed that a unique solution can only be obtained if a discontinuity in velocity is assumed to occur. He also indicated that such a discontinuity in a real gas would be smoothed out by molecular transport and, indeed, more recent work in shock wave theory has attempted to take molecular transport into account. Earnshaw (30) developed the simple wave equation for the flow of gases satisfying any relation in which pressure is a function only of density. Independently, Riemann (86) developed the theory of the simple wave and the general solution of the flow problem, but made the incorrect assumption that the transition across the shock is adiabatic and reversible. Rankine (79) showed that no steady adiabatic process in which the only forces are pressure forces can represent a continuous change over a small finite region from one constant

state to another. Instead, he proposed a non-adiabatic process in which heat may be communicated from one particle to another but in which no heat is received from outside. Rankine's condition agrees with the principle of conservation of energy, but Rayleigh (80) and Hugoniot (59) were the first to point out that an adiabatic reversible transition in a shock would violate the principle of conservation of energy. In fact, Hugoniot showed that in the absence of viscosity and heat conduction, conservation of energy implies conservation of entropy in continuous flow and also implies a change of entropy across a shock. From the conservation of energy, he also deduced the third shock condition in a form which is preferable to, although equivalent to, that of Rankine. Rayleigh (80) pointed out that the entropy must increase in crossing a shock front and, for this reason, a rarefaction shock cannot occur in a perfect gas.

The first recorded observation of shock waves in a tube may be credited to Vielle (115), though it is certain that they were produced unobserved previously in plumbing and flow devices. The class of combustion phenomena known as detonations was investigated by workers in the late nineteenth century. Chapman (19) and Jouguet (63) independently demonstrated the relation between this class of combustion and the aerodynamic theory of shock waves.

More recently, considerable work has been done with the shock tube to investigate its various properties and also to apply it to the achieving of high temperatures for the study of high temperature flows and chemical

reactions, as well as the more basic study of the shock properties themselves.

Considerable work has been done on the properties of shock waves in the shock tube, and several excellent compilations are available, especially Courant and Friedrichs (21) and Glass and Hall (39). Other pertinent work on shock wave properties has been done by Glass, Martin and Patterson (40, 41), Lieber and Wan (68), Travers (111), and Trimpi and Cohen (112). Work with particular emphasis on the shock tube as an experimental instrument or with particularly complete descriptions of the necessary equipment include Gluckstein (45), Henshall (50), Morrison (72), Russo and Hertzberg (89, 90), and White (116).

There has been considerable work on the use of the shock tube to achieve high temperatures, and particularly the works of Model (70), Resler et al (81), Turner (114), and Zeldovich and Leipunskii (121) are pertinent. Hertzberg (48) presents a review of this material.

The literature on the use of high temperature achieved from shock waves to achieve chemical reactions is quite extensive. Work on the mechanism of chemical reactions behind shock waves has been done by Duff (29), Glick et al (44), Greene (46), Hertzberg and Squire (51), Hornig (56, 57), and Steinberg and Lyon (100). A review by Hikita (52) is also available.

Work on the use of shock waves for the initiation of ignition or detonation has been done by Berets et al (5), Fay and Lekawa (35), Morrison (72), Schmidt (92), Steinberg and Kaskan (99) and Suzuki et al (107).

The dissociation of a pure diatomic gas behind a strong normal

shock wave has been studied by Jarre (61). Particular work on air and air products has been done by Carrington and Davidson (16, 17), Davidson and Schott (25), Feldman (36), Glick et al (43), Schott and Davidson (93), Toennies and Greene (109, 110), Wood (117), and Wurster (120). The halogens have been studied by Britton et al (7, 8, 9, 10), Palmer and Hornig (73), and Wray and Hornig (118, 119), the H_2-O_2 system has been studied by Bauer et al (2) and Fay (34). The hydrogen-deuterium exchange reaction was studied by Gluckstein (45).

The work on organic reactions in shock waves is fairly recent and not too extensive. Most of the work is concerned with acetylene decomposition and includes work by Aten and Green (1), Bennett (4), Glick (42), Greene et al (47), Hooker (55), and Jost (62).

The literature on ethane and ethylene decomposition, the two reactions studied in this thesis, is extensive and only the most pertinent will be discussed. Special reference will be made to several compilations of data which proved to be especially valuable. These are Brooks et al (11), Egloff (31), Laidler (66), and Steacie (97). A more complete listing of these references is contained in the bibliography.

II - THEORY

In this section, the equations for motion of a shock wave will be developed from the ideal gas standpoint and will be specialized for the development of the various flow parameters required for the determination of the conditions occurring in the shock tube used in this research. The sources of much of this material include Gluckstein (45), Glass and Hall (39), Courant and Friedrichs (21), and Laporte (122). The ideal gas standpoint is used because the equations become so complex that any more sophisticated and complicated viewpoint would lead to equations impossible to handle without a digital computer.

A. Definitions and Rankine-Hugoniot Equation

A shock wave may be defined as a pressure discontinuity in a compressible flow. This discontinuity is a disturbance in the fluid flow and so, will move at the disturbance velocity with respect to the gas behind the wave, i.e. at the velocity of sound with respect to the gas behind the wave. This velocity is a function only of the temperature, the heat capacity and the molecular weight of the fluid in question. In a one-dimensional flow, the disturbance will propagate both with and against the direction of motion of the fluid, so that with respect to a fixed laboratory system of coordinates:

$$\frac{dx}{dt} = u \pm C \tag{1}$$

where dx/dt is the disturbance velocity with respect to a fixed laboratory

system of coordinates, u is the velocity of the gas behind the wave with respect to the laboratory, and C is the local velocity of sound. From equation (1), it is clear that, although a shock wave propagates at the disturbance velocity with respect to the source of the shock wave, it can propagate at a much greater speed with respect to the laboratory, since the velocity of the source of the shock wave with respect to the laboratory may be quite high.

The fact that a discontinuity in pressure can exist in a compressible flow is due to the fact that the equations characterizing such a flow have more than one solution. These equations are simply the conservation of mass, conservation of momentum, and conservation of energy equations and, when written for the conditions before and after a shock, are known as the shock conditions. If the system is horizontal and there is no transfer of energy, mass, or momentum to the surroundings, they may be written as:

$$\rho_o v_o = \rho_1 v_1 \tag{2}$$

$$\rho_o v_o^2 + P_o = \rho_1 v_1^2 + P_1 \tag{3}$$

$$1/2\, v_o^2 + h_o = 1/2\, v_1^2 + h_1 \tag{4}$$

where the subscript o refers to the conditions before the shock and the subscript 1 refers to the conditions after the shock with the shock stationary in the coordinate system used. In the case in which there is a chemical

release of energy behind the shock, this energy may be included as part of the enthalpy term, h, in the energy equation.

These equations may be manipulated into the following form, known as the Rankine-Hugoniot Equation:

$$\frac{\rho_1}{\rho_o} = \frac{\beta \frac{P_1}{P_o} + 1}{\frac{P_1}{P_o} + \beta} \tag{5}$$

where $\beta = \frac{C_p + C_v}{C_p - C_v}$, if it is noted that the enthalpy h can be defined (for constant C_p and enthalpy equal to zero at 0^oR) by

$$h = C_p T \tag{6}$$

and the ideal gas law:

$$P = \frac{\rho R T}{m} \tag{7}$$

is taken into account. A complete derivation may be found in Appendix IA. This relationship between pressure and density is extremely useful and will be employed repeatedly in deriving the other necessary equations.

B. The Shock Tube

The shock tube is simply a tube sealed at both ends in which a diaphragm is placed to divide it into two sections. In one section, called the driver section, a gas is placed at high pressure, and in the other sec-

tion, called the test section, another gas is placed at low pressure. If the diaphragm is suddenly removed, the high pressure gas acts like a piston pushing down into the low pressure section. A shock wave precedes the high pressure gas into the low pressure section, causing compression and heating of the low pressure gas. At the same time, the expansion of the high pressure gas is accomplished by a rarefaction wave propagating back into the high pressure section, and the high pressure gas is cooled. These flow phenomena can best be illustrated on a diagram in which distance is plotted on the abscissa and time is plotted on the ordinate. Such a diagram is presented in Figure 1 along with ideal pressure and temperature profiles. It may be observed from the temperature profile that, at any point in the low pressure section, when the shock wave passes, there is local heating, and when the gas interface passes, there is local cooling. If the pressure ratio across the diaphragm is high enough, the temperature may rise several thousands of degrees behind the shock wave and, after a time interval, which may be of the order of less than one millisecond, the temperature may fall to as low a value as ten or twenty degrees absolute. It would seem, therefore, that the shock tube would be an ideal instrument for the study of rapid chemical reactions which must be initiated by high temperatures. Since it can achieve higher temperatures for a shorter period of time than can be obtained when gas mixtures are sent at a high rate of speed through a bed of heated pebbles, and since it can quench the gas mixture rapidly to extremely low temperatures, it could supersede this method

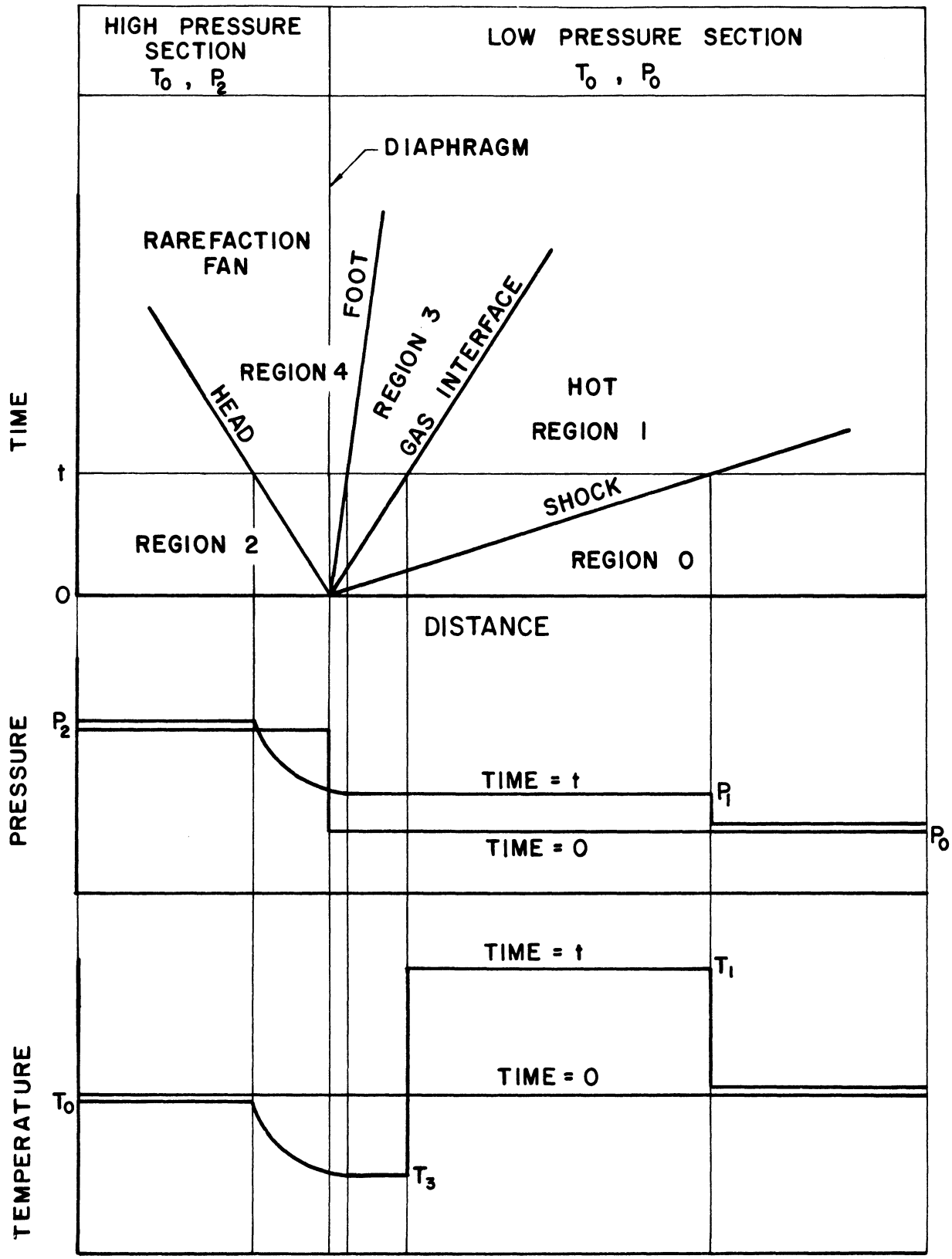

Figure (1) Wave Diagram with Temperature and Pressure Profiles

of studying such chemical reactions as hydrocarbon cracking, which require very rapid intense heating and quenching. Indeed, this is exactly the study performed in this research.

Before the study of the rate of chemical reactions in the shock tube can be begun, we must develop the various characteristics of a chemical system, such as temperature and residence time at high temperature for any particular particle of gas, in terms of the various shock flow parameters. This will be taken up in the rest of this section.

C. Pressure Rise Across a Shock Wave

It may be seen from the pressure profile in Figure 1, that the pressure in the reaction zone, marked region 1, is exactly the pressure behind the shock wave. Since it is prohibitively difficult to measure this pressure, it is desirable to find a relation for P_1 in terms of P_2, P_o, and other measurable quantities. Such an equation has been developed, and is known as the Taub Equation (122).

In order to derive this equation, some background must first be presented. We will first develop the equations for a perturbation in a compressible fluid. These equations can be developed by the method of similarities from the conservation of mass and conservation of momentum equations; as shown by Riemann (86).

$$\frac{\partial \rho}{\partial t} + \frac{\partial \rho u}{\partial x} = 0 \tag{8}$$

$$\rho \frac{\partial u}{\partial t} + \rho u \frac{\partial u}{\partial x} + C^2 \frac{\partial \rho}{\partial x} = 0 \tag{9}$$

Since $$C^2 = \frac{\partial P}{\partial \rho} \tag{10}$$

and $$P = k\rho^{\gamma} \tag{11}$$

for an adiabatic reversible flow, the conservation of mass and momentum equations can be manipulated to the form:

$$\frac{\gamma - 1}{2} C \frac{\partial u}{\partial x} + \frac{\partial C}{\partial t} + u \frac{\partial C}{\partial x} = 0 \tag{12}$$

$$\frac{\gamma - 1}{2} \left(\frac{\partial u}{\partial t} + u \frac{\partial u}{\partial x} \right) + C \frac{\partial C}{\partial x} = 0 \tag{13}$$

By similarity, we will assert that the perturbation is a function only of $x/t = \theta$.

So: $$\frac{\partial}{\partial x} = \frac{1}{t} \frac{\partial}{\partial \theta} \tag{14}$$

$$\frac{\partial}{\partial t} = \frac{-\theta}{t} \frac{\partial}{\partial \theta} \tag{15}$$

Substituting and multiplying through by t,

$$\frac{\gamma - 1}{2} C \frac{\partial u}{\partial \theta} - \theta \frac{\partial C}{\partial \theta} + u \frac{\partial C}{\partial \theta} = 0 \tag{16}$$

$$\frac{\gamma - 1}{2} \left(-\theta \frac{\partial u}{\partial \theta} + u \frac{\partial u}{\partial \theta} \right) + C \frac{\partial C}{\partial \theta} = 0 \tag{17}$$

thus indicating that the distribution is indeed a function only of θ, and not of x and t individually. Solving,

$$(u - \theta)^2 - C^2 = 0 \tag{18}$$

or, $\theta = u \pm C$ (19)

If the boundary condition, at $\theta = C_o$, $u = 0$, (since the fluid in front of the perturbation is at rest) is taken into account, further manipulation and integration of equations (16) and (17) together with the solution $\theta = u + C$, yields

$$u = \frac{2}{\gamma + 1} (\theta - C_o) \tag{20}$$

$$C = \frac{\gamma - 1}{\gamma + 1} \theta + \frac{2}{\gamma + 1} C_o \tag{21}$$

In the case of the rarefaction wave on Figure 1, u and θ are both negative, so

$$u = \frac{2}{\gamma + 1} (\theta + C_2) \tag{22}$$

$$C = - \frac{\gamma - 1}{\gamma + 1} \theta + \frac{2}{\gamma + 1} C_2 \tag{23}$$

since in this case, Region 2 is the region into which the disturbance is propagating. These equations hold at the foot of the rarefaction on the boundary of region 2, so they may be used to help derive the relation of P_2 to P_1.

These equations, along with equation (2), (3), (5), and the definition of the velocity of sound

$$C_o^2 = \frac{\gamma P_o}{\rho_o} \tag{24}$$

can be manipulated by a method described in Glass and Hall (39) as well as

in (122) into the final form of the Taub Equation:

$$\frac{P_2}{P_o} = \frac{P_1}{P_o}\left(1 - \frac{\beta_o - 1}{\beta_2 - 1}\,\frac{1}{\sqrt{\beta_o + 1}}\,\frac{C_o}{C_2}\sqrt{\frac{\frac{P_1}{P_o} - 1}{1 + \beta_o \frac{P_1}{P_o}}}\right)^{-(\beta_2 + 1)} \tag{25}$$

Curves for several representative gas combinations are shown in Figure 2. Further details of this derivation are given in Appendix IB.

D. Temperature Rise Across a Shock Wave

If we combine equation (4) with equations (6) and (7) and express the result in terms of v, γ, and C, since

$$C^2 = \frac{\gamma P}{\rho} \tag{24a}$$

and $$\gamma = \frac{C_p}{C_p - R}$$

we would obtain

$$v_o^2 + \frac{2}{\gamma - 1}\,C_o^2 = v_1^2 + \frac{2}{\gamma - 1}\,C_1^2 \tag{26}$$

We can eliminate v_1^2 by the equation

$$v_1^2 = \frac{C_o^2}{\beta_o + 1}\,\frac{\left(\frac{P_1}{P_o} + \beta_o\right)^2}{\beta_o \frac{P_1}{P_o} + 1} \tag{27}$$

(see Appendix IB)

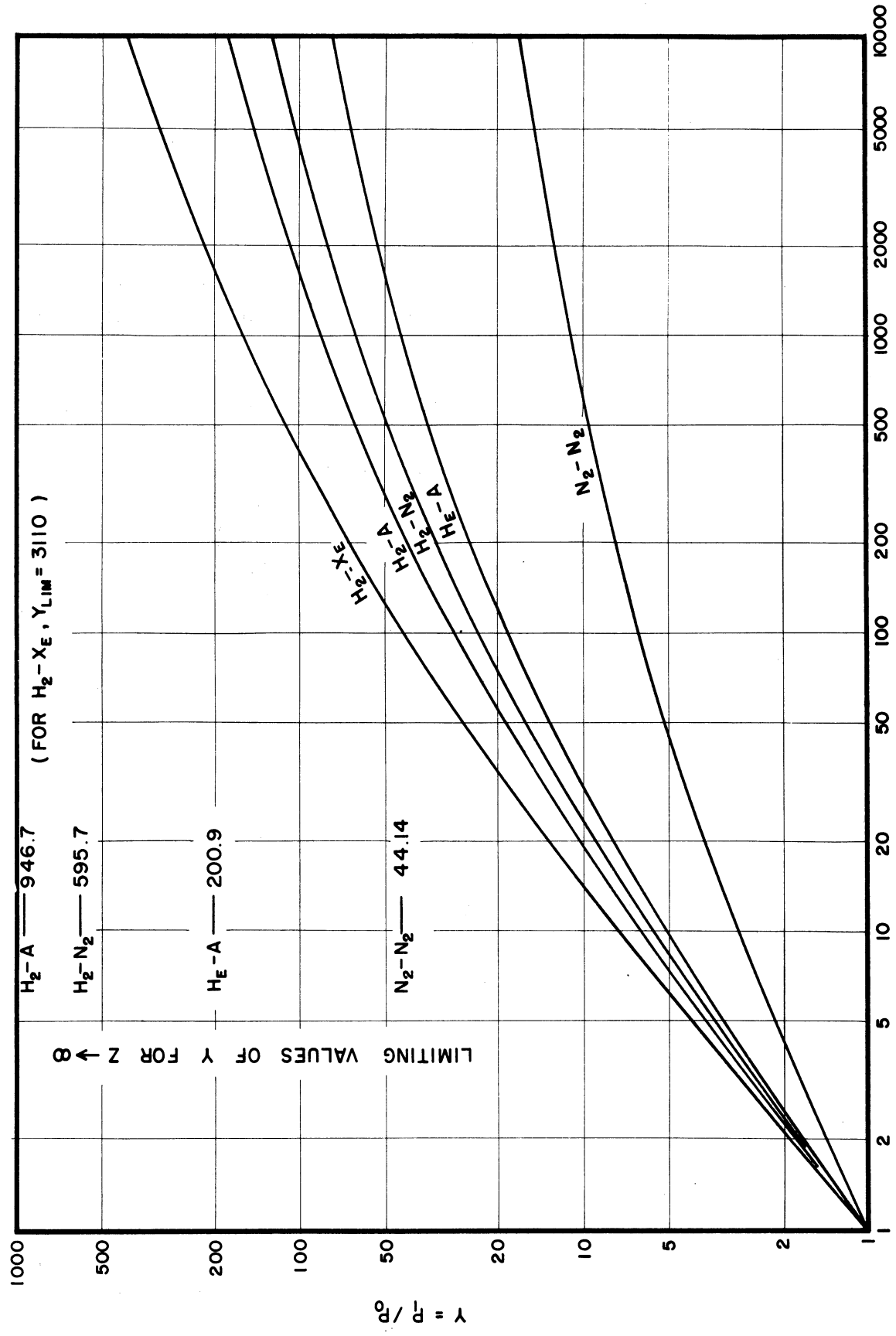

Figure (2) Classical Taub Equation Curves for Some Representative Gases

and then eliminate $\frac{P_1}{P_o}$ by the equation

$$v_o^2 = \frac{C_o^2}{\beta_o + 1} \left(\beta_o \frac{P_1}{P_o} + 1\right) \tag{28}$$

(see Appendix IB)

and rearrange, solving for $\frac{C_1^2}{C_o^2}$ in terms of γ and $M = \frac{v_o}{C_o}$. Since v_o is actually the wave velocity in the laboratory coordinate system, and M is the Mach Number, a dimensionless velocity, we would obtain

$$\frac{C_1^2}{C_o^2} = 1 + \frac{\gamma_o - 1}{2} \left(M^2 - \left(\frac{M + (\beta_o - 1)\frac{1}{M}}{\beta_o} \right)^2 \right) \tag{29}$$

Since $$C^2 = \frac{\gamma P}{\rho} = \gamma \frac{RT}{m} \tag{30}$$

$$\frac{C_1^2}{C_o^2} = \frac{T_1}{T_o} = 1 + \frac{\gamma_o - 1}{2} \left(M^2 - \left(\frac{M + (\beta_o - 1)\frac{1}{M}}{\beta_o} \right)^2 \right) \tag{31}$$

which is exactly the equation we are seeking. This equation is illustrated in Figure 3.

E. Gas Residence Time in the Reaction Zone

Before this term can be calculated, a few words must be said about the physical properties of the shock tube used in this work. Since the shock tube is sealed at both ends, a shock wave traveling down the tube would strike the downstream end and reflect with considerable reinforcement and heating. For the study of a chemical reaction, it is neces-

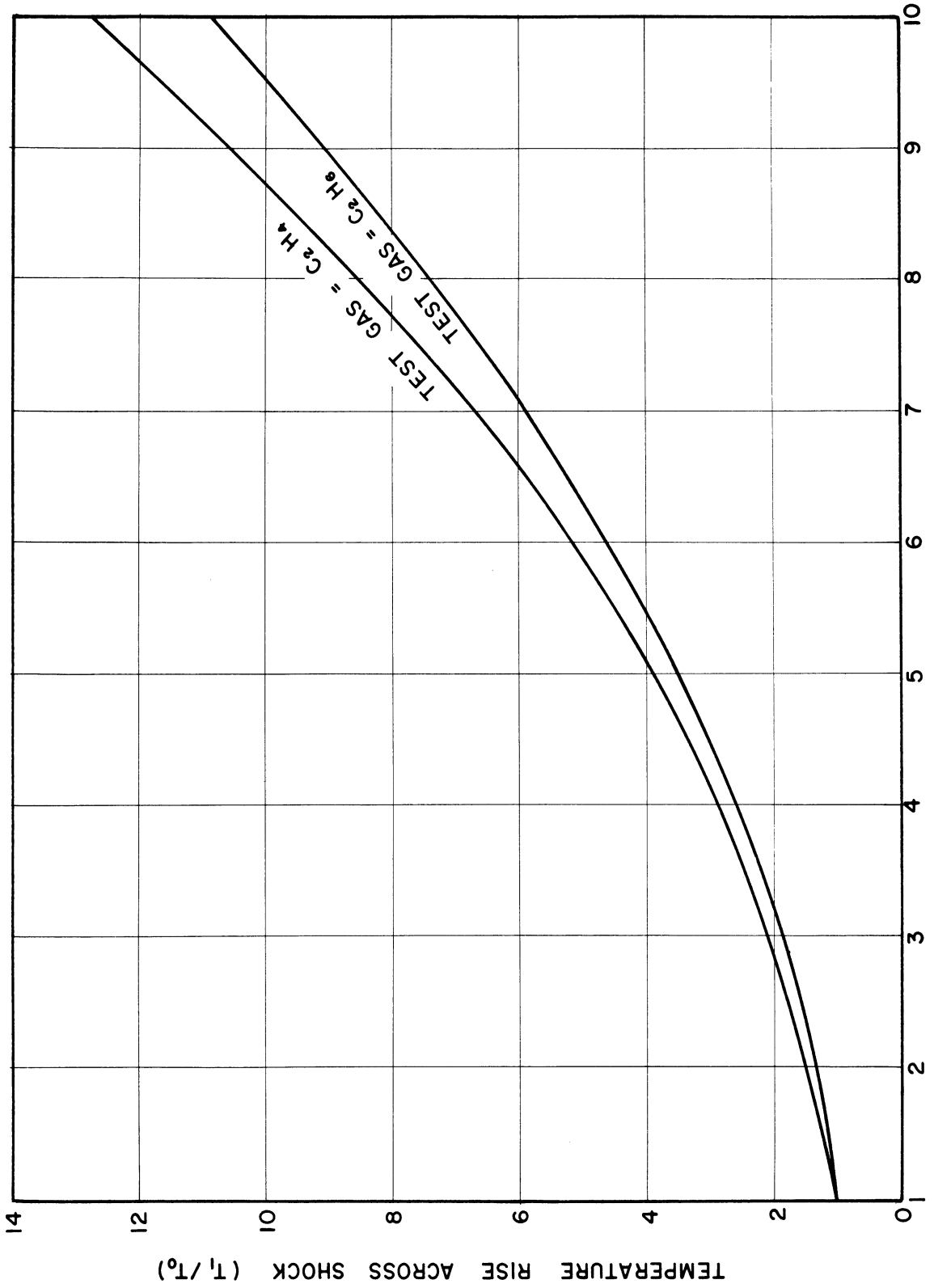

Figure (3) Temperature Rise Across Shock

sary that only a single reaction period occurs, or the results would be impossible to sort out. For this reason, many methods have been introduced to make sure that only a single reaction period occurs. For example, Gluckstein (45) uses a dump tank at the downstream end of the tube, Glick et al (42, 43, 44) uses a dump tank at the upstream end to generate a rarefaction which will quench the shock wave before it can reflect. Greene et al (47), however, does not prevent the reflected shock from occurring but, rather, uses the reaction period created by the reflected shock and eliminates that of the incident shock by making sure that the incident shock is so weak that, for all intents and purposes, no reaction occurs when the incident shock passes.

In this work, a somewhat different approach was used. If the high pressure section of the shock tube is short enough, the rarefaction wave propagating upstream will reflect from the upstream closed end and move downstream at a velocity high enough to catch the shock wave before it gets to the end of the tube and thereby, quench it. This method can best be illustrated on an x-t plot similar to that used in Figure 1. Such a plot is shown on Figure 4. By this method, all the equipment necessary to quench the wave can be eliminated and, also, all the equations necessary for the calculation of a reflected shock wave can also be eliminated. It is possible that, after the shock-rarefaction interaction, a weak shock will still propagate forward and reflect with some local heating. However, the reactions studied are so temperature sensitive that, unless the local temperature

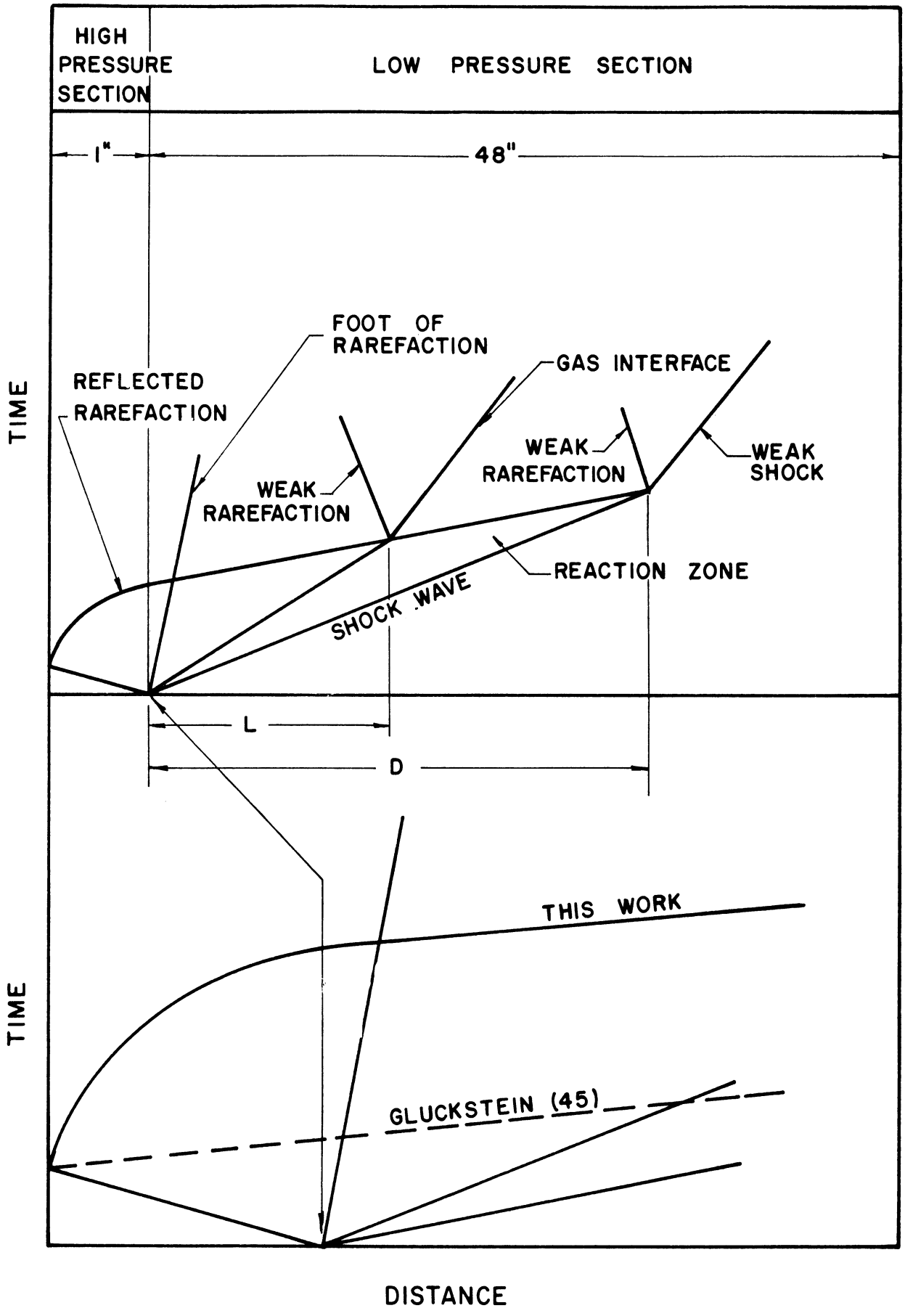

Figure (4) Wave Diagram for Interaction with Reflected Rarefaction

rises to a value very close to or greater than the value in the reaction zone, no marked effect on the reaction will be noted.

In calculating the flow conditions for the reflected rarefaction, some changes from the procedure used by Gluckstein (45) had to be made. After the rarefaction reflects from the upstream end of the tube, it passes through the rarefaction fan and is accelerated. Since the exact acceleration pattern is unknown, Gluckstein assumed that no acceleration occurs, and the rarefaction proceeds at its calculated velocity taking the pattern of the lowest line on the last part of Figure 4. However, when this pattern was assumed and the point of interaction was calculated, it was found to be much closer to the diaphragm than was observed through use of the pressure sensing devices mounted in the tube wall. It was noted that, although the pressure sensing devices recorded the passage of a shock wave, the usual calculation procedure indicated that no shock wave should be there. Therefore, this calculation procedure was rejected and another was substituted.

If it is assumed that the flow within the expansion fan is an ideal gas flowing horizontally with constant C_p and enthalpy equal to zero at $0^{\circ}R$, the conservation of energy equation may be written:

$$v^2 + A_2 T = A_1 \qquad (32)$$

(All A's are constants)

It is assumed that the temperature, T, is also related to the velocity, v, through another equation involving the change of thermal energy to kinetic

energy. Since it is known that an acceleration does occur, it is clear that this is not a relation of the same type as equation (32). Such a relation would lead to a constant value for v, which is exactly the functionality chosen by Gluckstein. For the purposes of this research, a functionality of the form

$$T = A_3 + A_4 v^2 + A_5 \frac{dv}{dt} \tag{33}$$

is assumed, implying a linear relationship between temperature and acceleration. In Gluckstein's work, $A_5 = 0$. Substituting equation (33) in equation (32) and rearranging,

$$A_6 + A_7 v^2 + A_8 \frac{dv}{dt} = 0 \tag{34}$$

In determining a distance-time relation for the rarefaction wave, it is seen that v is of the form x/t, where x is distance and t is time, so

$$A_9 + A_{10} \frac{x^2}{t^2} + A_{11} \frac{x}{t^2} = 0 \tag{35}$$

Multiplying through by t^2,

$$A_9 t^2 + A_{10} x^2 + A_{11} x = 0 \tag{36}$$

Completing the square and rearranging,

$$(x + A_{12})^2 + A_{13} t^2 = A_{14} \tag{37}$$

which is the equation of an ellipse on the x-t diagram. As a close approxi-

mation, it may be assumed that, rather than following an elliptical path through the rarefaction fan, the rarefaction follows a circular path on the x-t diagram. This is somewhat simpler to calculate and would lead to no appreciable error. This is represented by the highest line on the last part of Figure 4. As it turned out, interaction distances calculated using this functionality for rarefaction velocity within the rarefaction fan were very much in keeping with the experimental observations.

If the original shock Mach Number is large enough, the rarefaction will not catch up to the shock before it hits the end of the tube. In this case, a reflected shock wave will be formed accompanied by considerable heating. However, this reflected shock will be passing through a gas which has been considerably cooled below its initial temperature by the reflected rarefaction and, although the reflected shock will cause a temperature rise, the temperature will probably not rise to as high a value as the temperature in the reaction zone created by the incident shock and so, we will still have, in effect, a single reaction zone. This is borne out by the fact that reaction rates for the case where the rarefaction does catch up to the shock correlate quite well with those obtained for the case where the shock strikes the end of the tube before the reflected rarefaction can catch it.

In the shock tube used in this work, the high pressure section is one inch long, while the low pressure section is 48 inches long. This allows the rarefaction to catch up to the shock for a shock Mach Number

as high as seven or eight. For higher shock Mach Numbers, the shock will strike the end of the tube before the rarefaction can catch it. Most of the work conducted in this research was done at Mach Numbers less than eight. However, that work done at Mach Numbers greater than eight correlates extremely well with the rest, thus giving a strong indication that the analysis presented herein is valid.

The calculation of the distance, D, from the diaphragm site to the point of interaction of the shock wave with the reflected rarefaction is quite simple and straightforward. Since it would be convenient to express this distance in terms of the shock Mach Number, we will determine the shock strength $\frac{P_1}{P_o}$ as a function of the shock Mach Number. This can be done by slightly rearranging equation (28) to:

$$M^2 = \frac{v_o^2}{C_o^2} = \frac{1}{\beta_o + 1} \left(\beta_o \frac{P_1}{P_o} + 1\right) \tag{38}$$

or

$$\frac{P_1}{P_o} = \frac{(\beta_o + 1) M^2 - 1}{\beta_o} \tag{39}$$

A combination of this equation with the Taub Equation (25) and an equation found by eliminating θ between equations (22) and (23), yields the velocity of the particles of fluid behind the shock wave.

$$u = \frac{(\beta_o - 1)}{\beta_o} C_o \frac{M^2 - 1}{M} \tag{40}$$

(see Appendix IC)

It is interesting to note that this velocity turns out to be just a function of the properties of the low pressure gas and the shock Mach Number. Of course, it may be noted from the Taub Equation (25) that the shock Mach Number is very much a function of the properties of both fluids employed. In fact, the strongest shocks for any particular set of apparatus will be obtained if the high pressure gas has as low a molecular weight as is possible, hence the use of hydrogen, and the low pressure gas has as high a molecular weight as is possible. This is, of course, illustrated by Figure 2.

In order to determine the velocity of the rarefaction in the region after the rarefaction leaves the expansion fan, we must first find the sonic velocity in this region, marked Region 3 on Figure 1. This can be found by combining equation (25) with the condition expressing the definition of the disturbance velocity, equation (30) so that:

$$\left(\frac{C_3}{C_2}\right)^2 = \frac{T_3}{T_2} \tag{41}$$

If we combine equations (11) and (7), since the expansion region is taken as adiabatic with constant C_p and all process reversible,

$$\frac{T_3}{T_2} = \left(\frac{P_3}{P_2}\right)^{\frac{\gamma_2 - 1}{\gamma_2}} = \left(\frac{P_3}{P_2}\right)^{\frac{2}{\beta_2 + 1}} \tag{42}$$

Since $P_3 = P_1$, it is now obvious that

$$\left(\frac{C_3}{C_2}\right)^2 = \left(\frac{P_1/P_o}{P_2/P_o}\right)^{\frac{2}{\beta_2 + 1}} \tag{43}$$

Combining this equation with equation (25) yields

$$C_3 = C_2 \left(1 - \frac{\beta_o - 1}{(\beta_2 - 1)\beta_o} \frac{C_o}{C_2} \frac{M^2 - 1}{M}\right) \tag{44}$$

if we also take equation (39) into account. The rarefaction velocity is, then, the sum of equations (40) and (44).

If all distances on the x-t diagram are expressed in inches, the time interval between the time the diaphragm bursts and the time the reflected rarefaction reaches the site of the diaphragm, is equal to:

$$t_a = \sqrt{1 + \left(\frac{1}{C_2}\right)^2} \tag{45}$$

Then, the total time between the time the diaphragm bursts and the time the shock wave interacts with the rarefaction wave is:

$$t_i = \sqrt{1 + \left(\frac{1}{C_2}\right)^2} + \frac{D}{\frac{\beta_o - 1}{\beta_o} C_o \frac{M^2 - 1}{M} + C_2 \left(1 - \frac{\beta_o - 1}{\beta_o(\beta_2 - 1)} \frac{C_o}{C_2} \frac{M^2 - 1}{M}\right)} \tag{46}$$

where D is the distance between the diaphragm site and the interaction point, in inches. However, t_i also is equal to:

$$t_i = \frac{D}{C_o M} \tag{47}$$

Solving equations (46) and (47) for D, we obtain

$$D = \frac{\sqrt{1 + \left(\frac{1}{C_2}\right)^2}}{\frac{1}{C_o M} - \frac{1}{\frac{\beta_o - 1}{\beta_o} C_o \frac{M^2 - 1}{M} + C_2 \left(1 - \frac{\beta_o - 1}{(\beta_2 - 1)\beta_o} \frac{C_o}{C_2} \frac{M^2 - 1}{M}\right)}} \tag{48}$$

where D is expressed in inches. This equation is illustrated on Figure 5.

Similarly, we can find the distance between the diaphragm site and the point of interaction of the rarefaction wave with the gas interface, if it is recalled that the gas interface moves at the particle velocity, u:

$$L = \frac{\sqrt{1 + \left(\frac{1}{C_2}\right)^2}}{\frac{1}{\frac{(\beta_o - 1)}{\beta_o} C_o \frac{M^2 - 1}{M}} - \frac{1}{\frac{(\beta_o - 1)}{\beta_o} C_o \frac{M^2 - 1}{M} + C_2 \left(1 - \frac{\beta_o - 1}{(\beta_2 - 1)\beta_o} \frac{C_o}{C_2} \frac{M^2 - 1}{M}\right)}} \tag{49}$$

where L, this interaction distance is expressed in inches.

The gas particle which remains in the reaction zone longest is that which is originally at the diaphragm site when the diaphragm bursts. From Figure 7, it is obvious that this maximum residence time, τ_{max} is:

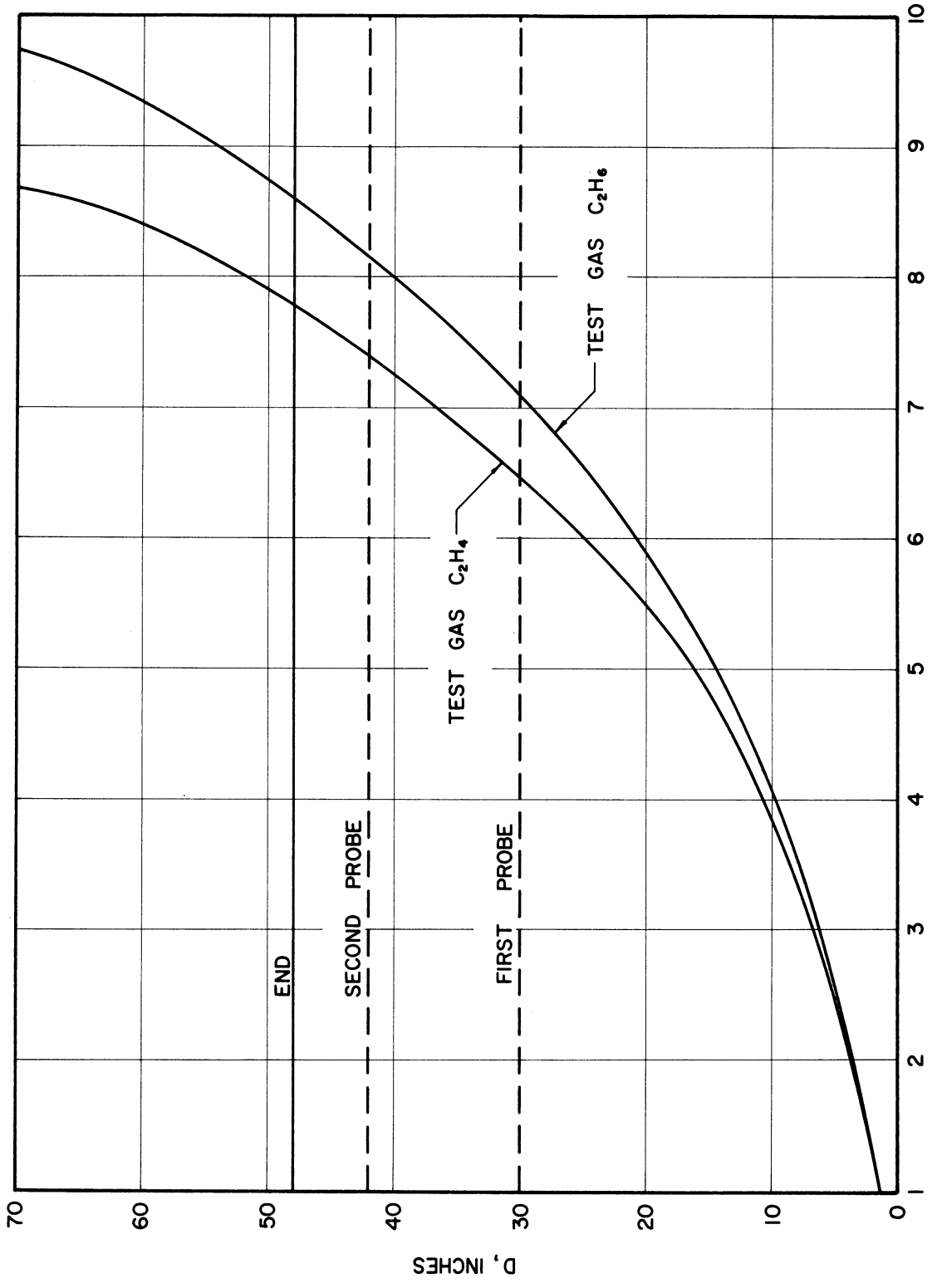

Figure (5) Distance Between Diaphragm Site and Interaction Point vs. Mach Number

$$\tau_{max} = \frac{L}{\left(\frac{\beta_o - 1}{\beta_o} C_o \frac{M^2 - 1}{M}\right)} \tag{50}$$

Curves for τ_{max} are presented on Figure 6.

Since the gas particles move according to Figure 7, it is also obvious that the residence time, τ , for a particle x inches from the diaphragm is equal to

$$\tau = \tau_{max}\left(1 - \frac{x}{D}\right) \tag{51}$$

provided x is smaller than D. If x is larger than D, $\tau = 0$.

F. Average Temperature In the Reaction Zone

During the course of the chemical reaction, the temperature will change because there is a finite heat of reaction. That is, the temperature of the mix will rise or fall (exclusive of compression effects) depending on whether the reaction gives off heat or absorbs heat during its course. We will now derive an expression for the average temperature in the reaction zone, taking this reaction heat into account.

If T_1 is the temperature at the beginning of the reaction, T_2 is this temperature plus the contribution due to heat of reaction, and T_{avg} is the average temperature during the course of the reaction, from the definitions of the rate constants (see ref. (58))

$$k_{1_{avg}} = Ae^{-\Delta E/RT_{avg}} \tag{52}$$

$$k_{1_1} = Ae^{-\Delta E/RT_1} \tag{53}$$

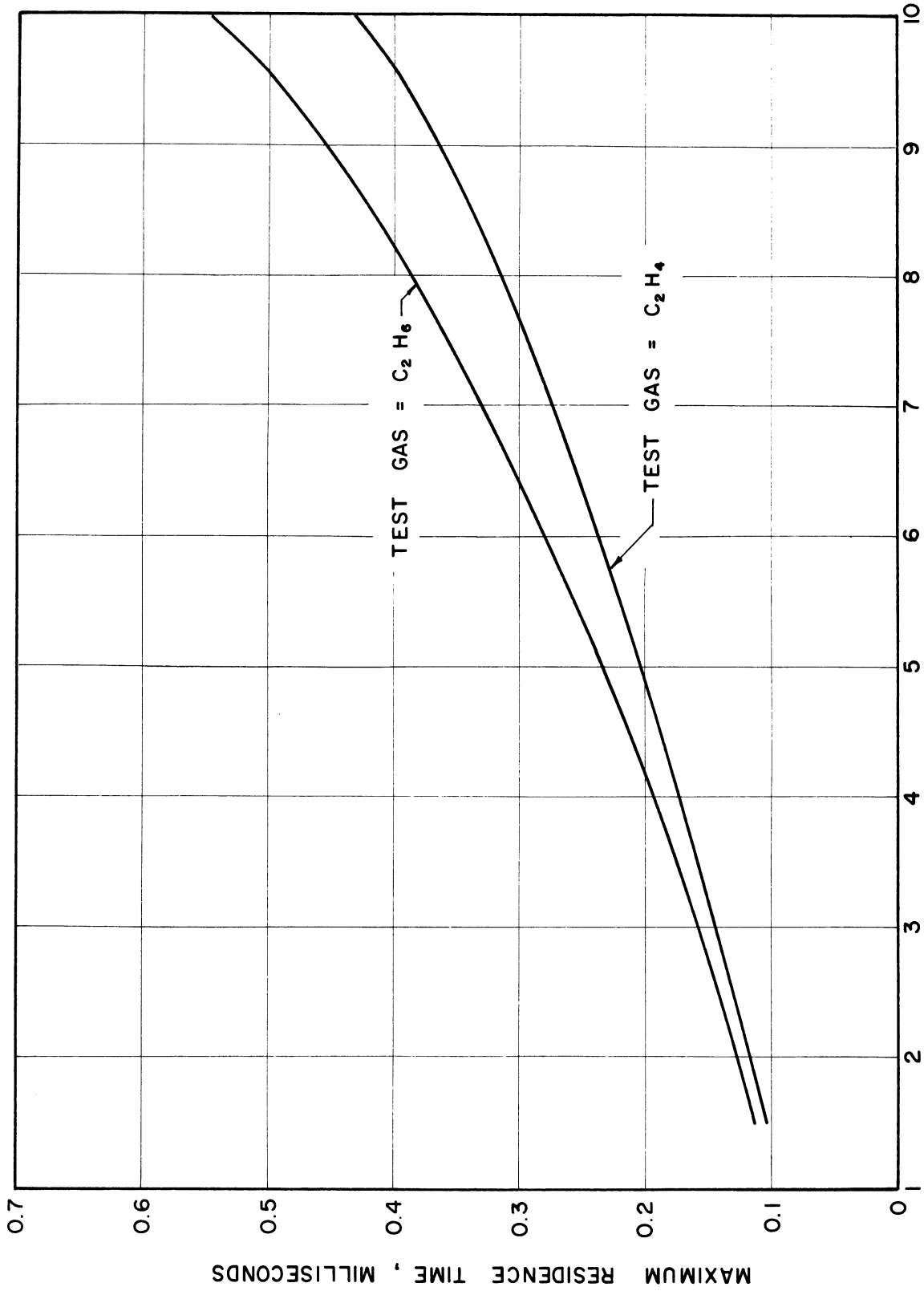

Figure (6) Maximum Residence Time as a Function of Mach Number

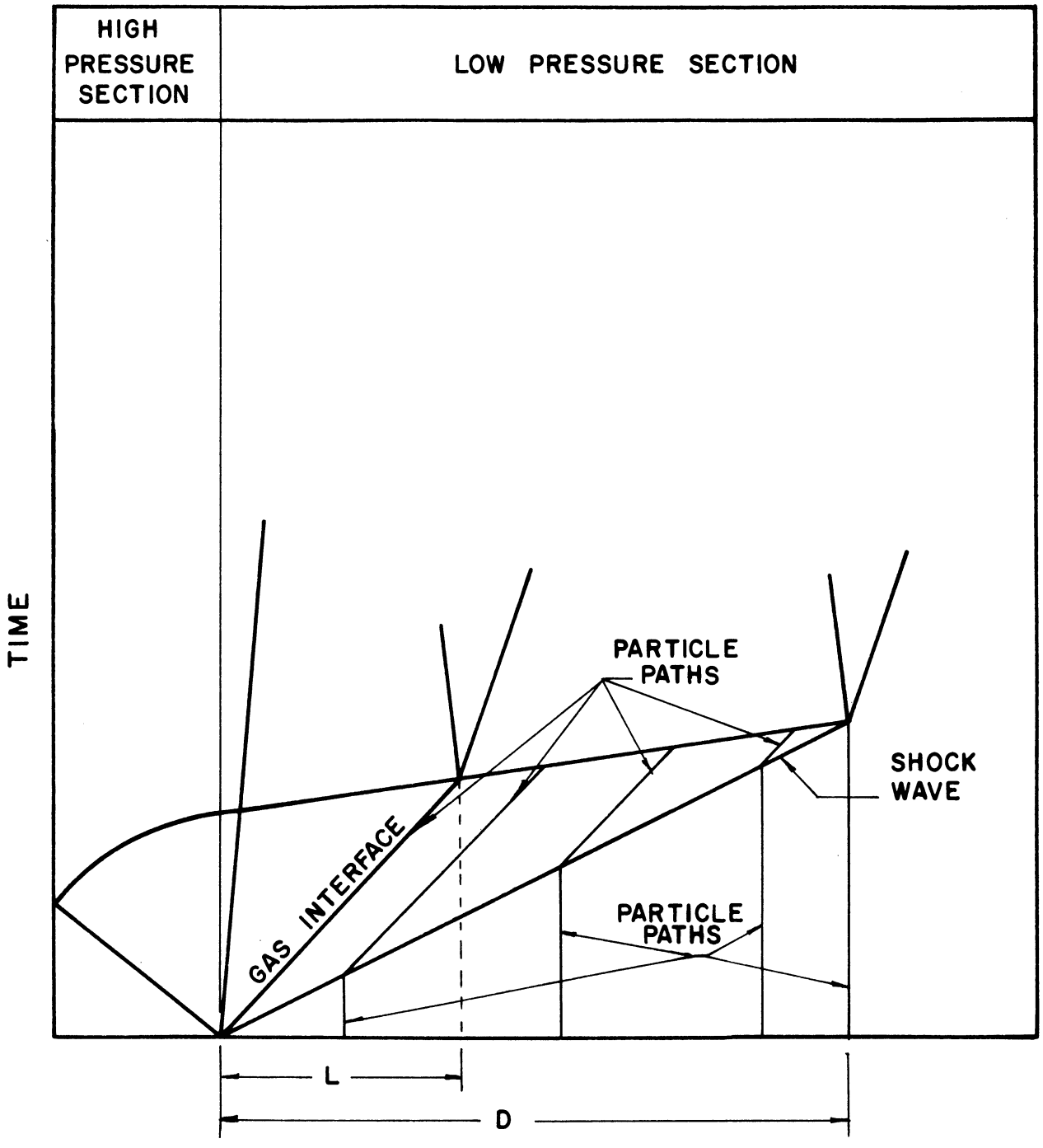

Figure (7) Particle Paths for Flow in Shock Tube

For a first order irreversible reaction,

$$\frac{dc}{dt} = k_1 (a-c) \tag{53}$$

$$\int_o^c \frac{dc}{k_1(a-c)} = \int_o^t dt \tag{54}$$

From the definition of k_1,

$$\int_o^c \frac{dc}{Ae^{-\Delta E/RT}(a-c)} = t \tag{55}$$

However, T may be defined from

$$T = T_1 + \left(\frac{\Delta H}{C_p}\right) c \tag{56}$$

so,
$$\int_o^c \frac{dc}{(a-c)\, Ae^{-\Delta E/R(T_1+(\frac{\Delta H}{C_p})c)}} = t \tag{57}$$

$k_{1_{avg}}$ can be defined by

$$k_{1_{avg}} = \frac{1}{t} \int_o^c \frac{dc}{(a-c)} \tag{58}$$

Combining equations (52), (57), (58) and simplifying (if ΔE is independent of c)

$$e^{\frac{1}{T_{avg}}} = \frac{\int_o^c e^{\frac{1}{T_1 + (\frac{\Delta H}{C_p})\, c}} \frac{dc}{(a-c)}}{\int_o^c \frac{dc}{(a-c)}} \tag{59}$$

Since there is only a very small temperature change during the course of the reaction (approximately 5%), T_{avg} can be taken as

$$\frac{1}{T_{avg}} = \frac{1}{2}\left(\frac{1}{T_1} + \frac{1}{T_2}\right) \tag{60}$$

since T_1 is the temperature at c = 0 (the lower limit) and T_2 is the temperature at c = c (the upper limit). (T_{avg} is also close to the arithmetic average of T_1 and T_2.)

In cases where the interaction of the rarefaction and the shock occurs close enough to the diaphragm so that we can detect the shock transmitted

mitted by the interaction, we can determine an average temperature for the entire low pressure region on a basis similar to that just used for determining what may be called the chemical average temperature, as contrasted to the interaction average temperature. We will now calculate this interaction average temperature.

Since the pressure sensing devices detect and measure the velocity of the shock caused by the shock-rarefaction interaction, we must first determine the velocity, and hence the temperature associated with the shock originating at the ruptured diaphragm. This can easily be done by a combination of equations (25) and (39) to give the shock Mach Number as a function of $\frac{P_2}{P_o}$ and the fluid properties. Of course, this equation would give the maximum Mach Number associated with the ideal case. In order to get a good estimate of the actual Mach Number, 10% can be subtracted from this maximum value as a fair estimate. (Fortunately, this procedure had to be invoked at only a very few points. At these points, however, the results turned out to be quite satisfactory).

If it is asserted that the average reaction rate constant is an average of the constants for the two parts, and since the interaction occurs D inches from the diaphragm, with the total length of the low pressure section being 48 inches,

$$Ae^{-\Delta E/RT_1} = \frac{D}{48}\left(Ae^{-\Delta E/RT_a}\right) + \frac{48 - D}{48}\left(Ae^{-\Delta E/RT_b}\right) \qquad (61)$$

Again expanding the exponential and dropping all but the first two

As a first approximation, equation (61) simplifies to:

$$\frac{1}{T_1} = \frac{D}{48}\left(\frac{1}{T_a}\right) + \frac{48 - D}{48}\left(\frac{1}{T_b}\right) \tag{62}$$

where T_a is the temperature of the hot zone created by the original shock and T_b is the temperature of the hot zone created by the shock which is produced by the shock-rarefaction interaction. T_1 is exactly the same T_1 used in equation (59) to determine the chemical average temperature.

G. Chemical Kinetic Equations

Since the reactions of interest in this work are the reactions

$$C_2H_6 \rightleftharpoons C_2H_4 + H_2 \quad \text{and}$$

$$C_2H_4 \rightleftharpoons C_2H_2 + H_2$$

both of the same form, we will develop chemical kinetic equations for the general reaction $E \rightleftharpoons F + G$. Some of the quantities necessary for calculation are:

$$E \underset{k_1'}{\overset{k_1}{\rightleftharpoons}} F + G$$

	E	F	G
moles at time = o	a	b	0
moles at time = t	a-c	b+c	c

k_1 is the rate constant of the forward reaction, while k_1' is the rate constant of the reverse reaction. The differential equation for the formation of B is:

$$\frac{dc}{dt} = k_1 (a - c) - k_1' (b + c)(c) \tag{63}$$

or, $$\frac{dc}{dt} = k_1 \left((a - c) - \frac{(b + c)(c)}{K_p} \right) \tag{64}$$

where $$K_p = \frac{k_1}{k_1'} \tag{65}$$

Since at equilibrium, $\frac{dc}{dt} = 0$, we have

$$o = k_1 \left((a - c_e) - \frac{(b + c_e)(c_e)}{K_p} \right) \tag{66}$$

and $$K_p = \frac{(b + c_e)(c_e)}{(a - c_e)} \tag{67}$$

so, $$\frac{dc}{dt} = k_1 \left((a - c) - \frac{(b + c)(c)}{(b + c_e)(c_e)} \quad (a - c_e) \right) \tag{68}$$

or, $$\frac{dc}{(a - c) - \frac{(b + c)(c)}{(b + c_e)(c_e)} \quad (a - c_e)} = k_1 \, dt \tag{69}$$

since at $t = 0$, $c = 0$, and at $t = t$, $c = c$, we can integrate between these limits

$$\int_o^c \frac{dc}{(a - c) - \frac{(b + c)(c)}{(b + c_e)(c_e)} \quad (a - c_e)} = k_1 \int_o^t dt \tag{70}$$

Integrating, we obtain:

$$k_1 t = \frac{b\,c_e + c_e^2}{ab + 2a\,c_e - c_e^2} \ln \left(\left(\frac{a(c_e + b) + c(a - c_e)}{a(c_e - c)} \right) \left(\frac{c_e}{c_e + b} \right) \right) \tag{71}$$

Define:

$$A = \frac{b\,c_e + c_e^2}{ab + 2a\,c_e - c_e^2} \tag{72}$$

$$B = a\,c_e \tag{73}$$

$$E = \frac{(a - c_e)(c_e)}{ce + b} \tag{74}$$

equation (65) becomes

$$k_1 t = A \ln \frac{B + Ec}{B - ac} \tag{75}$$

or, in a more convenient form (assuming Ec is much smaller than B)

$$c = \frac{B}{a}\left(1 - e^{-\frac{k_1 t}{A}}\right) \tag{76}$$

However, t is exactly τ as defined by equation (51) so

$$c = \frac{B}{a}\left(1 - e^{-\frac{k_1}{A}\left(\tau_{max}\left(1 - \frac{x}{D}\right)\right)}\right) \tag{77}$$

Now, define c_{avg} as

$$c_{avg} = \frac{1}{D}\int_o^D c\,(x)\,dx \tag{78}$$

so,
$$c_{avg} = \frac{B}{aD}\int_o^D \left(1 - e^{-\frac{k_1 \tau_{max}}{A}\left(1 - \frac{x}{D}\right)}\right)dx \tag{79}$$

or,
$$\frac{\frac{B}{a} - c_{avg}}{\frac{B}{a}} = \frac{A}{k_1 \tau_{max}}\left(1 - e^{-\frac{k_1 \tau_{max}}{A}}\right) \tag{80}$$

For the case where K_P is much greater than $\frac{(b + c)(c)}{(a - c)}$, so that c_e approaches a,

$$A \longrightarrow 1$$

$$B \longrightarrow a^2$$

$$E \longrightarrow 0$$

and equation (80) simplifies to

$$\frac{a - c_{avg}}{a} = \frac{1}{k_1 \tau_{max}} \left(1 - e^{-k_1 \tau_{max}}\right) \tag{81}$$

Since τ_{max} is known as a function of temperature, and also a and c_{avg} (since the products of the reaction for any particular Mach Number and, hence, any temperature can be determined) the first order rate constant for the forward reaction, k_1, as a function of temperature is known.

Now, the rate expressions for the case of the simultaneous decompositions will be derived:

$$E \underset{k'_1}{\overset{k_1}{\rightleftharpoons}} F + G$$

$$F \underset{k'_2}{\overset{k_2}{\rightleftharpoons}} J + G$$

A set of equations like these two would occur in the case where ethane decomposes to ethylene and hydrogen, and ethylene in turn decomposes into acetylene and hydrogen. If at time = 0, we have a moles of E, b moles of F, and none of the others, at time = t, we would have a - x moles of E, b + x - y moles of F, y moles of J, and x + y moles of G. If

the reverse reaction is neglected, the differential equations can be set up as follows:

$$\frac{dx}{dt} = k_1 (a - x) - k_2 (b + x - y) \tag{82}$$

$$\frac{dy}{dt} = k_2 (b + x - y) \tag{83}$$

Integrating, as in equation (70), setting $t = \tau_{max} (1 - \frac{x}{D})$ as in equation (77) and reintegrating as in equation (79),

$$\frac{b + x - y}{b + x} = \frac{1}{k_2 \tau_{max}} (1 - e^{-k_2 \tau_{max}}) \tag{84}$$

$$\frac{k_1 a - k_2 (b - y) - (k_1 + k_2) x}{k_1 a - k_2 (b-y)} = \frac{1}{(k_1 + k_2) \tau_{max}} (1 - e^{-(k_1 + k_2) \tau_{max}}) \tag{85}$$

where x and y are the mixed average values of the concentrations involved.

III - DESCRIPTION OF APPARATUS

A. General Remarks

The shock tube used in this research was essentially the same one used by Gluckstein (45). Several modifications will be described in detail in later parts of this section. The equipment consisted of the shock tube itself, related equipment for the mixing, introduction, and sampling of gas specimens, instruments for recording the pressure and temperature of the gas before the diaphragm was burst, electronic equipment for measuring the wave velocity, and means of determining the chemical composition of the gas samples taken. Figures 8 and 9 are photographs of the shock tube. These photographs show all the equipment used with the exception of the mass spectrometer used to analyze the gas samples. The labelled pieces of apparatus include:

A - Safety shield

B - Loading console

C - Manometer for determining pressure in test section

D - Reactant sample bulb

E - Driver gas

F - Pure hydrocarbon reactant gas

G - Mixing tank for introduction of mixed reactants

H - 3000 psi pressure gauge

I - 20, 000 psi pressure gauge

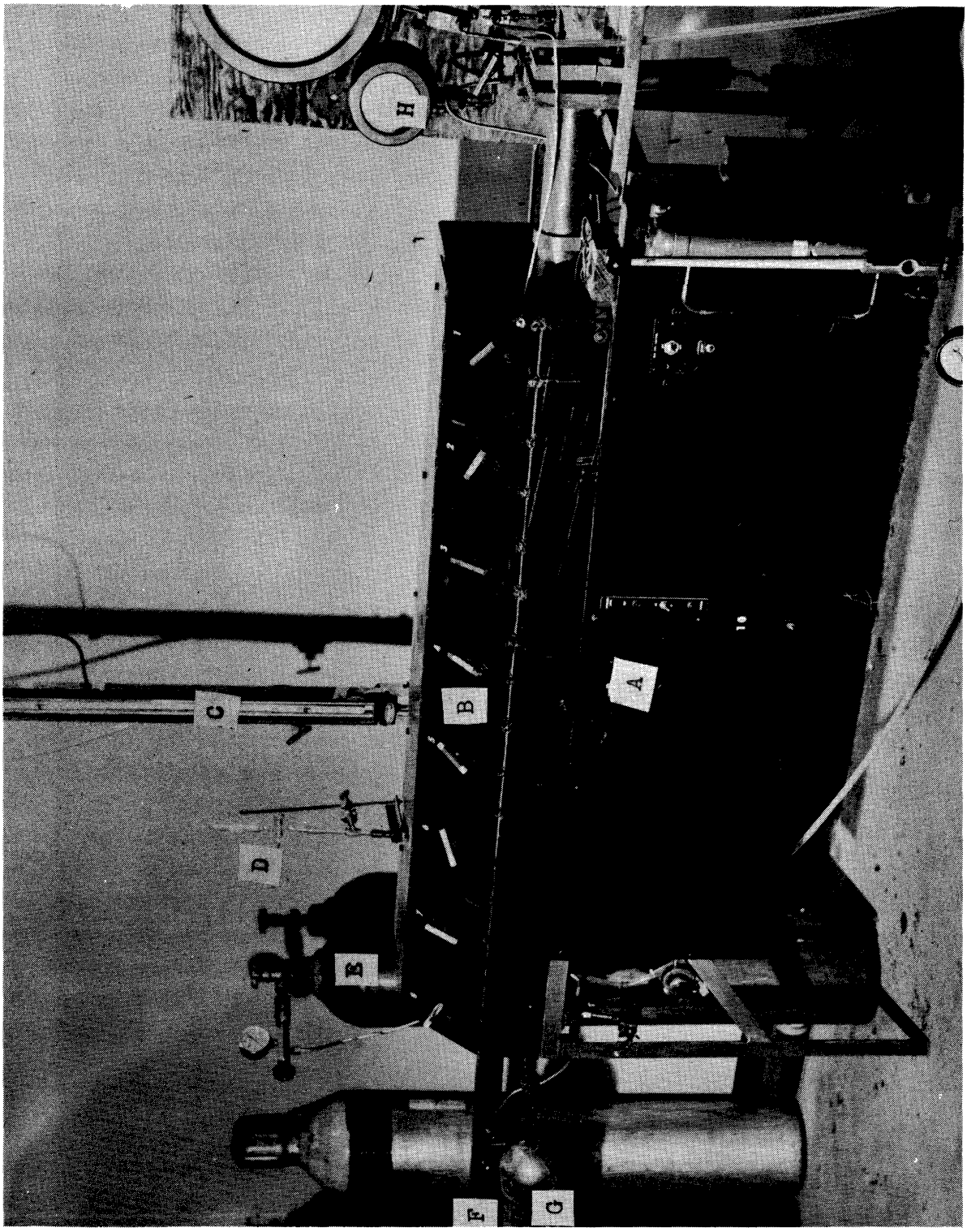

Figure (8) Loading Side of Shock Tube

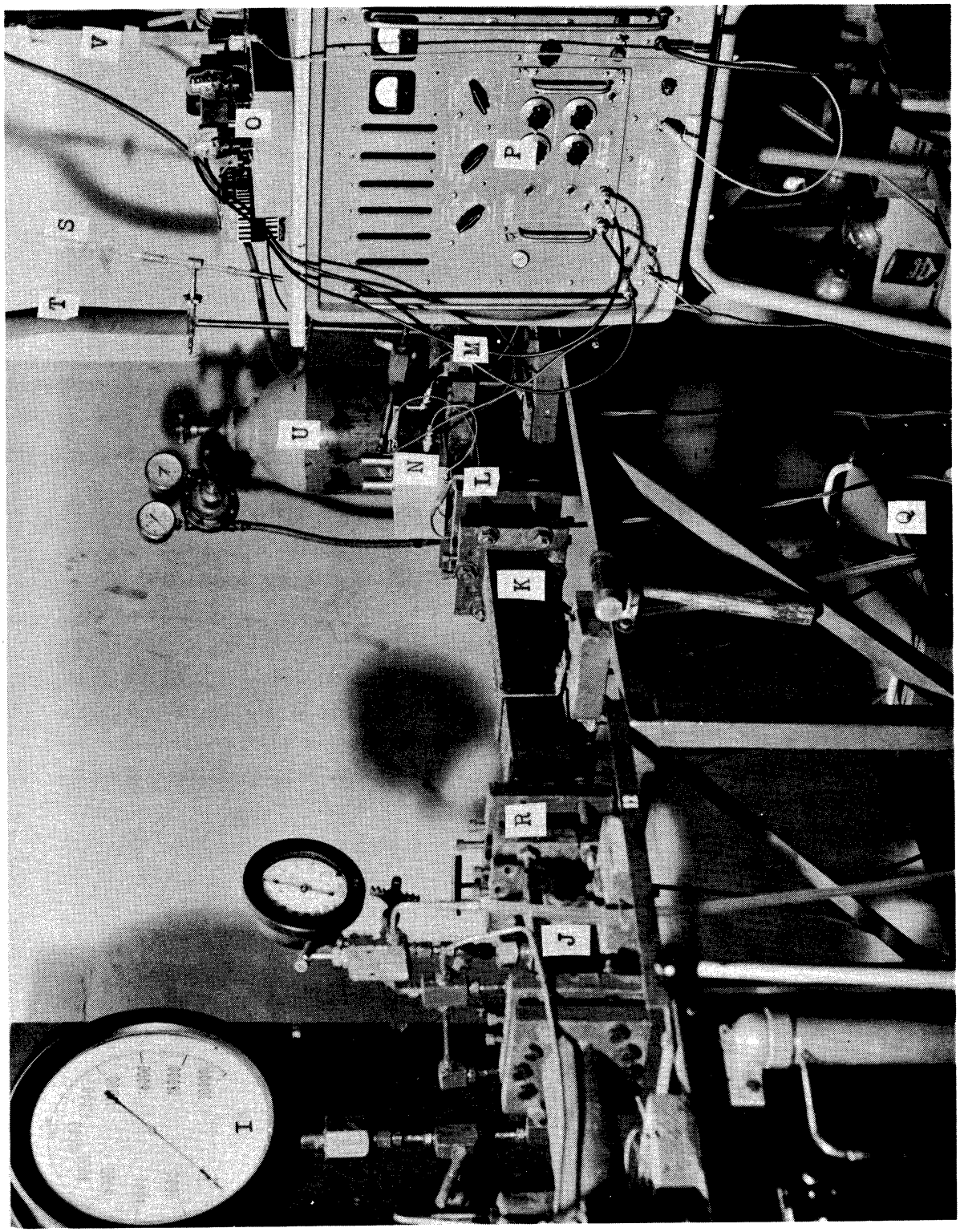

Figure (9) Test Side of Shock Tube

J - High pressure (driver) section

K - Low pressure (test) section

L - First velocity probe

M - Second velocity probe

N - Transducer signal amplifier

O - Thyratron circuitry

P - Electronic timer

Q - Power supply

R - Diaphragm mount

S - Product sample bulb

T - Exhaust for spent driver gas

U - Nitrogen for flushing exhaust tube

V - Manometer for measuring pressure in product sample bulb

Not Pictured - Vacuum pump, end plate on test section

B. Construction of the Shock Tube

Since the construction of the shock tube was described in Gluckstein (45), only a few pertinent observations will be made, and much of the detail will be neglected. The shock tube itself consists of a low pressure (test) section whose dimensions are 1/2" x 1/2" x 4'. At the downstream end of the test section, a one inch thick plate has been placed through which samples may be drawn through a small hole. At the upstream end of the test section is the high pressure (reservoir) section, separated from the test section by a diaphragm. This reservoir section has internal dimensions

of 1/2" x 1/2" x 1". It was originally constructed with an internal length variable from 12" on up. However, a fixed plug was inserted to shorten its length to one inch, and thus take advantage of the chance to use a rarefaction wave reflecting from the upstream wall of the reservoir section to quench the shock wave, and thus eliminate the need for a quench section, as used in Gluckstein (45).

The entire test section and reservoir were designed to withstand static pressure in excess of 100, 000 psi. As an added measure of safety, all valves, fittings, and connecting tubing for the test section, reservoir, high pressure storage vessels, and mixing console were of the superpressure type distributed by either Autoclave Engineers of Erie, Pennsylvania, or American Instrument Company of Silver Spring, Maryland. Sections of the equipment which operated between atmospheric pressure and 1000 psi were fabricated with commercial valves rated at 4000 psi working pressure or better, Ermeto fittings, and stainless steel or mild steel tubing of similar specifications.

All joints between adjacent sections or on removable components (i.e., velocity probes) were sealed by means of "O" rings or specially designed gaskets.

Calibrated Bourdon tube gauges were used to measure all positive pressures in excess of 30 psia and U-tube manometers were used for pressures below 30 psia.

The choice of the square cross section for the tube was caused

by a desire to increase its versatility and to permit the possible use of optical techniques in the determination of the wave properties. However, these techniques were not used. The entire tube was constructed of mild steel and the use of this material necessitated periodic dismantling and cleaning.

An overall schematic diagram of the shock tube and gas handling equipment is shown in Figure 10. The test section and reservoir were constructed by milling a 1/2" x 1/2" slot in a piece of 1-3/4" x 3" cold rolled steel. In addition, two 1/8" x 3/32" slots were milled on either side of the 1/2" x 1/2" slot to accommodate 1/8" round aluminum wire, which was used as a gasket for the test section, or 3/32" round neoprene wire (under tension), which was used as a gasket for the reservoir section. The upper covers of these "U" shaped channels were 1-1/4" x 3" cold rolled steel. The channels and cover plates were assembled by means of 3/8" - 24 NF Allen head screws located on 1" centers. Two dowel pins were located at the opposite ends of each section. After the initial assembly of the tops and bottoms of the sections, the ends were carefully machined square and finished. A diagram of the method of assembly of the test section is shown in Figure 11. The finishing consisted of machining "O" ring grooves, two in the test section faces, and one in the reservoir section face. The "O" ring groove details are shown in Figure 12. At the downstream end of the test section, a one-inch thick plate was placed with a 1/16" hole in its center to permit sampling of gases in the test section. Then the various sections were bolted together

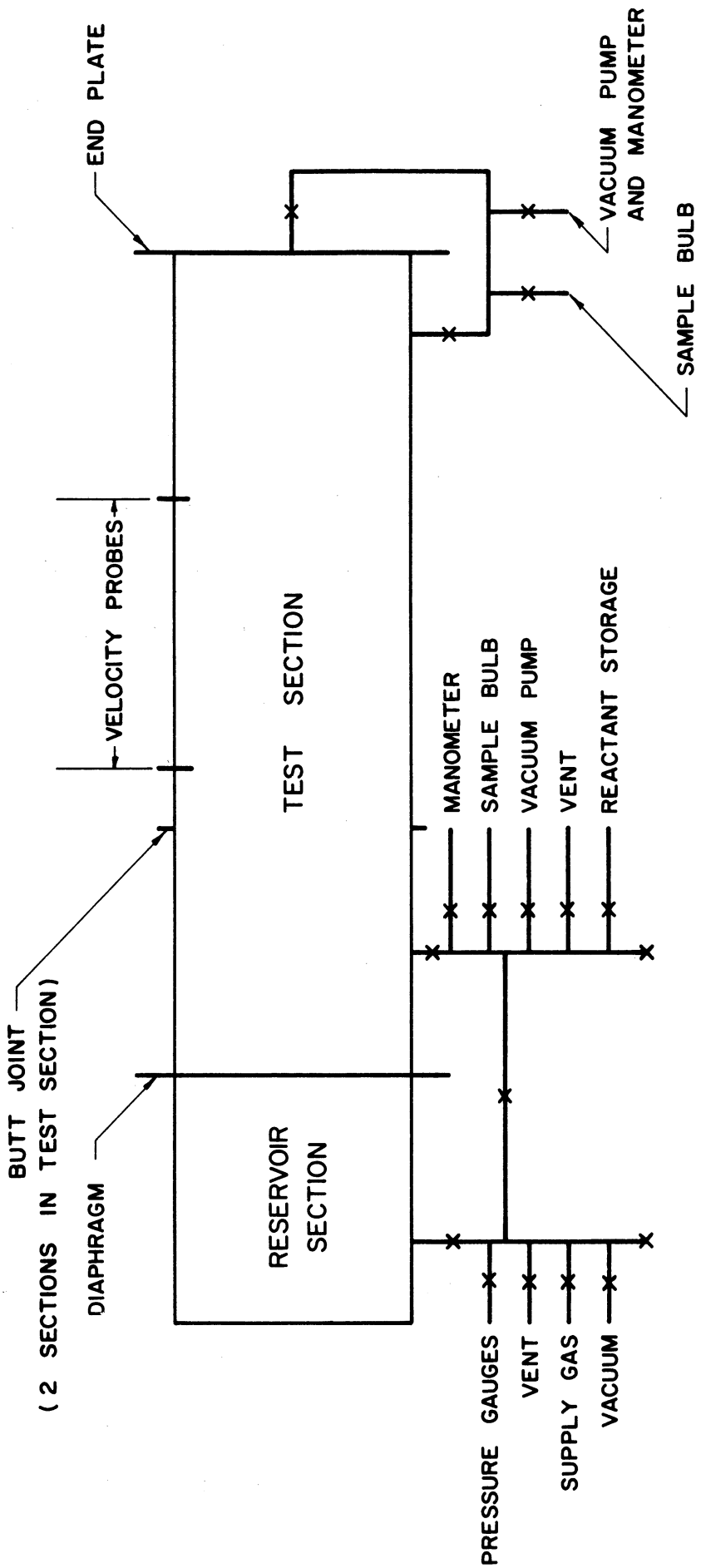

Figure (10) Diagram of the Shock Tube and Associated Lines

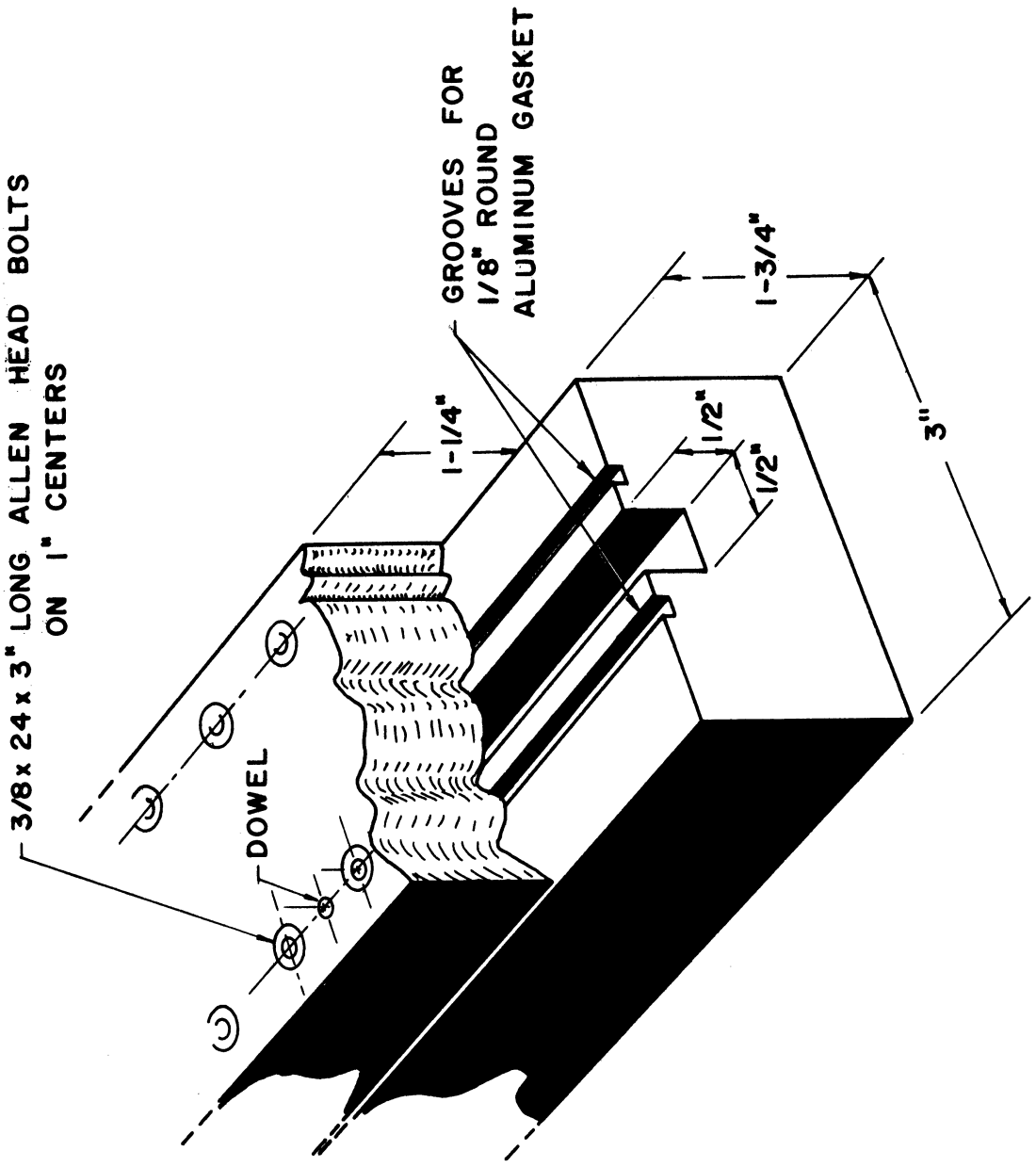

Figure (11). Method of Assembly of Test Section

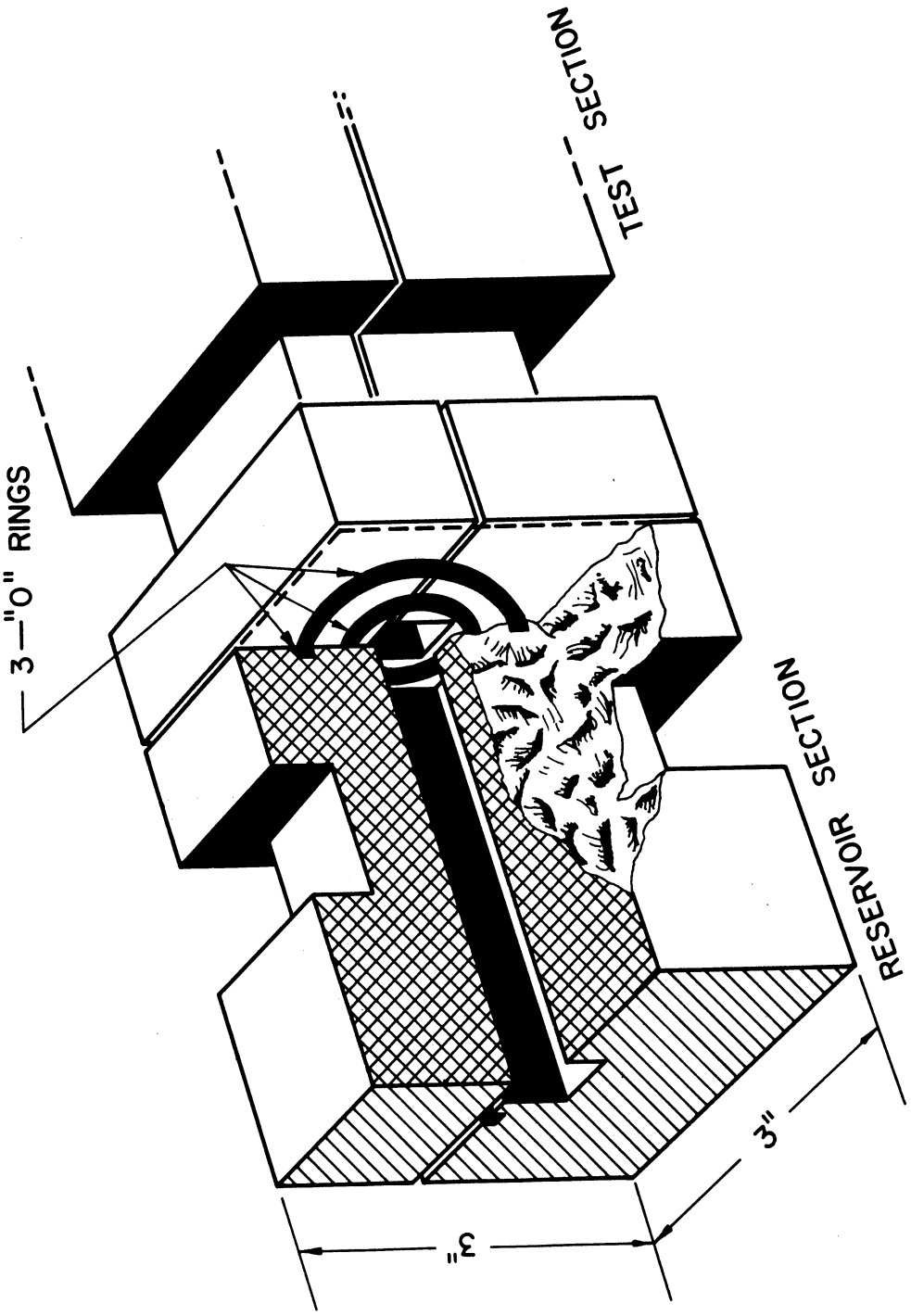

Figure (12) "O" Ring Groove Detail

by the use of flanges, a detail of which is shown in Figure 13.

Finally, the necessary openings for the gas lines and velocity probes were made and all face joinings on the split sections coated with a thin coat of Glyptal lacquer (General Electric Company) and air dried for 24 hours. The basic components were then assembled on an angle iron frame and connected. Alignment was achieved either by means of dowel pins or by passing a 1/2" x 1/2" x 6" square brass bar through the downstream end of the test section. When aligned, the sections were rigidly clamped to the frame, the plumbing system was installed, and a cover was made for the reservoir storage vessels and related lines. This cover served both as a safety shield and as a mounting plate for numerous valves.

The diaphragms separating the reservoir and test section were made of brass up to 0.010" thick. The thickness depended on the burst pressure desired. In all cases, the diaphragms were mechanically weakened by scoring diagonals across them. In this way, the center of the diaphragm, where the diagonals cross, became the weakest point and so, rupture could be insured with a minimum of flow eccentricity and disturbance.

Connections from the shock tube and its attendant piping to the sample bulbs and vacuum system were made by means of ground glass joints and short lengths of heavy wall, vacuum type tygon tubing. The sample bulbs themselves were simple glass test tubes, sealed at the

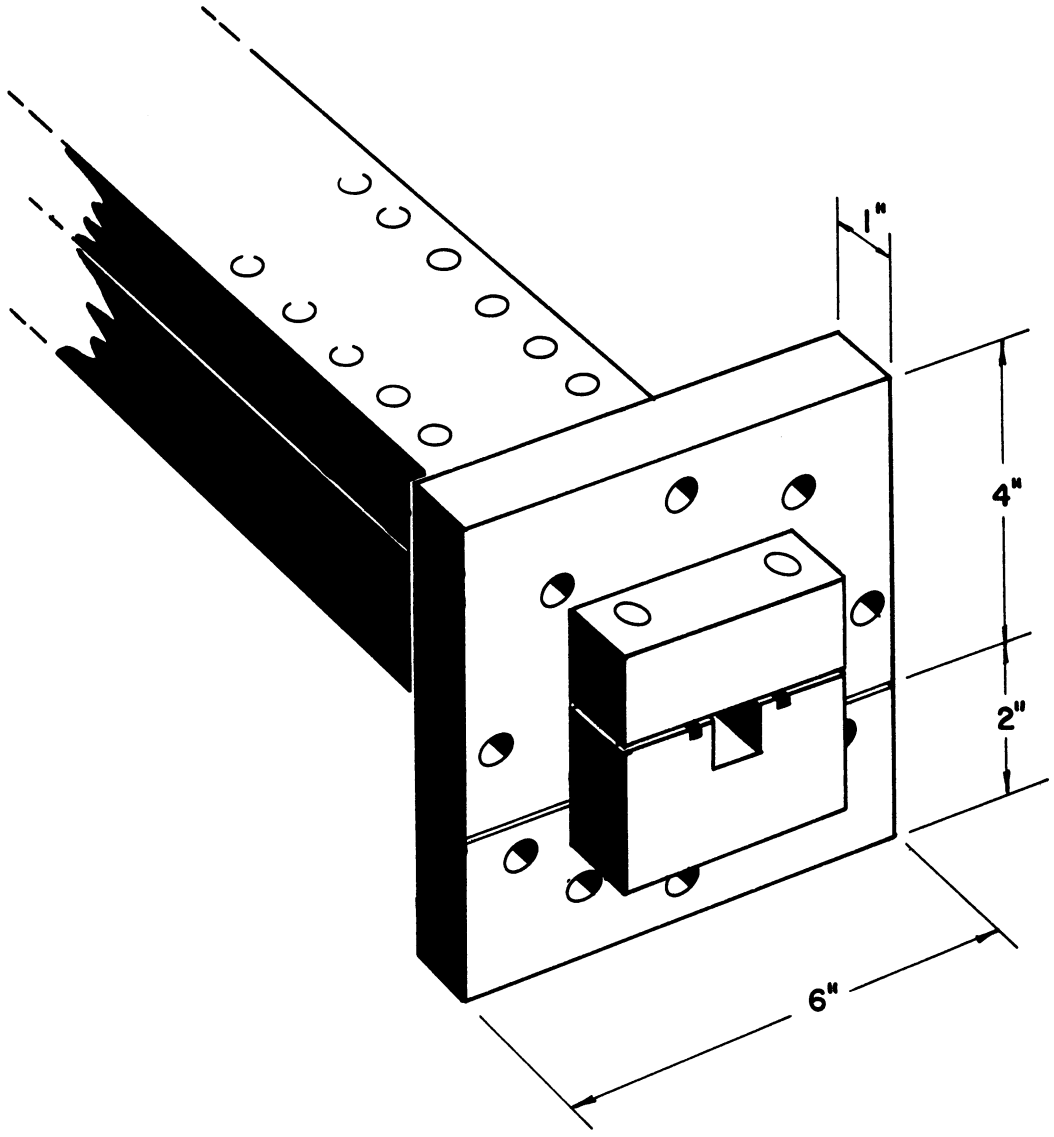

Figure (13) Detail of Flange

open end with a vacuum stopcock and ground glass joint. Vacuum was produced by a Cenco Megavac Pump.

C. The Velocity Probes and Timing Circuit

Before fixing on the final method used for measuring the wave velocity, considerable time and effort was expended in an effort to adapt the simple ionization type detectors used by Gluckstein (45) and Morrison (72) for use in this experiment. These ionization type detectors are best used to measure detonation velocity, but it was found that, when they are used to measure the shock velocities in this work with their correspondingly lower levels of ionization, they are too insensitive to be reliable. Many different designs of ionization probes were tried before this type of velocity detector had to be abandoned.

The method finally settled on involved use of two Kistler PZ-6 type quartz pressure transducers set in the test section wall at 30 inches and at 42 inches, respectively, from the diaphragm. The time interval between passage of the wave by each of these stations would directly give the wave velocity. Since the signal from such a transducer is extremely small, it must be amplified considerably before it can be used to trigger an electronic counter. To accomplish this, the signal from the transducer was fed to a high gain single stage pentode amplifier and the output of this amplifier was used to start a thyratron pulse maker which, in turn, started the timer. A signal from the second transducer followed a similar path and stopped the timer, which was a Hewlett-Packard Type 524 electronic

counter with a 525 B time interval unit. The operation of this circuitry is quite simple and can be readily seen by referring to Figures 14, 15, and 16. The time lag for the various pieces of electronic equipment was measured and the difference between the overall time lags for the start side and the stop side was found to be less than six microseconds. Since the time interval measured is of the order of 150 microseconds, this time lag was found to be quite small enough to give accurate time interval measurements.

D. Operation of the Shock Tube

In this section, the operation of the shock tube during an actual run will be described. Prior to the use of the shock tube for the experimental portion of this work, the shock tube, together with the piping and probes, was tested for pressure and vacuum tightness. The former test simply involved replacing the diaphragm with a solid steel insert, filling the sections with hydraulic fluid and applying pressure with the use of a hydraulic pump. A test pressure of 4000 psig was applied to the test section and high pressure piping and a leak rate of less than 5 percent per hour was observed. This was considered very satisfactory. Since the reservoir section is under considerably more strain than the test section, it was pressure tested to 11,000 psig and a leak rate of less than 5 percent per hour was observed. This was considered satisfactory. However, the leak rate increased with time and use and a periodic replacement of "O" rings at the diaphragm site was necessary. These "O" rings were replaced whenever the tube was taken apart

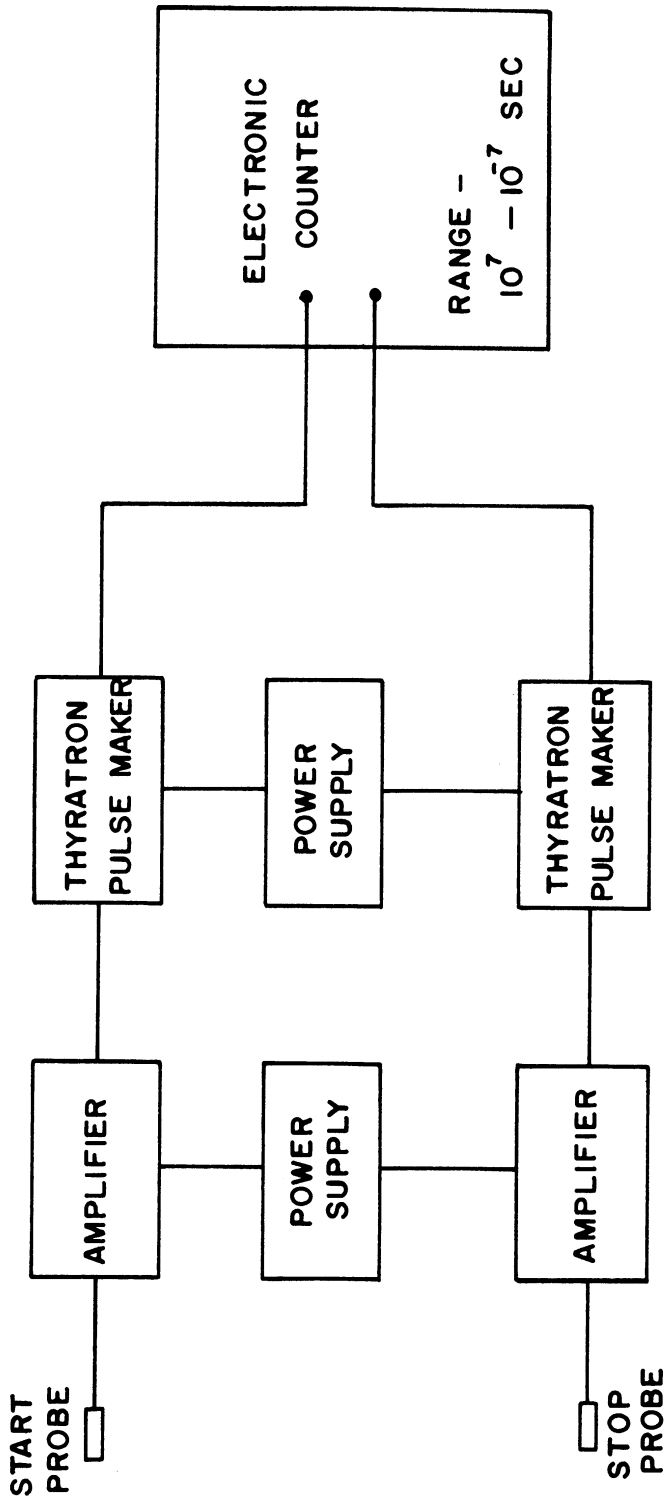

Figure (14) Block Diagram of Velocity Measurement Circuit

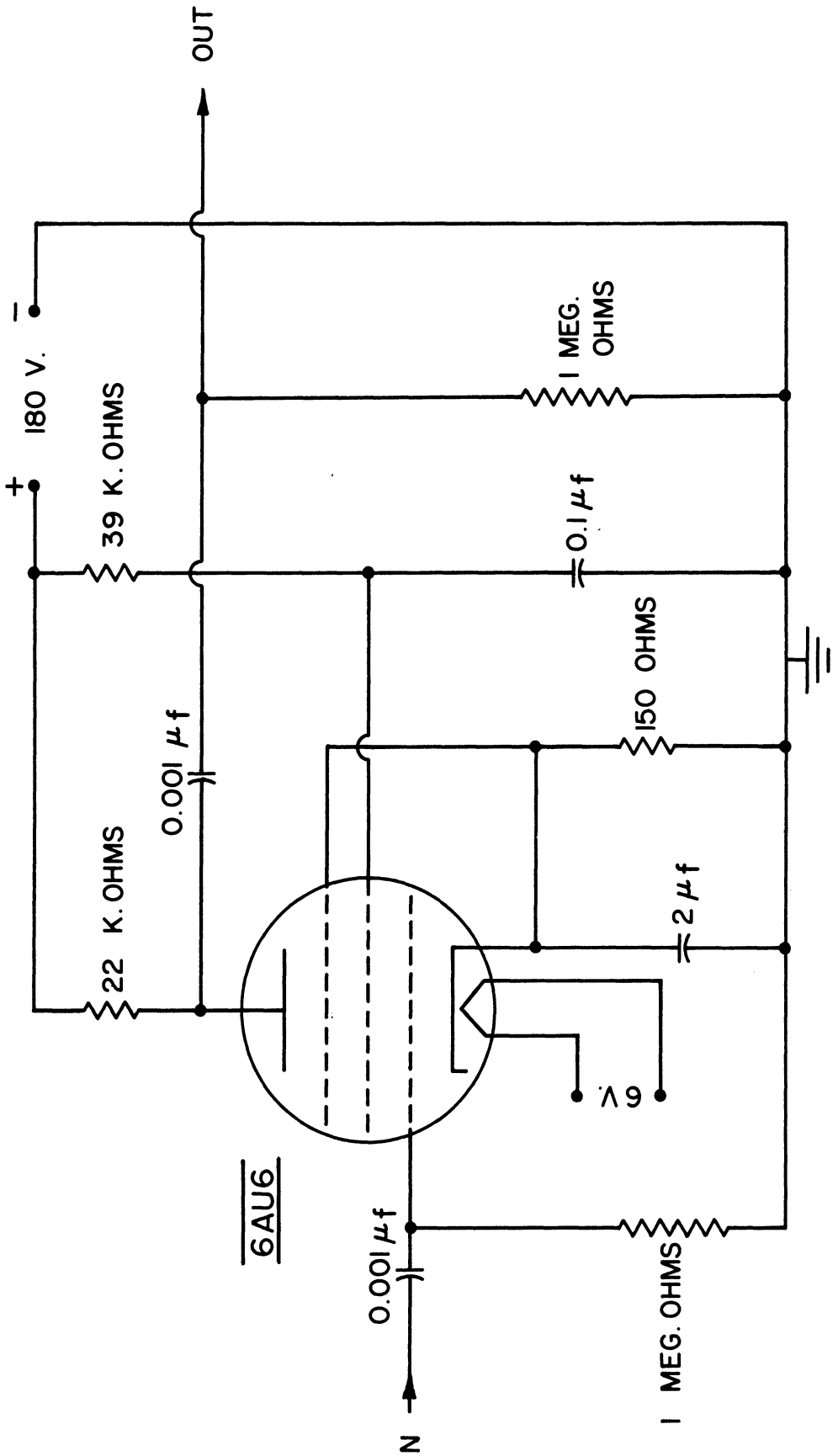

Figure (15) Circuit for Transducer Signal Amplifier

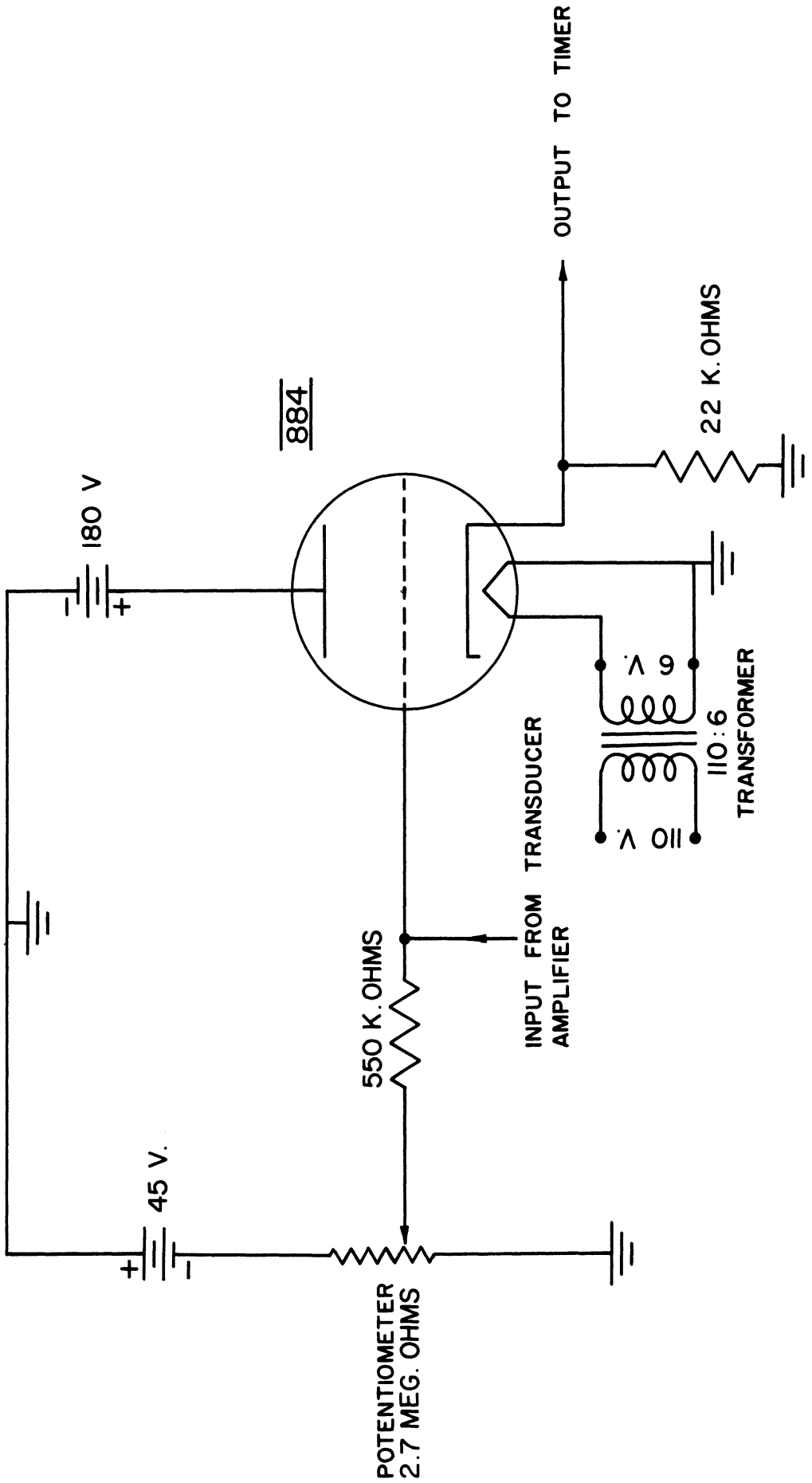

Figure (16) Circuit for Thyratron Pulse Maker

for periodic cleaning of the inside surface and tubing.

The entire shock tube and all components were vacuum tested collectively and individually. This test involved pumping down to maximum vacuum (less than 0.1 inch of mercury) and observing the leak rate. A leak rate for the entire system of less than one percent per hour was considered satisfactory. As a matter of fact, most of the components, as well as the gas sampling bulbs, were found to be leak free, within the ability of the gauges used to determine leaks.

The actual operation of the shock tube during a run will now be described. First, a scored brass diaphragm was mounted between the reservoir and test sections. Evacuated sample bulbs were placed in their receivers on the chassis. The entire system was evacuated to less than 0.1 inches of mercury and leak tested for periods of time from one-half hour to one hour. During the leak test, the ambient temperature and pressure were recorded. If the leak test showed the system to be tight, the test section was flushed with the test gas, re-evacuated, and a sample of the test gas was reintroduced to the test section and its pressure recorded. If desirable, a small amount of this test gas was sampled for analysis. Now, the driver gas was introduced into the reservoir section through a needle valve and its pressure was allowed to build up until the diaphragm burst. The burst pressure was recorded, as well as the time interval recorded by the electronic timer. A sample of the products of the reaction was taken for analysis, and the rest of the gas in the shock

tube was exhausted through a heavy rubber exhaust tube which was then flushed with nitrogen gas, to prevent any possibly dangerous accumulation of hydrogen.

Obviously, then, the operation of the shock tube is quite simple and rapid so that, in the absence of difficulties, a run could easily be made in less than two hours.

E. Preparation of Reactant Mixtures

In cases where a mixed test gas was used, the components were mixed to predetermined partial pressures in a previously evacuated stainless steel tank. After introducing the gases into the tank, they were allowed to mix for at least two days before use. The composition of all test gases was periodically checked by mass spectroscopic analysis.

F. Analytical Procedures

All gas samples were analyzed by use of a Consolidated Engineering Corporation Type 21-103 B mass spectrometer according to the manufacturers recommendations for use of this instrument. Basically, this procedure involves standardization of the instrument by means of samples of known composition and then determining the composition of the unknown sample by comparing its spectrum with those of the known standards. For the samples of reactant gas, a material balance was made and a total analysis was obtained, i.e., the percentage of each component was determined. For the product gases, this procedure could not be employed since, in these samples, often less than 0.5% of the mixture was prod-

uct, the remainder being excess driver gas. In these cases, the percentage of intermixed driver was not determined, and the product analysis was expressed by ratios of the various product components. The percentage of intermixed driver was not determined, because for adequate analysis of the products, the sensitivity of the mass spectrometer had to be set so high that the driver gas would simply overload the instrument if a driver gas analysis was attempted. This is, of course, a possible source of error but, when other possible sources of error are considered, it is apparent that any errors coming from this source are probably overshadowed by other errors for which no provision can be made. An example of this type of error would be the selective absorption of some of the hydrocarbons by such things as stopcock grease. Unsaturated hydrocarbons are more soluble than saturated hydrocarbons and so, the mass spectroscopic analysis could give erroneous results.

IV - EXPERIMENTAL RESULTS

A. Experimental Data Taken

During the course of a run, the information recorded included the diaphragm thickness, the driver gas used, the atmospheric pressure and temperature, the pressure in the low pressure section, P_o, the pressure in the high pressure section when the diaphragm bursts (with a maximum reading pressure gauge), P_2, the time interval between passage of the shock wave past two pressure sensing stations set one foot apart, the composition of the gas originally put in the low pressure section, and the composition of the products of the reaction as a mixed mean, as determined by the mass spectrometer.

From this information, a first order reaction rate constant may be calculated as a function of temperature. A detailed sample calculation of this type is presented in Appendix II. The best values of A and ΔE in equation (52) were determined by least squares using the data in Appendix III. It is exactly the results of just such a calculation which will be discussed in the next few parts of this section.

B. Cracking of Ethane

When runs were made using almost pure ethane (greater than 96% ethane) as the gas in the low pressure section, with hydrogen or helium in the high pressure section, and with varying shock strengths (and thus, varying effective reaction temperature), various values of k_1 as a function of temperature were determined. Since a first order irreversible reaction

mechanism is postulated, with a reaction rate constant given by the equation:

$$k_1 = Ae^{-\Delta E/RT} \tag{52a}$$

taking logarithms would lead to:

$$\ln k_1 = \ln A - \Delta E/RT \tag{86}$$

Figure 17, then, is a plot on which all the data obtained for the thermal decomposition of ethane is presented as $\ln k_1$ versus $1/T$. Considerable work on this reaction may be found in the literature and, indeed, data from such sources as Kuchler and Thiele (65), Storch and Kassel (106), Steacie and Shane (98), Sachsse (91), and Marek and McCluer (69) are presented in the lower part of Figure 17. The three points from the literature at the top of Figure 17 are from Greene et al (47). These points were not actually presented in the form plotted, but enough information was given so that $\ln k_1$ as a function of $1/T$ could be obtained. Since these three were also made in a shock tube (using a reflected wave) and since the reaction rate constants are somewhat higher than either those obtained in this work or in the previous non-shock-tube work, it was thought that the three might be used as a sort of check on any kinetic equation derived.

Several observations may be made on the data as presented on Figure 17. First of all, it is quite clear that there is much less scatter in the data obtained in the previous non-shock-tube work than in either the data of Greene (47) or in the data obtained in this work. This is

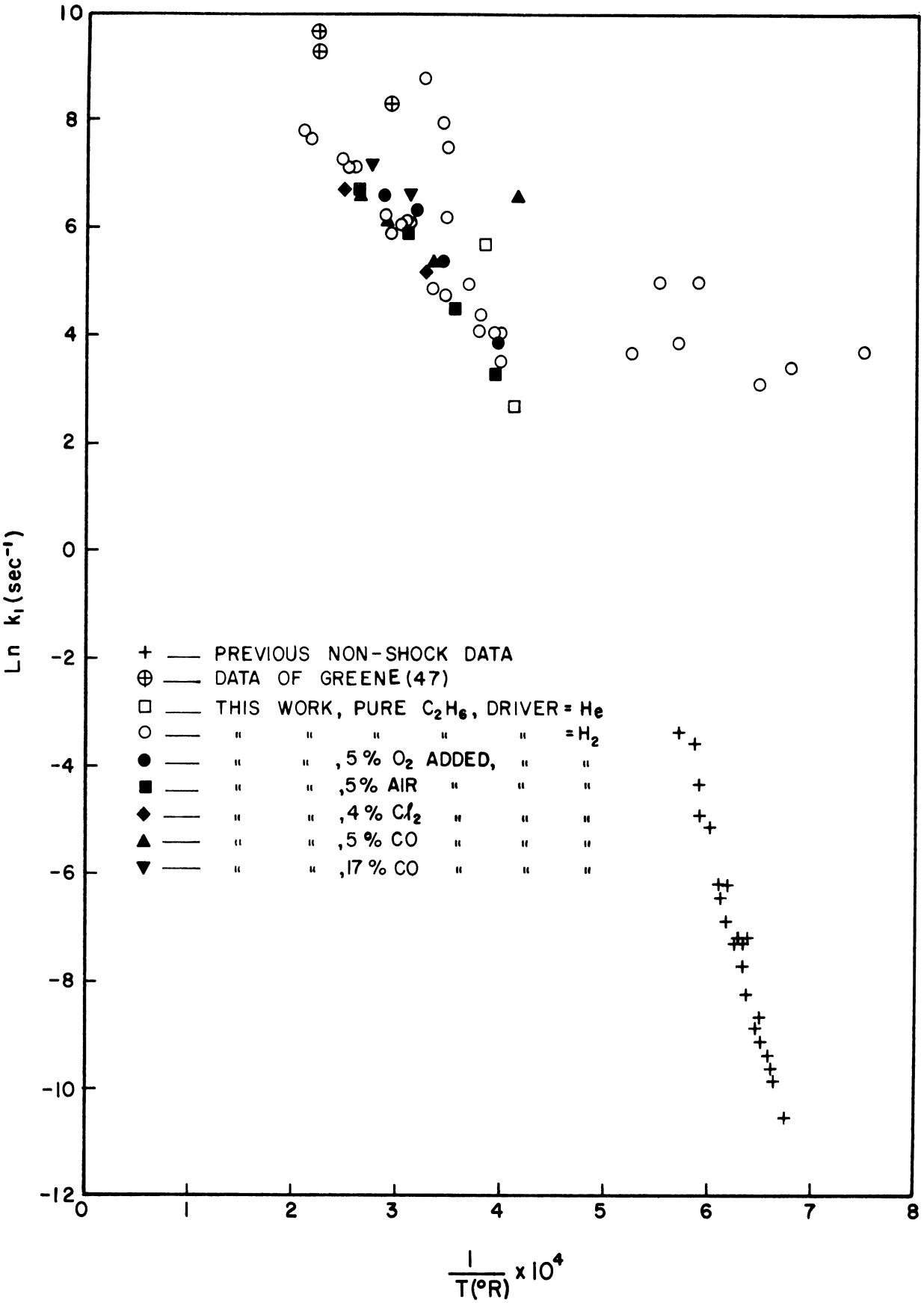

Figure (17) Data for the Reaction $C_2H_6 \rightleftharpoons C_2H_4 + H_2$

probably due to the fact that it is easier to measure such quantities as temperature accurately in the apparatus used in obtaining the non-shock-tube data than it is in the shock tube. Indeed, the reaction temperature in the shock tube is not be measured at all, but must be calculated from the flow conditions.

Another observation that can be made from Figure 17 is that the data obtained in this work agrees extremely well with the data obtained by Greene (47). Greene also used a shock tube, but employed a completely different system than the one used in this work. Greene made use of a reflected shock wave coming off the closed end of his shock tube to heat the reactant gases. Since the shock tube used in this work employed only an incident shock, the equations involved are quite different. However, the temperatures and time intervals involved are of the same order, quite different from the range of conditions employed in the non-shock-tube work.

A first order non-reversible reaction mechanism would be represented by a straight line on Figure 17. However, it may be noted that, although the data obtained in this work agrees extremely well with that of Greene (47), a straight line drawn through the non-shock data would not represent the shock tube data well at all. There are several possible explanations for this behavior. The first, and probably the one most likely true, is that the energy of activation of the reaction changes with temperature, as a result of some reaction steps which

were not important at low temperature becoming important at higher temperatures.

Another possible explanation could be that the reaction mechanism changes with temperature. The shock tube data was taken at considerably higher temperatures than was the non-shock data, so the discrepancy shown on Figure 17 can certainly be explained this way. If the reaction mechanism changes, then the energy of activation, represented by the slope of a curve drawn through the data on Figure 17, would also change. One such possible curve is shown on Figure 18, along with all the pure component data available.

Still another possible explanation for the discrepancy could be that there is no discrepancy at all, but the scatter in the data makes it appear that one exists. Since there is no adequate way to take any possible mechanism change into account or to determine the reason for the apparent discrepancy, it was decided to fit the best straight line through all the data by the method of least squares. Such a line, although it would not necessarily give a true picture of the actual reaction mechanism, would be the best available correlation for this reaction over the extremely wide range of conditions studied. In fitting the least squares line, the data of Greene (47) was left out so that they might serve as some sort of check on any least squares line derived. Such a least squares line is shown as the solid line on Figure 19. The equation for this line is

$$\ln k_1 = 19.365 - \frac{41640}{T(^{\circ}R)} \qquad (87)$$

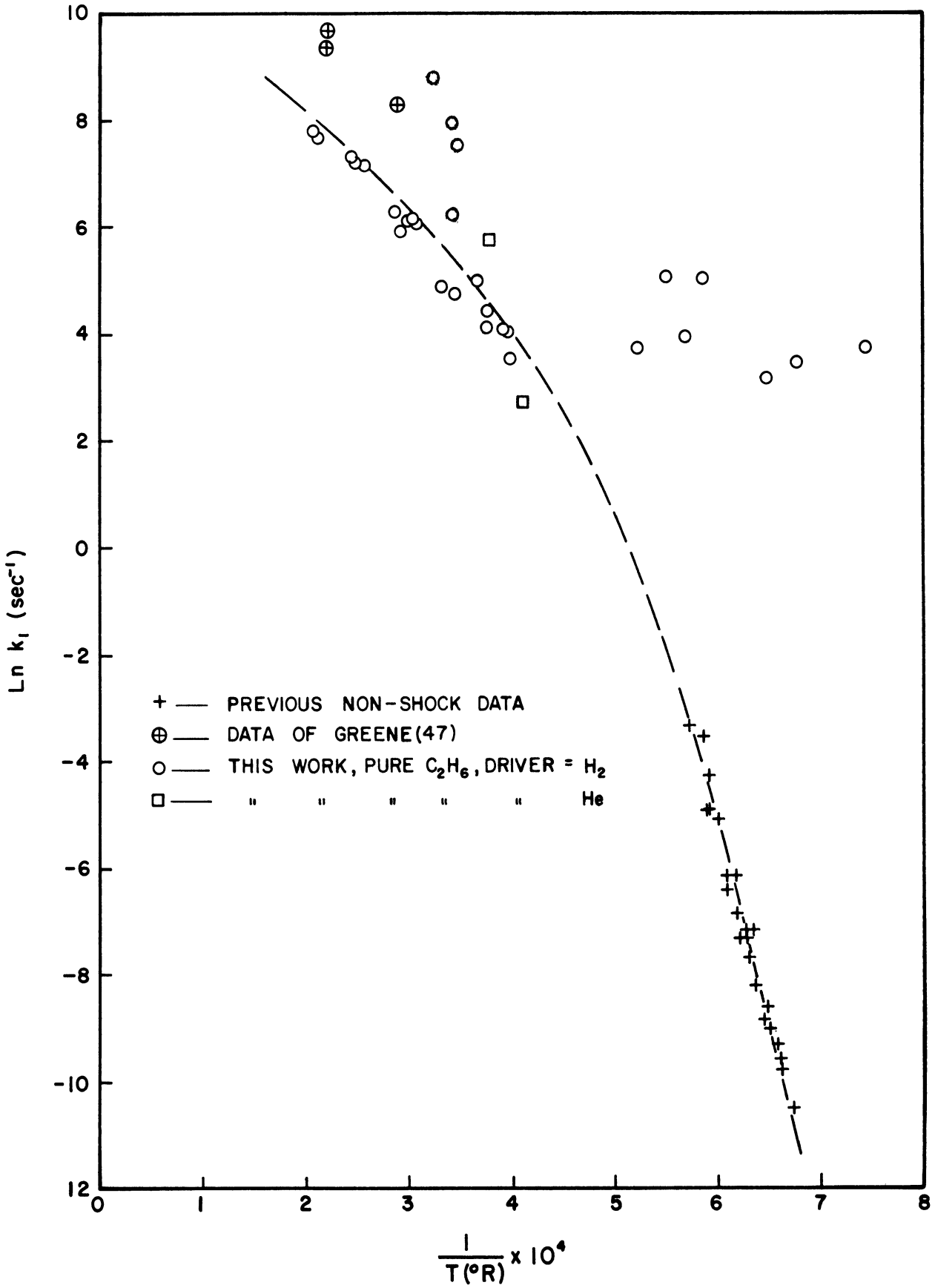

Figure (18) One Possible Way ln k_1 may be Related to T

This gives an apparent activation energy, ΔE, of 83,000 BTU/lb.-mole = 46 kcal/gm.-mole.

Steacie (97) presents a least squares correlation for the non-shock-tube data which is represented by the partially dotted line on Figure 19. This correlation can be put in the form

$$\ln k_1 = 34.75 - \frac{67036}{T(^{\circ}R)} \qquad (88)$$

This gives an activation energy of 133,000 BTU/lb.-mole = 74 kcal/gm.-mole, considerably higher than the value obtained for all the data. Indeed, other workers give values of ΔE much closer to 74 kcal/gm.-mole than does this work. For example, Paul and Marek (74) give the value ΔE = 77 kcal/gm.-mole. Sachsse (91) gives the value ΔE = 69.8 kcal/gm.-mole. Steacie and Shane (98) give the value ΔE = 68.7 kcal/gm.-mole, and Rice and Herzfeld (84) give the value ΔE = 66 kcal/gm.-mole.

Of course, all this work was done at considerably lower temperatures and longer residence times than was the work by Greene (47) or that done in this thesis. The reason why this should affect the value of ΔE is not really known, although a possible change in reaction mechanism has been discussed. It may be noted, from Figure 19, that the least squares line developed in this work fits Greene's data considerably better than does the least squares line presented by Steacie (97). This is to be expected, because Steacie used only the non-shock-tube data in deriving his equation. Exactly how much better will be discussed in the next section.

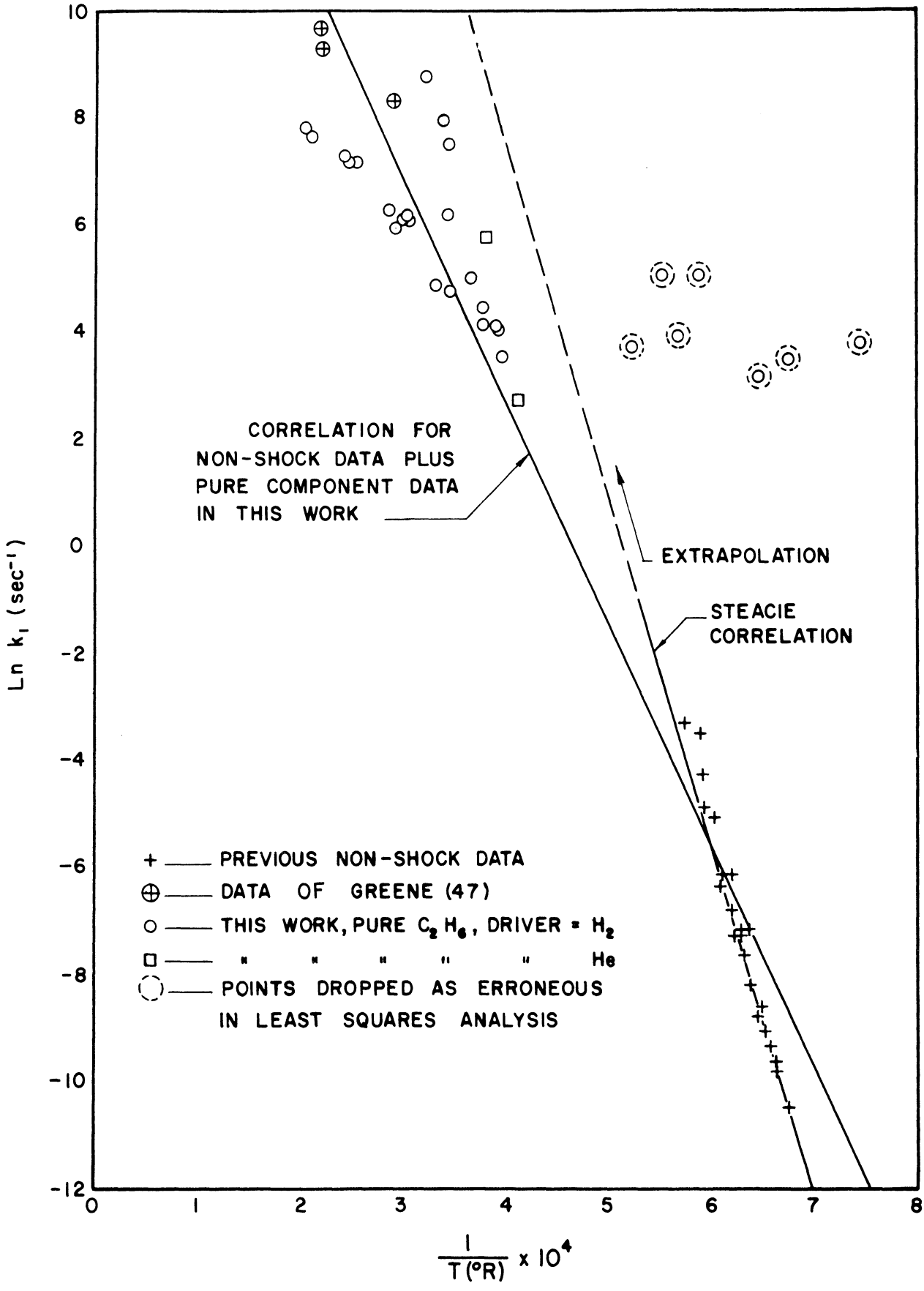

Figure (19) Least Squares Curves for Reaction $C_2H_6 \rightleftharpoons C_2H_4 + H_2$

C. Statistical Analysis of Ethane Data

For purposes of this work, a standard deviation may be defined by:

$$\sigma\ (\ln k_1) = \sqrt{\frac{\Sigma_N(\ln k_1 - \ln \bar{k}_1)^2}{N}} \qquad (89)$$

where $\ln k_1$ is the measured value, $\ln \bar{k}_1$ is the value predicted by the least squares curve at the same temperature, and N is the number of points. When this deviation was calculated for the various sections of Figure 19, it was found that the deviation for all the points on Figure 19 was 1.38, after those points considered erroneous were dropped. The criterion for dropping bad points was taken to be that all points whose deviation, defined by

$$\Delta = \left| \ln k_1 - \ln \bar{k}_1 \right| \qquad (90)$$

was greater than three times the standard deviation were dropped. This criterion was chosen because, for a normal distribution (see Cramer (22)), the probability for any point to have a deviation greater than three times the standard deviation is equal to 0.27%. It was felt that this probability was sufficiently small so that we can safely say that any points whose deviation is greater than three times the standard deviation in all probability are erroneous.

When the standard deviation was calculated for all the data using the Steacie equation, the standard deviation turned out to be 5.48, or

approximately four times the deviation from the equation derived in this work. Clearly, then, the equation determined in this work is considerably better for all the data than the Steacie equation which was derived for just the non-shock-tube data. When both equations were applied to determine the deviation of Greene's data, the equation derived in this work again turned out to be considerably better than the equation of Steacie. The standard deviation using the derived equation for Greene's data turned out to be 0.83, while the deviation using the Steacie equation turned out to be 9.32, or over ten times as great.

Of course, when both equations were applied to just the data Steacie used in deriving his equation, the Steacie equation turned out to be somewhat better. The deviation from the Steacie equation turned out to be 0.35, while the deviation from the equation derived in this work turned out to be 0.97. However, it should be remembered that considerably more data was used in this work than in the work of Steacie and that a much wider range of conditions is covered in this work than Steacie took into account. These results can best be shown in the following table:

TABLE I

STANDARD DEVIATIONS

Data Involved	Equation Derived Herein	Steacie
All pure component data	1.38	5.48
Greene's (47)	0.83	9.32
Data used by Steacie (97)	0.97	0.35

D. Uncertainty in the Value of k_1 for Ethane

From equation (86) it is apparent that the certainty in the value for $\ln k_1$ is very much dependent on the certainty in the value of ln A and $\frac{\Delta E}{R}$. Indeed, we can say that if:

$$\ln k_1 = \ln A - \left(\frac{\Delta E}{R}\right)\frac{1}{T} \tag{86}$$

then $$\ln k_1 \pm \Delta(\ln k_1) = \ln A \pm \Delta(\ln A) - \frac{1}{T}\left(\frac{\Delta E}{R} \pm \Delta\left(\frac{\Delta E}{R}\right)\right) \tag{91}$$

Subtracting equation (86) from equation (91) leaves

$$\Delta(\ln k_1) = \Delta(\ln A) \pm \frac{1}{T}\left(\Delta\left(\frac{\Delta E}{R}\right)\right) \tag{92}$$

so, the maximum uncertainty is:

$$\left|\Delta(\ln k_1)\right| = \left|\Delta \ln A\right| + \left|\frac{1}{T}\left(\Delta\left(\frac{\Delta E}{R}\right)\right)\right| \tag{93}$$

The values for $\Delta \ln A$ and $\Delta\left(\frac{\Delta E}{R}\right)$ may be taken as the standard deviatio in the values which will be defined as:

$$\Delta(\ln A) = \sqrt{\frac{\Sigma_N (\ln A - \ln \bar{A})^2}{N}} \tag{94}$$

$$\Delta\left(\frac{\Delta E}{R}\right) = \sqrt{\frac{\Sigma_N \left(\frac{\Delta E}{R} - \frac{\overline{\Delta E}}{R}\right)^2}{N}} \tag{95}$$

where $\ln \bar{A}$ and $\overline{\Delta E}$ are the mean values of the quantities, i.e., the values used in the least squares equation, and ln A and ΔE are defined from:

$$(\ln A) = \ln k_1 + \frac{1}{T} \left(\frac{\overline{\Delta E}}{R} \right) \tag{96}$$

$$\left(\frac{\Delta E}{R} \right) = \frac{\ln \bar{A} - \ln k_1}{\frac{1}{T}} \tag{97}$$

where $\ln k_1$ is the actual value measured at the point in question.

If we now apply equations (96) and (97) and use the values derived in equations (94) and (95), we can determine the quantities in equation (93) to derive an equation for $\Delta(\ln k_1)$

$$\Delta(\ln k_1) = 1.37 + \frac{0.434}{T\ (^{\circ}R)} \tag{98}$$

This equation represents the statistical uncertainty in $\ln k_1$ and is represented by the dotted lines on Figure 20. The band bounded by the dotted lines, then, represents the region where, statistically at least, the values of $\ln k_1$ fall.

Another reason for uncertainty in the value for k_1 is the inability to obtain an exact chemical analysis of the product gases. In the calculation of k_1, the amount of conversion to C_2H_4 is crucial, and there is some uncertainty in the mass spectrometer analysis. A conservative estimate for the uncertainty in measuring the peak heights on the mass spectrometer record was taken (uncertainty = 0.5 divisions) and the corresponding values for $\ln k_1$ were determined. This uncertainty can best be shown on a graph, Figure 20., where the uncertainty is represented by a line through each of the points whose length covers the region of uncertainty.

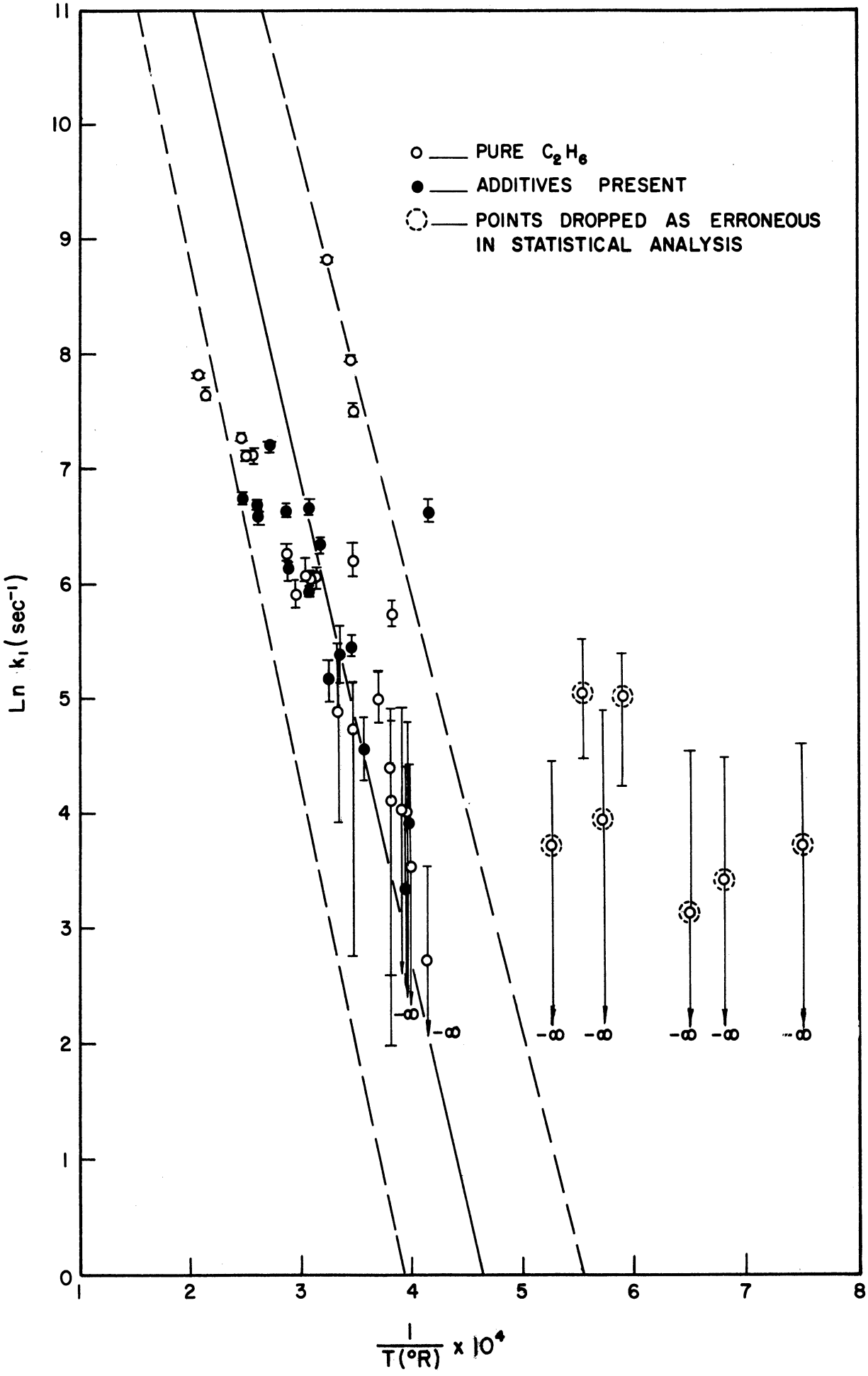

Figure (20) Uncertainty in the Value of ln k_1

From this figure, it may be seen that those points with the biggest deviations (those points furthest right on the figure surrounded by dotted lines) are those which were dropped in the statistical analysis. These points represent the smallest conversions. It is a strong possibility, then, that the reason for their large deviation from the least squares line may be due to the uncertainty in the analysis. Of course, this estimate of the uncertainty is conservative, and the actual range of uncertainty for any given point is probably considerably less than that indicated by the figure.

E. Analytical Methods for Eliminating Uncertainty

Several attempts were made to lessen the uncertainty in the chemical analysis. One method employed was to attempt concentration of the hydrocarbons present in the gas samples. Most of the uncertainty in the analysis is due to the fact that the gas samples taken consist mostly of hydrogen, the driver gas, occasionally to as high a percentage as 99.8%. An attempt was made to remove most of the hydrogen by immersing the gas sample bulbs in liquid nitrogen for twenty-four hours, pumping off most of the residual gas, warming the gas samples to evaporate the hydrocarbons condensed during the immersion and analyzing this residue. Indeed, this method served to concentrate the hydrocarbon portion by about ten to twenty times. No significant changes in the analysis was found over the analysis for the original gas sample. The concentrations were more certain in the frozen samples. The frozen samples also afforded a chance to look for any material present in small amounts which might be

the product of a reaction competing with the reaction

$$C_2H_6 \rightleftharpoons C_2H_4 + H_2$$

For example, the presence of CH_4, C_3, or C_4 hydrocarbons would be evidence of further cracking or polymerization not taken into account in the derivation of the chemical equations. However, no significant amounts of hydrocarbons other than C_2H_6, C_2H_4, or C_2H_2 (present in the very high temperature runs) was detected.

Another possible reaction might be a complete breakdown of hydrocarbon to carbon and hydrogen. This effect would not show up in the gas analysis performed, because the carbon would be a solid, and the hydrogen would be masked by the driver hydrogen. This effect could be detected if helium were substituted for the hydrogen driver, and an analysis made to determine the amount of hydrogen formed by the reaction. A comparison of this amount with the amount of unsaturated hydrocarbon formed would immediately make apparent any significant amounts of carbon formed, since for each atom of carbon formed, one and one-half molecules of hydrogen gas would be formed. This analysis would also indicate if enough driver hydrogen were carried into the reaction zone on the hydrogen-driver shocks to significantly repress the cracking because of the equilibrium $C_2H_6 \rightleftharpoons C_2H_4 + H_2$. Two such runs (with helium driver) were made, and the results plotted on Figure 19 indicate that perhaps a small but not very significant increase in reaction rate does occur, i.e., perhaps there is a little suppression of the cracking by driver hydrogen, but not very much.

An analysis based on just the hydrogen-hydrocarbon portion of the product gas for the two helium driven runs is presented in the following Table:

TABLE II

ANALYSIS OF HELIUM DRIVEN RUNS FOR ETHANE

	Run 203	Run 204
Temperature (^{o}R)	2620	2422
% C_2H_6	84.75 $\pm$ 0.50	94.26 $\pm$ 0.28
% C_2H_4	8.43 $\pm$ 0.23	2.90 $\pm$ 0.13
% H_2	6.82 $\pm$ 0.22	2.84 $\pm$ 0.12

From Table II, it is quite clear that a significant amount of carbon is not formed by the reaction (if no carbon is formed, % C_2H_4 = % H_2) since, although there is a difference between the amounts of C_2H_4 and H_2, this difference is in the wrong direction, i.e., too little hydrogen for just the simple cracking to ethylene. However, this difference is small enough to be accounted for by losses of the highly volatile and penetrating hydrogen through leakage, absorption by stopcock grease, or adsorption on the walls of the various pieces of equipment in contact with the hydrogen. Cracking of ethane to pure carbon can probably be ruled out as can any other reaction which does not leave equal amounts of ethylene and hydrogen present.

F. The Effect of Certain Additives on Ethane Cracking

During the course of the work on the cracking of ethane, small amounts of various additives were added to the ethane to see if they had

any effect on the effective reaction rate. The reaction rate constants for these runs are plotted on Figure 17. As may be seen from this Figure, none of the additives exhibited any really significant effect.

In the work of Glick (42), it was noted that the amount of C_2H_4 formed in the cracking of C_2H_6 dropped as the amount of CO formed increased. This CO formation was brought about by the addition of water vapor. Because of the possibility of forming some CO, small amounts of air and O_2 were added to the ethane. If CO formed and thus suppressed the formation of C_2H_4, the reaction rates would be lower than those for the pure C_2H_6. If, on the other hand, the oxygen reacted with any hydrogen which may have come into the reaction zone, and thus raised the effective reaction temperature, the reaction rates would be higher than for the runs made with pure C_2H_6. The amounts of O_2 and air added were deliberately kept small to prevent the formation of oxygenated hydrocarbons, and were thus kept to 5% additive. Both O_2 and air were tried in an attempt to detect any differences due to the smaller amounts of O_2 present in the air additive. The effect, if any, of either O_2 or air additive was within the uncertainty of the analysis.

It was then thought that perhaps the effect observed by Glick (42) was not due to the formation of CO, but rather to the presence of CO as some sort of inhibiter. With this in mind, several runs were made on C_2H_6 with 5% CO additive, and then with 17% CO additive. Again no significant effect was noted, so this notion was discarded.

One further attempt at observing additive effects was made when 4% Cl_2 was added to the C_2H_6, thus taking advantage of the heat of chlorination to raise the reaction rates. Again, no particular effect was noted, probably due to the small amounts of chlorine used.

G. Cracking of Ethylene

In several of the runs at the highest temperatures in the cracking of ethane, significant amounts of acetylene were noted, a result of the reaction:

$$C_2H_4 \rightleftharpoons C_2H_2 + H_2$$

It was therefore thought that a logical extension of the work on the cracking of ethane would be a study of the kinetics of ethylene decomposition to acetylene. This is especially true, considering the fact that very little data is available on this reaction. A group of runs was, therefore, made using pure ethylene in the low pressure section and the results are shown on Figure 21, along with two points from the work of Greene et al (47) obtained in exactly the same way as were the three points from Greene used in the ethane cracking study. No other data were found on this reaction.

By a method exactly analogous to that used for the ethane decomposition, a least squares line was fitted to the data for the decomposition of the pure C_2H_4. The equation for this line is:

$$\ln k_1 = 10.756 - \frac{18940}{T(^{\circ}R)} \qquad (99)$$

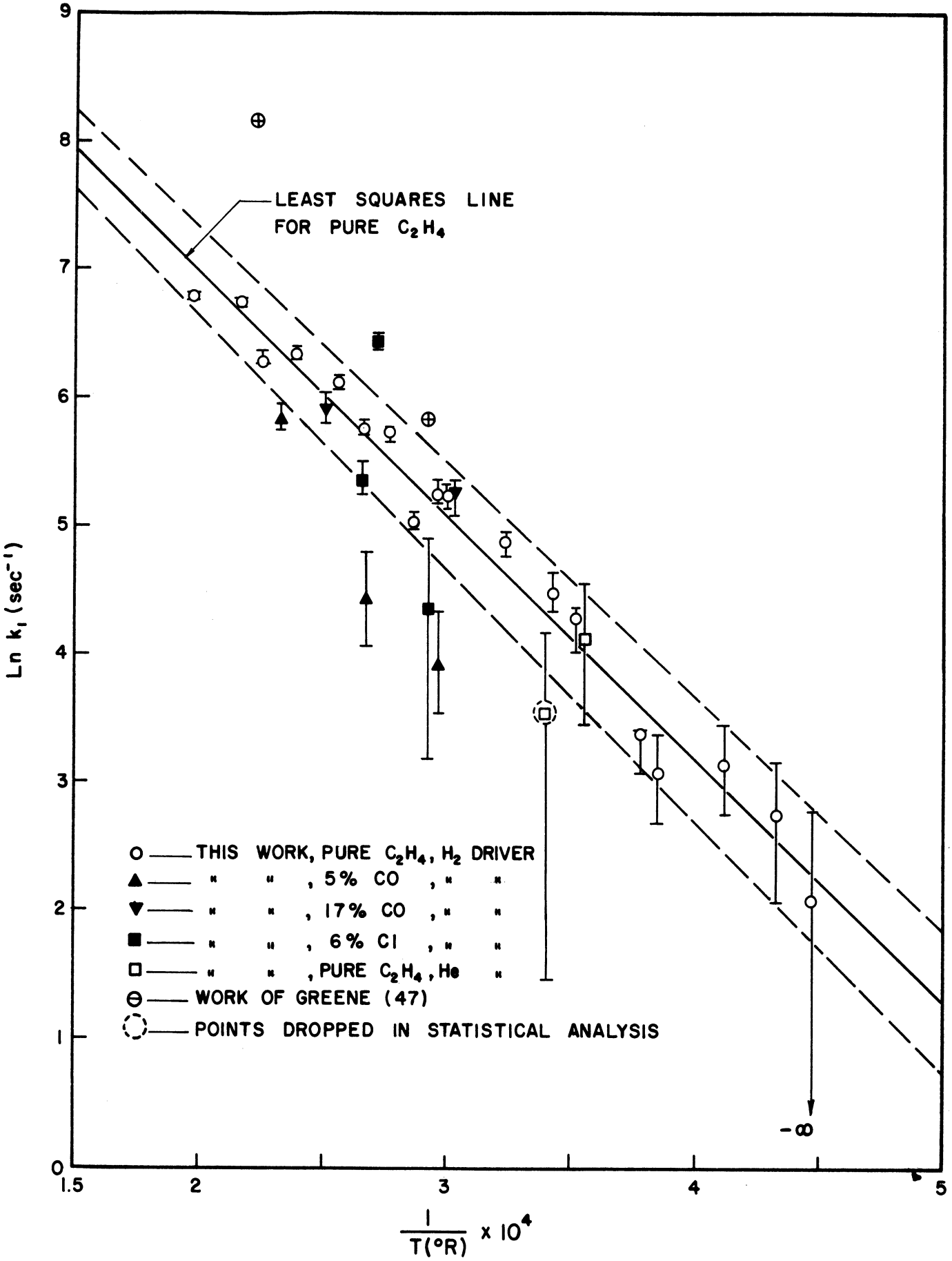

Figure (21) $\ln k_1$ vs. $\frac{1}{T}$ for $C_2H_4 \rightleftharpoons C_2H_2 + H_2$

The apparent activation energy for the reaction $C_2H_4 \rightleftharpoons C_2H_2 + H_2$ from equation (99) then is 21 kcal/gm mole. There is some discussion in the literature on the mechanism of this reaction, though no specific rate data are given. Molera and Stubbs (71) report an activation energy of 57.8 - 75.0 kcal/gm mole depending on the pressure, while Taylor and van Hook (108) speculate on a value for the activation energy of about 85 kcal/gm mole. This value is in doubt.

Of course, there is some uncertainty in the value of $\ln k_1$ computed in this work, both statistical uncertainty and uncertainty caused by uncertainty in the chemical analysis. Application of equations (93) - (97) gives an equation representing the statistical uncertainty in $\ln k_1$. This turns out to be

$$\Delta(\ln k_1) = 0.206 + 0.067 \left(\frac{1}{T}\right) \qquad (100)$$

so that the value of $(\ln k_1)$ is not nearly so uncertain for ethylene as it is for ethane. This is caused by the fact that there is considerably less scatter in the ethylene data than in the ethane data. As a matter of fact, the standard deviation for the ethylene data, defined by equation (89), turned out to be $\sigma\ (\ln k_1) = 0.214$, as compared to 1.38 for the ethane decomposition data. The average deviation of equation (99) from the two points of Greene (47) is somewhat greater, being equal to 1.20. The boundaries of the region of statistical uncertainty are represented by dotted lines on Figure 21.

An estimate of the uncertainty in the value of $\ln k_1$ caused by

uncertainty in the analysis was made in exactly the same way as for the ethane decomposition, and this uncertainty is represented by the lines through each point on Figure 21.

Several authors have pointed to the possibility of a reaction opposing the formation of acetylene. The main reaction pointed out is

$$2\ C_2H_4 \rightleftharpoons C_4H_8$$

This reaction has been mentioned by such authors as Burk et al (12), Molera and Stubbs (71), Lenher (67), and Storch (104). It should be pointed out that the polymerization is favored by high pressure. Pease (75) asserts that, for pressures greater than ten atmospheres, the polymerization reaction is the only one that occurs. Since polymerization may happen, an investigation was made to determine if any polymerization could be detected. This was done by concentrating the hydrocarbons by a freeze-out technique exactly the same as the technique for ethane freeze-out, and then analyzing the residue on the mass spectrometer for traces of hydrocarbons heavier than ethane. No noticeable concentrations of heavier hydrocarbons were detected by this procedure.

Another possible reaction would be the breakup of ethylene to form carbon and hydrogen. This possibility was checked by using a helium driver and then analyzing for the hydrogen formed and comparing it to the acetylene formed. As in the ethane decomposition, an investigation involving helium driver would also check to see if any driver hydrogen coming into the reaction zone suppresses the reaction

by causing it to go in the reverse direction. This could be noted if the reaction rates using helium driver would be significantly higher than the rates using hydrogen driver at the same temperature. This did not turn out to be the case, however, and it was concluded that mixing of driver gas into the reaction zone is negligible. The results of the product analysis, based on just the hydrogen and hydrocarbon, is presented in Table III.

TABLE III

ANALYSIS OF HELIUM DRIVEN RUNS FOR ETHYLENE

	Run 200	Run 202
Temperature (^{o}R)	2820	2940
% C_2H_4	92.37 $\pm$ 0.49	96.28 $\pm$ 0.48
% C_2H_2	1.33 $\pm$ 0.22	0.74 $\pm$ 0.21
% H_2	6.30 $\pm$ 0.21	2.98 $\pm$ 0.20

Unlike the ethane decomposition runs, it will be noted in this case that considerably more hydrogen is presented than could be accounted for by just the reaction $C_2H_4 \rightleftharpoons C_2H_2 + H_2$. Two possibilities present themselves. Either some of the ethylene decomposes to carbon and hydrogen, or some of the acetylene formed by the reaction decomposes (or both). Since no other compounds were detected in the product stream, any other reaction is ruled out (except, of course, loss of one or more components by physical means, such as leakage, absorption, etc.). Since there is no way to adequately take into account the formation of carbon, this effect was neglected in the reaction rate analysis. One possible cause of this carbon

formation could be that the temperatures involved in the ethylene cracking are higher than those for ethane cracking.

As in the study of ethane decomposition, some study was made of the effect of additives on the ethylene decomposition. In particular, 5% CO, 17% CO, and 6% Cl_2 were tried, and the results are plotted on Figure 21. Very little, if any, effect of adding these materials was noted.

H. Decomposition of a Mixture of Ethane and Ethylene

One method for checking the validity of the two least squares equations, (87) and (99), would be to run a mixture of ethane and ethylene and try to predict, on the basis of equations (84) and (85) what the conversions to ethylene and acetylene would be. These values may then be compared to the actual measured conversions for the runs. The results of this analysis is presented in Table IV. The values of x and y are defined as x being equal to the mole fraction of ethane converted to ethylene, and y being equal to the mole fraction of ethylene converted to acetylene. The analysis was made on a mixture whose initial composition was 51.4% C_2H_6 and 48.6% C_2H_4.

TABLE IV

PREDICTION OF CONVERSION FOR MIXTURES OF C_2H_6 and C_2H_4

Run	Temp. (°R)	x predicted	x measured	y predicted	y measured
153	3720	0.205	0.095 ± 0.003	0.026	0.009 ± 0.001
157	3380	0.071	0.080 ± 0.002	0.016	0.002 ± 0.001
163	3130	0.027	0.047 ± 0.003	0.010	0.000 ± 0.001
165	3140	0.016	0.042 ± 0.005	0.006	0.000 ± 0.001
167	2690	0.007	0.033 ± 0.004	0.004	0.000 ± 0.001

It may be noted that there is considerable discrepancy between the predicted and measured values of x and y. This is to be expected since the statistical uncertainty in the values of k_1 allows the predicted values of x and y to fall in a fairly wide range. For example, in Run 153, the statistical uncertainty allows the value of x predicted to fall anywhere in the range 0.021 - 0.414 and the value of y predicted to fall anywhere in the range 0.010 - 0.106. This is caused by the fact that equations (84) and (85) involve the values of k rather than the values of ln k, so any uncertainty in ln k is considerably magnified in k. Taking this into account, it should be noted that the predicted values of x and y really have very little meaning, although they do show trends in the right direction.

I. General Notes on the Decomposition of Hydrocarbons in the Shock Tube

In the analysis of the products of both the ethane and the ethylene decomposition, it was noted that only negligible amounts of hydrocarbons other than those predicted by the main decomposition reaction were noted. This is to be contrasted with most of the hydrocarbon decomposition work done in pebble bed heaters and other such devices (see 65, 106, 98, 91, and 69) where an entire spectrum of hydrocarbons, from the lightest to the heaviest, was found. Apparently, the difference lies in the fact that the degrees of conversion involved in the shock tube work are so much lower than those obtained elsewhere. In the work done by other methods, residence times were greater than in the shock tube, thus leading to greater conversions. Larger residence times and greater conversions would give reactions slower than the main reaction a chance

to occur, and so, would lead to the formation of a spectrum of hydrocarbons, provided, of course, that the temperature is high enough to crack the reactants significantly.

There is a possibility that the reaction rates investigated in this work are obscured somewhat by the effect of inhibition by such materials as ethylene and acetylene. There is considerable work in the literature on inhibition of chain reactions, particularly the work of Rice and Polly (85), Stavely and Hinshelwood (96) and Eshevskaya (33). In these works, and elsewhere, it is pointed out that ethylene is a free radical inhibitor. Since the decompositions studied in this thesis have free radical mechanisms, this would indicate that the reactions are self-inhibiting and so, the reaction rates measured may not be really the true rates for the decompositions.

In the ethane decomposition, then, the larger the amount of ethylene formed, the slower the rate of formation of further ethylene would be, exclusive of the effect of the reverse reaction and the equilibrium. Of course, there is a limit to the inhibiting effect of ethylene, and it is not known at what concentration of ethylene the inhibiting effect reaches its limit. If the limit is not reached until large amounts of ethylene are present, the slope of the $\ln k_1$ vs $\frac{1}{T}$ line would not be constant, but would tend to flatten out and tend toward the horizontal as the concentrations of ethylene got higher. This effect was not observed, so it is supposed that the inhibiting effect of ethylene reaches its limit at rather low concentrations of ethylene.

A note may be included on the use of helium as a driver gas in the shock tube. It may be noted that, when helium was used as the driver gas in place of hydrogen, the values of the Mach Number (from equations (25) and (39)) predicted were much closer to the measured Mach Number than they were for the hydrogen driver (see Appendix III). Why this should be so is not really known. There may be a vibrational excitation effect in the hydrogen which has not been taken into account. By this it is meant that some of the energy which would ideally go to increasing the velocity of the hydrogen is, instead, used up in exciting the vibrational states in the hydrogen. This would lead to measured Mach Numbers for hydrogen which are too low. This is exactly what was observed. Since helium is monatomic, of course, no such effect would exist.

A further note may be included on the possibility of producing acetylene directly from ethane. It may be noted that in two runs on pure ethane (100 and 101), substantial amounts of acetylene were produced directly from ethane (see Appendix III). These runs were the strongest run on pure ethane, and it is probable that, if higher shock strengths could be obtained, even greater amounts of acetylene could be produced.

J. Considerations for the Attainment of Continuous Decomposition by a Shock Wave

Since the shock tube is strictly a batch reactor, involving

considerable effort for each run in which only a small amount of product is manufactured, it would not be a very practical instrument for industrial manufacture of ethylene or acetylene. However, it is possible to achieve the conditions occurring in the shock tube by other means. If the reactant gas is fed into a converging-diverging nozzle of the type in the following Figure,

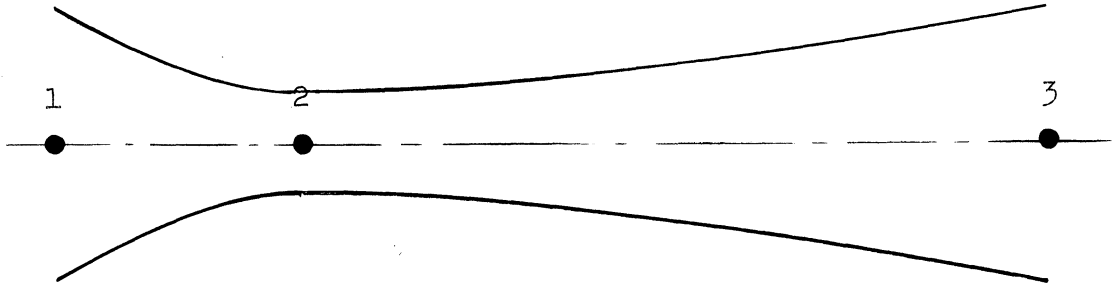

Figure (22) Schematic Diagram of Converging-Diverging Nozzle

it can be accelerated to very high supersonic velocities. The acceleration of the fluid is governed by the de Saint Vernant-Wantzel-Hugoniot Equation (122), assuming one dimensional adiabatic frictionless flow of an ideal gas:

$$\frac{du}{dx} = -\frac{1}{A}\,\frac{u}{1-\frac{u^2}{c^2}}\,\frac{dA}{dx} \qquad (101)$$

where u is the gas velocity, A is the cross-sectional area, c is the sonic velocity, and x is distance. From this equation and Figure 22 it can be seen that, when the gas is fed into the entrance of the nozzle (1) at low velocity, it will be accelerated until u = c. This will occur at the throat

of the nozzle (2), and now, as the gas continues into the diverging section, it will continue to be accelerated, since u is now greater than c, to any velocity we might wish. However, since the nozzle is insulated from the surroundings, the internal energy of the gas will be converted to kinetic energy and the gas will naturally cool. However, heat can be added through the walls of the nozzle to maintain the gas temperature, and thus achieve the velocity and other gas properties necessary for the establishment of a strong standing shock at point 3 in the nozzle. It is the purpose of this section to determine the amount of heat required to maintain the temperature and establish the other properties of the gas stream to duplicate the conditions of several of the runs in the shock tube.

For this purpose, it is assumed that the feed gas is available at one atmosphere pressure and 520°R, and the amount of energy required to change its conditions to the pressure in the low pressure section for the run we are trying to duplicate and its velocity to the velocity of the shock wave in that run will be calculated, assuming the temperature remains constant throughout the expansion.

For this purpose, an energy balance was made, which took the form (refs. 28, 58) of:

$$Q = \frac{u_3^2}{2g_c} - \frac{RT}{m} \ln \frac{P_3}{P_1} + \frac{T}{m} \left((S_3^* - S_3) - (S_1^* - S_1) \right) + \frac{T_c}{m} \left(\frac{(H_1^* - H_1)}{T_c} - \frac{(H_3^* - H_3)}{T_c} \right) \tag{102}$$

where Q is the heat requirement per lb. of fluid, S is the entropy, H the enthalpy, T_c the critical temperature, and the asterisk indicates that the measurement is made at a pressure approaching zero, to eliminate real gas effects. If a nozzle exit size is assumed, the heat requirement per unit time can also be calculated. For purposes of this calculation, a nozzle exit diameter of six inches was assumed. The results obtained in this calculation are given in Table V.

TABLE V

REQUIREMENTS FOR STANDING SHOCK WAVE TO DUPLICATE SHOCK TUBE RUNS

	Runs Duplicated		
	61	99	121
u_3 (ft/sec.)	6120	8590	8750
P_3 (atm.)	0.0268	0.0087	0.0094
Q (Btu/lb.)	873	1634	1704
W (lb./hr.)	9150	4190	4290
q (Btu/hr.)	8,000,000	6,850,000	7,310,000

Although the heat requirement is rather high, it is not necessarily impossible to attain. For example, the nozzle can be made smaller, thus cutting down the mass flow rate and with it, the heat flux. A bank of nozzles can be used to increase overall amounts of products. Of course, the crucial quantity is the heat flux density requirement, Btu/hr - ft^2, which cannot be estimated until the exact configuration of the nozzle is decided upon. The minimum overall nozzle

size is also a gas dynamic design problem, and will not be discussed here. All that can be said is that perhaps such a scheme for continuously cracking hydrocarbons by shock waves may be possible.

V - CONCLUSIONS

It may be concluded on the basis of the information obtained in the course of this work that shock waves can indeed be used to cause thermal decomposition in ethane and ethylene. The temperatures and the residence times of the hydrocarbon reactant in the hot zone are of such a magnitude as to make the gathering of reaction rate data quite convenient over a wide range of conditions.

The quenching of the shock wave by use of a reflected rarefaction in indeed feasible and the results obtained through use of this method are quite in keeping with the results obtained by more conventional quenching methods.

In the study of the cracking of ethane to form ethylene and hydrogen, it was found that the kinetic data obtained was reasonably consistent with previous non-shock-tube data, although the activation energy derived is lower than that derived previously. The kinetic data obtained in this work is, however, very much consistent with data obtained in another, quite different, shock tube.

In the study of the cracking of ethylene to form acetylene and hydrogen, it was found that the data indicate a first-order irreversible reaction mechanism with relatively little scatter as compared to the ethane decomposition study. This data is consistent with data obtained in another, quite different, shock tube, although the activation energy derived is smaller than that derived previously.

The effect of additives on the cracking of ethane and ethylene was also studied. It was found that small amounts of oxygen, air, carbon monoxide, or chlorine do not appreciably affect the rates of cracking of either ethane or ethylene.

Indications were present that there is some carbon formation in the ethylene decomposition reaction, but little or none in the ethane decomposition reaction. Also, apparently, there is no appreciable mixing of driver gas into the reaction zone.

Apparently, there are fewer side reactions occurring in the shock tube study than in the previous non-shock tube work. This is probably due to the shorter residence times and lower degrees of conversion obtained in the shock tube, as compared to other methods.

Finally, by application of the equations governing the flow in a shock tube and in a converging-diverging nozzle, and from rate data obtained in the shock tube, it should be possible to design a device through which reactants will flow on a continuous basis through a standing shock wave which will initiate the reaction. One possible use for such a device could be to produce acetylene directly from ethane, a reaction which was noted in the course of this research.

Future work in this field should include work on determining the mechanism of the reactions exactly. This can be done by varying the contact time at constant temperature with the other variables held constant and thus determining the effect of contact time on conversion.

APPENDIX I

FLOW EQUATIONS

A. Derivation of Rankine-Hugoniot Equation:

$$h = C_p T \tag{6}$$

$$T = \frac{mP}{\rho R} \tag{7a}$$

$$h = \frac{m C_p P}{\rho R} = \left(\frac{\gamma}{\gamma - 1}\right)\frac{P}{\rho} \tag{103}$$

where $\gamma = C_p / C_v$ (104)

and $C_p - C_v = R$ (105)

so, $h_o - h_1 = \frac{1}{2}(v_1^2 - v_o^2)$ (4a)

$$\frac{\gamma}{\gamma - 1}\left(\frac{P_o}{\rho_o} - \frac{P_1}{\rho_1}\right) = 1/2\,(v_1^2 - v_o^2) \tag{106}$$

but from $\rho_o^2 v_o^2 - \rho_1^2 v_1^2 = 0$ (2a)

and $\rho_o v_o^2 - \rho_1 v_1^2 = P_1 - P_o$ (3a)

it can be easily seen that

$$v_1^2 - v_o^2 = (P_o - P_1)\left(\frac{1}{\rho_o} + \frac{1}{\rho_1}\right) \tag{107}$$

so $$\frac{\gamma}{\gamma - 1}\left(\frac{P_o}{\rho_o} - \frac{P_1}{\rho_1}\right) = 1/2\,(P_o - P_1)\left(\frac{1}{\rho_o} + \frac{1}{\rho_1}\right) \tag{108}$$

since $\beta = \frac{\gamma + 1}{\gamma - 1}$, this equation can easily be rearranged to

$$\frac{\rho_1}{\rho_o} = \frac{\beta(P_1/P_o) + 1}{P_1/P_o + \beta} \tag{5}$$

which is the Rankine-Hugoniot Equation.

B. Notes on the Derivation of the Taub Equation:

For the standing shock, where the coordinate system is centered on the shock and the fluid flows past, we note that, from equations (2) and (3):

$$v_o^2 = \frac{P_o - P_1}{\rho_o - \rho_1} \frac{\rho_1}{\rho_o} \tag{109}$$

$$v_1^2 = \frac{P_o - P_1}{\rho_o - \rho_1} \frac{\rho_o}{\rho_1} \tag{110}$$

If equations (5) and (24) are included, it is a relatively easy matter to obtain

$$v_o^2 = \frac{C_o^2}{\beta_o + 1} \left(\beta_o \frac{P_1}{P_o} + 1\right) \tag{28}$$

$$v_1^2 = \frac{C_o}{\beta_o + 1} \frac{\left(\frac{P_1}{P_o} + \beta_o\right)^2}{\beta_o \frac{P_1}{P_o} + 1} \tag{27}$$

If the coordinates are transformed to the case where the shock is moving into stagnant fluid, the shock velocity, U, becomes

$$U = v_o = \frac{C_o}{\sqrt{\beta_o + 1}} \sqrt{\beta_o \frac{P_1}{P_o} + 1} \tag{111}$$

and the velocity of the gas behind the shock, $v_o - v_1$, becomes:

$$v_o - v_1 = C_o \frac{(\beta_o - 1)}{\sqrt{\beta_o + 1}} \frac{\frac{P_1}{P_o} - 1}{\sqrt{\beta_o \frac{P_1}{P_o} + 1}} \tag{112}$$

Combining equations (22) and (23) to eliminate θ, and applying it at the foot of the rarefaction,

$$C_3 = C_2 - \frac{\gamma_2 - 1}{2} u_3 \tag{113}$$

Since $u_3 = v_o - v_1$ and

$$C_3 = \sqrt{\gamma_2 \frac{P_3}{\rho_3}} = \sqrt{\gamma_2 \frac{P_1}{\rho_2} \left(\frac{P_2}{P_1}\right)^{1/\gamma_2}} \tag{114}$$

from $\frac{P}{\rho^{\gamma_2}}$ = constant (the rarefaction fan is adiabatic) and the fact that $P_3 = P_1$, we can set up an equation involving just P_2, P_o, P_1 and the various sonic velocities and heat capacities of the fluids in question. This equation is exactly equation (25).

C. Notes on Particle Velocity

A combination of equation (25) with equation (39) yields:

$$\frac{P_2}{P_o} = \frac{P_1}{P_o} \left(1 - \frac{\beta_o - 1}{\beta_2 - 1} \frac{1}{\beta_o} \frac{1}{\sqrt{\beta_o + 1}} \frac{C_o}{C_2} \frac{(\beta_o + 1)(M^2 - 1)}{\beta_o(\sqrt{\beta_o + 1})\, M}\right)^{-(\beta_2 + 1)} \tag{115}$$

which simplifies to:

$$\frac{P_2}{P_o} = \frac{P_1}{P_o}\left(1 - \frac{\beta_o - 1}{\beta_2 - 1}\,\frac{1}{\beta_o}\,\frac{C_o}{C_2}\,\frac{M^2 - 1}{M}\right)^{-(\beta_2 + 1)} \tag{116}$$

Substituting from equation (43) we obtain

$$C_3 = C_2\left(1 - \frac{\beta_o - 1}{\beta_2 - 1}\,\frac{1}{\beta_o}\,\frac{C_o}{C_2}\,\frac{M^2 - 1}{M}\right) \tag{117}$$

Eliminating θ from equation (22) and (23) and applying the resulting equation to region 3, we obtain

$$C_3 = C_2 - \frac{\gamma_2 - 1}{2}\,u_3 \tag{113}$$

$$C_3 = C_2 - \frac{1}{(\beta_2 - 1)}\,u_3. \tag{118}$$

Eliminating C_3 between equation (117) and equation (118) yields the required result.

APPENDIX II

SAMPLE CALCULATION

A sample calculation will be made for Run No. 99. The measurements made during the run were:

Diaphragm = 0.006 inches thick scored brass

Atmospheric Pressure = 29.67" Hg.

Atmospheric Temperature = 60.0°F.

P_o = 0.26" Hg.

P_2 = 700 psig

Time Interval = 116.6 microseconds

High Pressure Gas = Hydrogen

Mass Spectroscopic Analyses:

Gas fed to low pressure section =
97.3% C_2H_6, 2.7% C_2H_4

Reaction products (based on total hydrocarbons) =
76.0% C_2H_6, 24.0% C_2H_4, a trace of C_2H_2

The necessary properties of the feed material and the products of reaction were obtained from Rossini (88), Perry (77), and Hougen and Watson (58). These include such values as γ_o = 1.20, γ_2 = 1.40, C_o = 1020 ft/sec. (at T = 520°R), C_2 = 4600 ft/sec., heat of reaction = 55,700 Btu absorbed per lb. mole ethane cracked, and C_{p_o} = 12.0 Btu/lb. mole-°R. We can now easily calculate all the parameters necessary for the reaction rate analysis by applying the equations developed in the theory section of this thesis.

Since we know the length of time required for the wave to go one foot, and since we know the sonic velocity in the test gas at the ambient temperature, we also know the shock Mach Number:

M observed = 8.41

Since we know β_o (= 11), β_2 (= 6), C_o, C_2, and $\frac{P_2}{P_o}$, we can apply equation (25) to obtain $\frac{P_1}{P_o}$. This turns out to be

$$\frac{P_1}{P_o} = 62.5$$

Now, we can apply equation (38) to obtain the maximum Mach Number possible, i.e., that Mach Number which would be observed if the diaphragm burst perfectly:

M calculated = 9.75

or, about 14% higher than the observed value. Application of equation (48) shows that the shock wave and the reflected rarefaction will interact more than 48 inches from the diaphragm. Since this interaction will not occur in the shock tube, application of equation (62) becomes unnecessary. Application of equation (31) yields the temperature behind the shock wave, T_1, assuming no chemical reaction. This temperature turns out to be

$T_1 = 4260^oR$

Application of equation (60) and (59) for one mole of material yields

$T_{avg} = 4000^oR$, corresponding to a Mach number change of from 8.41 to 8.23, a negligible amount.

On the basis of data in Hougen and Watson (58), the value of K_p turns out to be

$$K_p = 7800$$

Since $\frac{(b+c)(c)}{(a-c)} = 0.067$, the reverse reaction is indeed negligible, and we are on safe ground insofar as the kinetic equations are concerned.

Application of equations (49) and (50) yields the value of τ_{max}, which turns out to be:

$$\tau_{max} = 0.412 \text{ milliseconds}$$

We now know all the terms necessary to calculate k_1 from equation (81). This value turns out to be:

$$k_1 = 1240 \text{ sec}^{-1}$$

Since a first order decomposition reaction is assumed, with a rate constant defined by equation (52), we can take logarithms of both sides of equation (52) to obtain:

$$\ln k_1 = \ln A - \frac{\Delta E}{RT} \qquad (86)$$

If we now plot $\ln k_1$ against $(\frac{1}{T})$, we should obtain a straight line of slope $(\frac{-\Delta E}{R})$ and intercept (ln A), thus determining the exact kinetic equation. For this run $\ln k_1 = 7.13$, $\frac{1}{T} = 2.50 \times 10^{-4}$.

For the runs where C_2H_4 is the gas in the low pressure section, the data used is: $\gamma_o = 1.24$, $C_{p_o} = 10.38$ Btu/lb mole - ^oR, $C_o = 1070$ ft./sec., and heat of reaction = 71,800 Btu absorbed per lb. mole ethylene cracked to acetylene.

Since there may be a run in which the reverse reaction becomes important, it was decided to pick that run in which the reverse reaction

would be most significant and determine if any effect of the reverse reaction could be noted. The run used was Run 55. For this run, $K_p = 890$, while $\frac{(b+c)(c)}{(a-c)} = 1.15$. Since, even for this run, the reverse reaction is negligible, it was neglected for all runs.

APPENDIX III

EXPERIMENTAL INFORMATION

A. Data Obtained During the Course of the Runs

1. Cracking of Pure Ethane (Analysis Based on 100% Hydrocarbons)

Run	M	P_o(atm)	P_2(psia)	Reactants		Products	
				$\%C_2H_6$	$\%C_2H_4$	$\%C_2H_6$	$\%C_2H_4$
52	7.33	0.0100	700	96.3	3.7	61.3	38.7
55	7.87	0.0090	825	"	"	34.8	65.2
56	8.46	0.0167	695	"	"	72.3	27.7
57	6.70	0.0525	665	"	"	71.3	28.7
58	6.50	0.0591	680	"	"	88.3	11.7
61	6.01	0.0268	715	97.3	2.7	95.3	4.7
62	5.32	0.0344	635	"	"	96.4	3.6
64	4.41	0.0782	685	"	"	95.2	4.8
65	4.20	0.0900	675	"	"	95.3	4.7
68	4.32	0.0803	625	"	"	96.6	3.4
69	4.56	0.0686	655	"	"	96.7	3.3
72	6.55	0.0194	730	"	"	95.1	4.9
75	3.90	0.1047	665	"	"	97.0	3.0
78	3.75	0.1132	645	"	"	96.9	3.1
79	3.51	0.1450	655	"	"	96.8	3.2
82	6.40	0.0214	685	"	"	96.1	3.9
83	6.79	0.0164	725	"	"	95.5	4.5
85	7.43	0.0124	725	"	"	89.8	10.2
86	8.29	0.0074	705	"	"	76.0	24.0
91	6.03	0.0191	215	"	"	96.8	3.2
95	7.29	0.0064	665	"	"	90.2	9.8
98	7.52	0.0127	745	"	"	91.1	8.9
99	8.41	0.0087	715	"	"	76.0	24.0
100	9.40	0.0033	785	"	"	59.5	32.9
				(7.6% C_2H_2 in product)			
101	9.55	0.0037	815	"	"	55.0	34.6
				(10.4% C_2H_2 in product)			
102	6.39	0.0217	775	"	"	96.4	3.6
103	6.26	0.0256	795	"	"	96.5	3.5
203	6.45	0.0120	1075	"	"	90.6	9.4
204	6.07	0.0114	885	"	"	97.0	3.0
205	7.68	0.0160	840	"	"	88.2	11.8
206	7.34	0.0208	865	"	"	90.2	9.8

2. Cracking of Ethane Containing 5% O_2 (Analysis Based on 100% Hydrocarbons)

111	6.86	0.0204	835	97.3	2.7	93.2	6.8
112	7.19	0.0157	715	"	"	88.3	11.7
114	6.22	0.0274	865	"	"	96.6	3.4
115	7.73	0.0120	775	"	"	84.6	15.4

EXPERIMENTAL INFORMATION (Cont'd)

3. Cracking of Ethane Containing 5% Air (Analysis Based on 100% Hydrocarbons)

Run	M	P_o(atm)	P_2(psia)	Reactants		Products	
				$\%C_2H_6$	$\%C_2H_4$	$\%C_2H_6$	$\%C_2H_4$
116	8.19	0.0104	785	97.3	2.7	83.2	16.8
117	7.34	0.0147	685	"	"	91.1	8.9
118	6.69	0.0211	835	"	"	95.8	4.2
119	6.26	0.0291	840	"	"	96.9	3.1
4. Cracking of Ethane Containing 5% CO							
168	6.18	0.0154	805	"	"	87.2	12.8
180	8.15	0.0140	1015	"	"	84.4	15.6
181	7.65	0.0181	985	"	"	89.4	10.6
182	6.92	0.0218	975	"	"	93.7	6.3
5. Cracking of Ethane Containing 17% CO							
189	7.27	0.0217	840	"	"	85.1	14.9
190	7.89	0.0150	905	"	"	76.4	23.6
6. Cracking of Ethane Containing 4% Cl_2							
192	8.27	0.0134	935	"	"	82.2	17.8
193	7.06	0.0227	885	"	"	94.4	5.6

EXPERIMENTAL INFORMATION (Cont'd)

7. Cracking of Pure Ethylene (Reactant = 100% ethylene)

Run	M	P_o(atm)	P_2(psia)	Products (based on 100% hydrocarbons)	
				$\%C_2H_4$	$\%C_2H_2$
120	7.21	0.0151	715	94.9	5.1
121	8.17	0.0094	805	89.7	10.3
125	8.90	0.0080	885	82.7	17.3
128	8.47	0.0060	715	84.5	15.5
129	7.38	0.0144	725	94.5	5.5
130	7.90	0.0104	710	89.8	10.2
131	6.80	0.0184	725	97.0	3.0
132	6.90	0.0194	735	96.8	3.2
135	6.50	0.0221	795	98.0	2.0
136	6.28	0.0244	765	98.7	1.3
137	6.15	0.0264	760	99.1	0.9
138	6.15	0.0277	805	99.1	0.9
139	5.82	0.0377	805	99.7	0.3
140	5.88	0.0334	725	99.6	0.4
141	5.41	0.0421	705	99.8	0.2
142	5.59	0.0382	735	99.7	0.3
143	5.32	0.0435	730	99.9	0.1
198	7.59	0.0137	1000	92.2	7.8
199	7.00	0.0211	885	97.5	2.5
200	6.15	0.0137	990	98.6	1.4
202	6.29	0.0120	1010	99.2	0.8
8. Cracking of Ethylene Containing 5% CO					
184	7.94	0.0134	1005	93.6	6.4
185	7.29	0.0187	985	98.4	1.6
186	6.85	0.0234	1050	99.1	0.9
9. Cracking of Ethylene Containing 17% CO					
187	6.81	0.0207	965	97.0	3.0
188	7.32	0.0147	815	93.8	6.2
10. Cracking of Ethylene Containing 6% Cl_2					
194	7.39	0.0144	845	89.6	10.4
195	7.36	0.0187	865	96.2	3.8
197	6.92	0.0227	865	98.7	1.3

EXPERIMENTAL INFORMATION (Cont'd)

B. Reaction Parameters Calculated from Raw Data

1. Cracking of Pure Ethane

Run	P_1/P_o	Predicted M	D"	T(°R)	(milliseconds) τ_{max}	ln k_1
52	47.0	9.55	>48	2920	0.340	7.97
55	55.0	9.90	>48	3090	0.378	8.81
56	63.0	8.88	>48	4060	0.415	7.29
57	39.3	7.26	32.0	2880	0.344	7.51
58	37.0	7.13	30.9	2900	0.338	6.21
61	31.6	8.28	34.5	3020	0.304	4.90
62	24.5	7.79	29.5	2530	0.330	4.02
64	17.0	6.77	21.0	1810	0.280	5.04
65	15.2	6.55	19.9	1700	0.273	5.01
68	16.2	6.61	20.3	1750	0.276	3.96
69	18.0	6.90	22.2	1910	0.290	3.74
72	37.5	8.72	38.9	2720	0.307	5.00
75	13.2	6.33	18.7	1540	0.267	3.14
78	12.1	6.20	17.9	1475	0.260	3.44
79	10.7	5.89	16.3	1340	0.249	3.72
82	35.9	8.51	36.1	2640	0.300	4.41
83	40.1	8.95	41.4	3110	0.318	4.75
85	48.4	9.33	45.8	3310	0.356	6.09
86	60.5	9.98	>48	3860	0.409	7.13
91	31.6	7.11	23.8	2520	0.299	3.54
95	46.1	10.08	>48	3210	0.345	6.07
98	49.5	9.33	45.8	3400	0.359	5.91
99	62.5	9.75	>48	4000	0.412	7.13
100	77.0	11.05	>48	4700	0.485	7.68
101	80.0	11.00	>48	4840	0.498	7.81
102	35.9	8.69	38.5	2640	0.300	4.11
103	34.2	8.45	36.0	2550	0.293	4.04
203	45.2	6.62	>48	2620	0.452	5.75
204	40.8	6.52	>48	2422	0.400	2.71
205	65.0	9.16	44.0	3500	0.368	6.28
206	59.1	8.90	41.2	3250	0.350	6.09

2. Cracking of Ethane Containing 5% O_2

111	41.2	8.88	40.5	2920	0.324	5.44
112	45.3	9.00	42.0	3130	0.339	6.36
114	33.5	8.50	36.5	2520	0.291	3.90
115	52.5	9.46	47.1	3510	0.372	6.64

EXPERIMENTAL INFORMATION (Cont'd)

3. Cracking of Ethane Containing 5% Air

Run	P_1/P_o	Predicted M	D"	T(°R)	(milliseconds) τ_{max}	ln k_1
116	59.0	9.64	>48	3850	0.398	6.70
117	47.0	9.33	45.8	3270	0.349	5.92
118	39.3	8.80	39.7	2820	0.313	4.59
119	34.1	8.38	35.3	2540	0.293	3.32
4. Cracking of Ethane Containing 5% CO						
168	41.9	9.16	43.7	2400	0.288	6.61
180	73.0	9.59	>48	3840	0.396	6.60
181	64.0	9.16	43.7	3480	0.367	6.14
182	52.3	8.99	42.0	2980	0.327	5.40
5. Cracking of Ethane Containing 17% CO						
189	57.9	8.78	39.5	3250	0.346	6.67
190	68.5	9.35	46.0	3700	0.380	7.20
6. Cracking of Ethane Containing 4% Cl_2						
192	75.0	9.57	>48	4030	0.404	6.75
193	55.0	8.80	39.5	3070	0.334	5.19
7. Cracking of Pure Ethylene						
120	50.4	9.00	>48	3620	0.342	5.74
121	65.0	9.80	>48	4450	0.397	6.29
125	77.2	10.13	>48	5050	0.447	6.78
128	70.0	10.22	>48	4630	0.417	6.72
129	53.0	9.06	>48	3740	0.350	5.74
130	61.0	9.45	>48	4170	0.381	6.34
131	45.0	8.72	>48	3320	0.320	5.23
132	52.5	8.65	48.0	3380	0.325	5.25
135	46.5	8.60	47.0	3090	0.304	4.88
136	43.1	8.41	44.0	2920	0.293	4.49
137	42.0	8.28	42.3	2840	0.287	4.14
138	42.0	8.30	42.7	2840	0.287	4.14
139	37.5	8.13	40.6	2600	0.272	3.09
140	38.0	7.92	38.2	2640	0.273	3.38
141	32.1	7.58	34.5	2300	0.253	2.76
142	34.0	7.78	36.5	2420	0.260	3.14
143	31.1	7.58	34.5	2240	0.249	2.08
198	63.0	9.55	>48	3910	0.362	6.11
199	54.0	8.80	>48	3500	0.330	5.01
200	42.0	6.27	>48	2820	0.444	4.14
202	43.9	6.35	>48	2940	0.461	3.54

EXPERIMENTAL INFORMATION (Cont'd)

8. Cracking of Ethylene Containing 5% CO

Run	P_1/P_o	Predicted M	D"	T(°R)	(milliseconds) τ_{max}	ln k_1
184	69.5	9.58	>48	4270	0.384	5.85
185	59.0	9.10	>48	3730	0.346	4.43
186	51.8	8.90	>48	3380	0.323	3.96

9. Cracking of Ethylene Containing 17% CO

187	51.8	8.94	>48	3320	0.321	5.23
188	93.5	9.16	>48	3980	0.349	5.91

10. Cracking of Ethylene Containing 6% Cl_2

194	60.5	9.26	>48	3680	0.351	6.44
195	60.4	8.93	>48	3770	0.350	5.37
197	52.8	8.67	>48	3430	0.327	4.37

BIBLIOGRAPHY

1. Aten, C. F., and E. F. Greene, "Rate of Formation of Carbon from the Pyrolysis of Acetylene in Shock Waves," Disc. Faraday Society, 22, pg. 162. (1956).

2. Bauer, S. H., G. L. Schott, and R. E. Duff, "Kinetic Studies of Hydroxyl Radicals in Shock Waves I - The Decomposition of Water Between 2400 and 3200°K," J. Chem. Phys., 28, pg. 1089, (1958).

3. Belchetz, L., and E. K. Rideal, "Decomposition of Hydrocarbon Vapors on C Filaments," J. Am. Chem. Soc., 57, pg. 1168, (1935).

4. Bennett, E. N., "Carbon Formation From Acetylene in the Shock Tube," CIT, Guggenheim Jet Propulsion Center, AF 18 (603) TR 2, June 1956, 85 pp., 12 refs.

5. Berets, D. J., E. F. Greene, and G. B. Kistiakowsky, "Gaseous Detonations II - Initiation by Shock Waves," J. Am. Chem. Soc., 72, pg. 1086, (1950).

6. Berlie, M. R. and D. J. Le Roy, "The Reaction of Atomic Hydrogen with Ethane," Disc. Faraday Society, 14, pg. 50, (1953).

7. Britton, D., and N. Davidson, "Hydrogen - Bromine Reaction in a Nonsteady State," J. Chem. Phys., 23, pg. 2461, (1955).

8. Britton, D., N. Davidson, W. Gehman, and G. Schott, "Shock Waves in Chemical Kinetics: Further Studies on the Rate of Dissociation of Molecular Iodine," J. Chem. Phys., 25, pg. 804, (1956).

9. Britton, D., and N. Davidson, "Shock Waves in Chemical Kinetics: Rate of Dissociation of Molecular Bromine," J. Chem. Phys., 25, pg. 810, (1956).

10. Britton, D., N. Davidson, and G. Schott, "Shock Waves in Chemical Kinetics: Rate of Dissociation of Molecular Iodine," Disc. Faraday Society, 17, pg. 58, (1954).

11. Brooks, B. T., C. E. Boord, S. S. Kurtz, Jr., and L. Schmerling, "The Chemistry of Petroleum Hydrocarbons," Vol. II, Reinhold Publishing Corp., New York, 1955.

12. Burk, R. E., B. G. Baldwin, and C. H. Whitacre, "Thermal Reactions of C_2H_4," Ind. and Eng. Chem., 29, pg. 326, (1937).

13. Burington, R. S., "Handbook of Mathematical Tables and Formulas," Handbook Publishers, Inc., Sandusky, Ohio, 1953.

14. Calderbank, P. H., and V. P. Hovnanian, "Pyrolysis of Ethane," Ind. Chemist, 33, pg. 557, (1957).

15. Carpenter, R. A., and F. C. Fowler, "Ethylene by Steam Pyrolysis of Ethane," Petroleum Refiner, 31, No. 4, pg. 148, (1952).

16. Carrington, T., and N. Davidson, "Photoelectric Observation of the Rate of Dissociation of Nitrogen Tetroxide by a Shock Wave," J. Chem. Phys., 19, pg. 1313, (1951).

17. Carrington, T., and N. Davidson, "Shock Waves in Chemical Kinetics: The Rate of Dissociation of N_2O_4," J. Phys. Chem., 57, pg. 418, (1953).

18. Challis, J., "On the Velocity of Sound," Philosophical Magazine, (3), 32, pg. 494, (1848).

19. Chapman, D. L., "Rate of Explosion of Gases," Philosophical Magazine, (5), 47, pg. 90, (1899).

20. Corneille, J. L., and R. Brais, "Thermal Dehydrogenation of Ethane," Ann. ACFAS, 17, pg. 88, (1951).

21. Courant, R., and K. O. Friedrichs, "Supersonic Flow and Shock Waves," Interscience Publishers, Inc., New York, 1956.

22. Cramér, H., "The Elements of Probability Theory and Some of its Applications," John Wiley and Sons, New York, 1955.

23. Dahlgren, G. Jr., and J. E. Douglas, "Kinetics of The Thermal Reactions of Ethylene," J. Am. Chem. Soc., 80, pg. 5108 (1958).

24. Danby, C. J., B. C. Spall, F. J. Stubbs, and C. N. Hinshelwood, "The Irreversible Formation of Methane in the System Ethane-Ethylene-Hydrogen," Proc. Roy. Soc., A 218, pg. 450 (1953).

25. Davidson, N., and G. L. Schott, "The Role of NO_3 in the Thermal Decomposition of NO_2," J. Chem. Phys., 27, pg. 317, (1957).

26. Dintses, A. L., D. A. Kyvatkovskii, A. D. Stepukhovich, and A. V. Frost, "Decomposition of Hydrocarbons IV. Kinetics of the Decomposition of C_2H_6 at Pressures Below Atmospheric," J. Gen. Chem. USSR, 7, pg. 1754, (1937).

27. Dintses, A. L., V. R. Zharkova, A. V. Zherko, and A. V. Frost, "Kinetics and Mechanism of Decomposition of Hydrocarbons IV. Effect of Pressure On the Rate and Direction of Decomposition of C_2H_6," J. Gen. Chem., USSR, 7, pg. 1063, (1937).

28. Dodge, B. F., "Chemical Engineering Thermodynamics," McGraw-Hill Book Company, Inc., New York, 1944.

29. Duff, R. E., "Relaxation Time for Reactions Behind Shock Waves and Shock Wave Profiles," Phys. Fluids, pg. 242, (1958).

30. Earnshaw, S., "On the Mathematical Theory of Sound," Trans. of the Royal Society, 150, pg. 133, (1860).

31. Egloff, G., "The Reactions of Pure Hydrocarbons," Reinhold Publishing Corp., New York, 1937.

32. Eltenton, G. C., "Detection of Free Radicals," J. Chem. Phys., 10, pg. 403, (1942). ibid. 15, pg. 455, (1947).

33. Eshevskaya, M. P., "Kinetics and Mechanism of the Decomposition of Hydrocarbons VII. Inhibiting Effect of Unsaturated Hydrocarbons on the Thermal Decomposition of Iso-octane," Refiner Natural Gasoline Mfr., 19, pg. 264, (1940); also, J. Gen. Chem. USSR, 9, pg. 2162 (1939).

34. Fay, J. A., "Initiation of Detonation in 2 H_2 - O_2 Mixtures by Uniform Shock Waves," 4th Symposium on Combustion, Williams and Wilkins Co., Baltimore, 1953, pg. 501.

35. Fay, J. A. and E. R. Lekawa, "The Ignition of Combustible Gases by Converging Shock Waves," ASTIA Rept. AD 73694, June 30, 1955.

36. Feldman, S., "Some Shock Tube Experiments on the Chemical Kinetics of Air at High Temperatures," J. Fluid Mechanics, 3, Part 3, pg. 225, (1957).

37. Frey, F. E., and D. F. Smith, "Thermal Decomposition of Ethane, Ethylene, Propane, and Propylene," Ind. and Eng. Chem., 20, pg. 948, (1928).

38. Frolich, P. K., A. White, and H. P. Dayton, "Production of C_2H_2 from CH_4 (I) Cracking in Vacuo," Ind. and Eng. Chem., 22, pg. 20, (1930).

39. Glass, I. I. and J. G. Hall, "Shock Tubes - Part I - Theory and Performance of Simple Shock Tubes; Part II - Production of Strong Shock Waves; Shock Tube Applications, Design, and Instrumentation," UTIA Review No. 12, May, 1958.

40. Glass, I. I., W. Martin, and G. N. Patterson, "A Theoretical and Experimental Study of the Shock Tube," UTIA Rep. 2, Nov. 1953, 281 pp., 73 refs.

41. Glass, I. I., and G. N. Patterson, "A Theoretical and Experimental Study of Shock-Tube Flows," J. Aero. Sci., Feb. 1955, pg. 73.

42. Glick, H. S., "Shock Tube Studies of Reaction Kinetics of Aliphatic Hydrocarbons," 7th Symposium on Combustion, Preprints, Butterworth's Scientific Publications, London, 1958, pg. 76.

43. Glick, H. S., J. J. Klein, and W. Squire, "Single-Pulse Shock Tube Studies of the Kinetics of the Reaction $N_2 + O_2 \rightleftharpoons 2\ NO$ Between 2000-3000°K," CAL Rept. No. AD-959-A-1, AFOSR TN-57-407, AD 132485 (Sept. 1957), J. Chem. Phys., 27, No. 4, pg. 850, (1957).

44. Glick, H. S., W. Squire, and A. Hertzberg, "Shock-Tube Technique for the Study of High-Temperature Gas-Phase Reactions," 5th Symposium on Combustion, Reinhold Publishing Company, New York, 1955, pg. 393.

45. Gluckstein, M. E., "Shock Induced Chemical Reactions," Univ. of Mich. Industry Program, Rept. IP-208, Feb. 1957, (Ph. D. Thesis, University of Michigan, 1957).

46. Greene, E. F., "Chemical Reactions in Strong Shock Waves," J. Am. Chem. Soc., 76, pg. 2127, (1954).

47. Greene, E. F., R. L. Taylor, and W. L. Patterson, Jr., "Pyrolysis of Simple Hydrocarbons in Shock Waves," J. Phys. Chem., 62, pg. 238, (Feb. 1958).

48. Hertzberg, A., "The Application of the Shock Tube to the Study of High Temperature Phenomena in Gases," Appl. Mechanics Revs., 9, pg. 505, (1956).

49. Hague, E. N. and R. V. Wheeler, "Mechanism of the Thermal Decomposition of the Normal Paraffina," J. Chem. Soc., 1929, pg. 378.

50. Henshall, B. D., "The Use of Multiple Diaphragms in Shock Tubes," Gt. Brit. ARC, CP 291, 1956, 44 pp.

51. Hertzberg, A., and W. Squire, "The Use of The Shock Tube for Studying Chemical Kinetics," Phys. Rev., 91, pg. 469, (1953).

52. Hikita, T., "Chemical Reactions in the Shock-Tube," Kagaku (Kyoto), 12, pg. 823, (1957).

53. Hobbs, J. E., and C. N. Hinshelwood, "Mechanism of Chain Breaking in the Thermal Decomposition of Ethane," Proc. Roy. Soc., A 167, pg. 439, (1938).

54. Hobbs, J. E., and C. N. Hinshelwood, "Reaction Chains in the Thermal Decomposition of Hydrocarbons - Comparison of Methane, Ethane, Propane, and Hexane," Proc. Roy. Soc., A 167, pg. 447, (1938).

55. Hooker, W. J., "Shock Tube Studies of Acetylene Decomposition," CIT Guggenheim Jet Prop. Cen. TR 7, (AFOSR TN 58-293), AD 154202, Apr. 1958; also, 7th Symposium on Combustion, Preprints, Butterworth's Scientific Publications, London, 1958, pg. 180.

56. Hornig, D. F., "The Production of Unstable Species in Shock Waves," Ann. N. Y. Acad. Sci., 67, pg. 463, (1957).

57. Hornig, D. F., "Spectroscopic Studies on Reactions at High Temperatures," Molecular Spectroscopy, Rept. Conf. Inst. Petroleum, London, 1954, pg. 183, (Pub. 1955).

58. Hougen, O. A., and K. M. Watson, "Chemical Process Principles," John Wiley and Sons, Inc., New York, (1949).

59. Hugoniot, H., "On the Propagation of Motion in Bodies and Especially in a Perfect Gas," Journal de l'Ecole Polytechnique, 53, pg. 1, (1889).

60. Ingold, K. U., F. J. Stubbs, and C. N. Hinshelwood, "Kinetics of the Thermal Decomposition of Normal Paraffin Hydrocarbons III - Activation Energies and Mechanisms of Molecular Reactions," Proc. Roy Soc., A 203, pg. 486, (1950).

61. Jarre, G., "The Dissociation of a Pure Diatomic Gas Behind a Strong Normal Wave," Z. Angew. Math. u. Phys., 9b, pg. 389, (1958). Also, Torino Polytech. Appl. Mec. Lab. TN 3, (AFOSR TN-58-7), AD 148046, Nov. 1957, 17 pp.

62. Jost, W., "Rapid Gas Reactions in Flames and Shock Waves," Chem. Ing. Tech., 28, pg. 708, (1956).

63. Jouguet, E., "Mechanics of Explosives," O. Dour et Fils, Paris, 1907.

64. Kistiakowsky, G. B., and A. G. Nickle, "Ethane-Ethylene and Propane-Propylene Equilibria," Disc. Faraday Society, 10, pg. 175, 1951.

65. Kuchler, L., and H. Thiele, "Thermal Decomposition of C_2H_6 in the Presence of Foreign Gases," Z. Physik. Chem., B 42, pg. 359, (1939).

66. Laidler, K. J., "Chemical Kinetics, "McGraw-Hill Book Co., Inc., New York, 1950.

67. Lenher, S., "Direct Reaction Between O and C_2H_4," J. Am. Chem. Soc., 53, pg. 3752, (1931).

68. Lieber, P., and K. S. Wan, "On a Statistical Theory for One-Dimensional Real Gas Flows," RPI Dept. Geol. Rep. (AFOSR TN 57-478) AD 136470, Sept. 1957, 23 pp.

69. Marek, C. F., and W. B. McCluer, "Velocity Constants for the Thermal Dissociation of C_2H_6 and C_3H_8," Ind. and Eng. Chem., 23, pg. 878, (1931).

70. Model, I. Sh., "Measurement of High Temperatures in Strong Shock Waves in Gas," Zhur. Eksptl. i Theoret. Fiz., 32, pg. 714, (1957).

71. Molera, M. J., and F. J. Stubbs, "Kinetics of the Thermal Decomposition of Olefins," J. Chem. Soc., 1952, pg. 381.

72. Morrison, R. B., "A Shock Tube Investigation of Detonative Combustion," Ph. D. Thesis, University of Michigan, Ann Arbor, 1952.

73. Palmer, H. B., and D. F. Hornig, "Rate of Dissociation of Bromine in Shock Waves," J. Chem. Phys., 26, pg. 98, (1957).

74. Paul, R. E., and L. K. Marek, "Primary Thermal Dissociation Velocity Constants for Propane, Butane, and Isobutane, Ind. and Eng. Chem., 26, pg. 454, (1934).

75. Pease, R. N., "Thermal Dissociation of Ethane, Propane, Butane, and Isobutane," J. Am. Chem. Soc., 50, pg. 1179, (1928)
ibid., 51, pg. 3470, (1929)
ibid., 52, pg. 1158, (1930)
ibid., 53, pg. 613, (1931)
ibid., 54, pg. 1878, (1932)

76. Pease, R. N., and E. S. Durgan, "Equilibrium in the Reaction $C_2H_6 \rightleftharpoons C_2H_4 + H_2$," J. Am. Chem. Soc., 50, pg. 2715, (1928).

77. Perry, J. H., Editor, "Chemical Engineers' Handbook," McGraw-Hill Book Company, Inc., New York, 1950.

78. Potolovskii, L. A., and A. Atal'yan, "Thermal Dehydrogenation of C_2H_6 to C_2H_4," Petroleum Engr., 10, No. 11, pg. 4, (1939).

79. Rankine, W. J. M., "On the Thermodynamic Theory of Finite Longitudinal Disturbances," Trans. of the Royal Society, 160, pg. 277, (1860).

80. Rayleigh, Lord, "Aerial Waves of Finite Amplitude," Proc. of the Royal Society, 84, pg. 247, (1910).

81. Resler, E. L., S. C. Lin, and A. Kantrowitz, "The Production of High Temperature Gases in Shock Tubes," J. Appl. Phys., 23, pg. 1390, (1952).

82. Rice, F. O., "Thermal Decomposition of Organic Compounds from the Standpoint of Free Radicals III. Calculation of the Products Formed from Paraffin Hydrocarbons," J. Am. Chem. Soc., 55, pg. 3035, (1933).

83. Rice, F. O., and M. D. Dooley, "Thermal Decomposition of Organic Compounds From the Standpoint of Free Radicals IV. Dehydrogenation of Paraffins and the Strength of the C-C Bond," J. Am. Chem. Soc., 55, pg. 4245, (1933).
ibid., 56, pg. 2747, (1934).

84. Rice, F. O., and K. F. Herzfeld, "Thermal Decomposition of Organic Compounds - Free Radicals IV. Chain Reactions," J. Am. Chem. Soc., 56, pg. 284, (1934).

85. Rice, F. O., and O. L. Polly, "Inhibition of Homogeneous Organic Decompositions," J. Chem. Phys., 6, pg. 273, (1938).

86. Riemann, B., "Collected Mathematical Works," Teubner Verlog, Leipzig, 1892.

87. Robertson, A. J. B., "Pyrolysis of Methane, Ethane, and Butane on a Pt. Filament," Proc. Roy. Soc., A 199, pg. 394, (1949).

88. Rossini, F. D., et al., "Selected Values of Thermodynamic Properties," Circular 500, National Bureau of Standards, U. S. Gov't. Printing Office, Washington, D. C., 1952.

89. Russo, A., and A. Hertzberg, "A Method for Improving the Performance of Shock Tubes," Jet Propulsion, 27, No. 11, pg. 1 (1957).

90. Russo, A. L., and A. Hertzberg, "Modifications of the Basic Shock Tube to Improve its Performance," CAL Rep. AD-1502-A-7 (AFOSR TN 58-716) AD 162251, Aug. 1958, 43 pp., 11 refs.

91. Sachsse, H., and F. Patat, "Concentration of H Atoms and the Thermal Dissociation of Some Organic Molecules," Z. Electrochem, 41, pg. 493, (1935). Also, Z. Physik. Chem., B 31, pg. 87, (1935).

92. Schmidt, E., "Ignition in the Shock Tube," Brennstoff-Wärme-Kraft, 10, pg. 295, (1958).

93. Schott, G., and N. Davidson, "Shock Waves in Chemical Kinetics: The Decomposition of N_2O_5 at High Temperatures," J. Am. Chem. Soc., 80, pg. 1841, (1958)

94. Silcocks, C. G., "The Kinetics of the Thermal Decomposition and Polymerization of Ethane and Ethylene," Proc. Roy. Soc., A 233, pg. 465, (1956).

95. Spall, B. C., F. J. Stubbs, and C. N. Hinshelwood, "Influence of NO on the Two Opposing Reactions of the Equilibrium $C_2H_6 \rightleftharpoons C_2H_4 + H_2$," Proc. Roy. Soc., A 219, pg. 312, (1953).

96. Stavely, L. A. K., and C. N. Hinshelwood, "Reaction Chains in the Decomposition of Organic Compounds," J. Chem. Soc., 1937, pg. 1568.

97. Steacie, E. W. R., "Atomic and Free Radical Reactions," Second Edition, Reinhold Publishing Company, New York, 1954.

98. Steacie, E. W. R., and G. Shane, Can J. Research, B 18, pg. 203, (1940).

99. Steinberg, M., and W. E. Kaskan, "The Ignition of Combustible Mixtures by Shock Waves," 5th Symposium on Combustion, Reinhold Publishing Company, New York, 1955, pg. 664.

100. Steinberg, M., and T. F. Lyon, "Study of Chemical Relaxation Behind Shock Waves," WADC Tech. Rep. 56-394, (ASTIA AD 118050), Jan. 1957, 18 pp.

101. Stepukhovich, A. D., and F. M. Mitenkov, "Kinetics of Ethane Decomposition at Pressures Higher than Atmospheric," Zhur. Fiz. Khim., 25, pg. 203, (1951).

102. Stokes, E. E., "On a Difficulty in the Theory of Sound," Philosophical Magazine (3), 33, pg. 349, (1848).

103. Storch, H. H., "Acetylene Formation in the Thermal Decomposition of Hydrocarbons," Ind. and Eng. Chem., 26, pg. 56, (1934).

104. Storch, H. H., "Kinetics of Ethylene Polymerization," J. Am. Chem. Soc., 56, pg. 374, (1934).

105. Storch, H. H., and P. L. Golden, "Synthesis of Acetylene by Pyrolysis of Methane," Ind. and Eng. Chem., 25, pg. 768, (1933).

106. Storch, H. H., and L. S. Kassel, "Pyrolysis of C_2H_6," J. Am. Chem. Soc., 59, pg. 1240, (1937).

107. Suzuki, M., H. Miyama, and S. Fujimoto, "The Ignition of Methane-Oxygen Mixture by Shock Wave," Bull. Chem. Soc. Japan, 31, pg. 232, (1958).

108. Taylor, H. A., and A. van Hook, "Polymerization and Hydrogenation of C_2H_2," J. Phys. Chem., 39, pg. 811, (1935).

109. Toennies, J. P., and E. F. Greene, "Dissociation Energies of Carbon Monoxide and Nitrogen from Reflected Shock Wave Studies," J. Chem. Phys., 26, pg. 655, (1957).

110. Toennies, J. P., and E. F. Greene, "Dissociation of Nitrogen in Shock Waves," J. Chem. Phys., 23, 1366, (1955).

111. Travers, S., "Present State and Value of the Hydrothermodynamic Theory of Explosions and Shocks II. The Thickness of the Shock Wave and the Mechanism of Ignition in The Combustion Wave," Mem. Artillerie Franc., 25, pg. 421, (1951).

112. Trimpi, R. L., and N. B. Cohen, "A Theory for Predicting the Flow of Real Gases in Shock Tubes with Experimental Verification," U. S. N. A. C. A. TN-3375, Mar. 1955, 69 pp.

113. Tropsch. H., and G. Egloff, "Pyrolysis of Gaseous Paraffin Hydrocarbons," Ind. and Eng. Chem., 27, pg. 1063, (1935).

114. Turner, E. B., "The Production of Very High Temperatures in the Shock Tube with Application to Spectral Line Broadening," PhD. Thesis, University of Michigan, 1956.

115. Vielle, P., "On the Discontinuities Produced by the Sudden Release of a Compressed Gas," Comptes Rendus, 129, pg. 1228, (1899).

116. White, D. R., "Influence of Diaphragm Opening Time on Shock Tube Flows," J. Fluid Mech., Nov. 1958, pg. 585, 12 refs.

117. Wood, G. P., "Calculations of the Rate of Thermal Dissociation of Air Behind Normal Shock Waves at Mach Numbers of 10, 12, and 14," U. S. N. A. C. A. TN 3634, Apr. 1956, 40 pp., 21 refs.

118. Wray, K. L., and D. F. Hornig, "Dissociation Energy of Fluorine," J. Chem. Phys., 24, pg. 1271, (1956).

119. Wray, K. L., "Dissociation Energy of Fluorine from Shock-Wave Measurements," Univ. Microfilms (Ann Arbor, Mich.) Publ. No. 13, 194. Dissertation Abstract 15, 1328, (1955).

120. Wurster, W. H., "Final Report Summarizing Research in Rate of High Speed Reactions," CAL Rept. AD-959-A-2, (AFOSR TR 58-8) AD 148054, Jan. 1958, 19 pp., 14 refs.

121. Zeldovich, Ya. B., and O. I. Leipunskii, "Obtaining Extremely High Temperatures," Journal of Physics, USSR. 7, pg. 245, (1953).

122. Laporte, O., Private Communication. Also, Class Notes for Physics 233 - "Special Topics in Fluid Dynamics."

NOMENCLATURE

A = a constant; area; defined by equation (72).

a = initial concentration of reactant, mole fraction.

B = defined by equation (73).

b = initial concentration of product, mole fraction.

C = sonic velocity (ft./sec.).

C_p = heat capacity at constant pressure (BTU/lb. mole - ^oR).

C_v = heat capacity at constant volume (BTU/lb. mole - ^oR).

c = mole fraction reactant converted to product.

c_e = mole fraction reactant converted to product at equilibrium.

D = distance between diaphragm site and point of interaction of reflected rarefaction with shock wave; (inches).

E = reactant in generalized chemical reaction; as defined by equation (74).

ΔE = activation energy in reaction rate equation, (BTU/lb. mole or kcal/gm. mole).

e = base of natural logarithms.

F = product in generalized chemical reaction.

G = product in generalized chemical reaction.

g_c = gravitational constant ($32.2 \frac{\text{lb. mass ft.}}{\text{lb. force sec}^2}$).

ΔH = heat of reaction (BTU/lb. mole).

h = enthalpy (BTU/lb. mole).

J = product in generalized chemical reaction.

K_p = equilibrium constant for reversible reaction (in terms of partial pressures).

k = a constant.

k_1 = reaction rate constant for forward reaction (sec^{-1}).

k_2 = when two simultaneous reactions occur, the reaction rate constant for the second forward reaction. (sec^{-1}).

k_1' = reaction rate constant for reverse reaction. (sec^{-1}).

k_2' = when two simultaneous reactions occur, the reaction rate constant for the second reverse reaction. (sec^{-1}).

L = distance between diaphragm site and point of interaction between reflected rarefaction and gas interface (inches).

ln = natural logarithm (to the base e).

M = Mach Number.

m = molecular weight (lb./lb. mole).

N = number of points in statistical analysis.

n = number of moles.

P = pressure (atm., psia, or inches Hg).

Q = heat requirement per unit weight of fluid (Btu/lb.)

q = heat requirement per unit time (Btu/hr.).

R = universal gas constant ($1.987 \frac{\text{Btu}}{\text{lb. mole } ^{o}R}$).

S = entropy of fluid ($\frac{\text{Btu}}{\text{lb. mole } ^{o}R}$).

T = temperature of fluid (^{o}R).

T_c = critical temperature of fluid (^{o}R).

t = time (sec.).

t_a = defined from equation (45) (sec.).

t_i = defined from equation (46)(sec.).

U = shock velocity, laboratory coordinate system (ft./sec.).

u = gas velocity, laboratory coordinate system (ft./sec.).

v = gas velocity, stationary shock coordinate system (ft./sec.).

W = mass rate of flow (lb./hr.).

x = distance (inches); mole fraction E converted to F.

Y = P_1/P_o.

y = mole fraction F converted to J.

Z = P_2/P_o.

Greek Letters

γ = C_p/C_v.

Δ = defined by equation (90); deviation from average value.

θ = x/t.

ρ = density of fluid ($lb./ft^3$).

Σ = summation symbol.

τ = gas residence time in reaction zone. (sec.)

σ = standard deviation.

τ_{max} = maximum gas residence time in reaction zone. (sec.)

β = $\dfrac{C_p + C_v}{C_p - C_v}$.

Symbols and Subscripts

0 = initial state in low pressure region.

1 = state behind shock.

2 = initial state in high pressure region.

3 = state in cold flow behind gas interface.

4 = state within rarefaction fan.

$\frac{dx}{dt}$ = disturbance velocity with respect to laboratory coordinate system.

$\sqrt{\quad}$ = square root.

$\int$ = integral.

$\overline{(\quad)}$ = value of ( ) determined from least squares equation; mean value of ( ).

avg = average.

max = maximum.